IDENTIFY SUSTAINABLE AND ACCESSIBLE COOLING STRATEGIES TO KEEP INDIVIDUALS COOL DURING EXTREME HEAT EVENTS

SUSHANT SURESH BHUVAD

PhD

The Hong Kong Polytechnic University

2025

The Hong Kong Polytechnic University

Department of Building Environment and Energy Engineering

Identify Sustainable and Accessible Cooling Strategies to Keep Individuals Cool During Extreme Heat Events

BHUVAD Sushant Suresh

A thesis submitted in partial fulfillment of the requirements for the Degree of Doctor of Philosophy

July 2025

CERTIFICATE OF ORIGINALITY

I hereby declare that this thesis is my own work and that, to the best of my knowledge and belief, it reproduces no material previously published or written, nor material that has been accepted for the award of any other degree or diploma, except where due acknowledgement has been made in the text.

(Signed)

Sushant Suresh Bhuvad (Name of Student)

Department of Building Environment and Energy Engineering

The Hong Kong Polytechnic University

Hong Kong, China

July 2025

ABSTRACT

Abstract of the thesis entitled: Identify Sustainable and Accessible Cooling Strategies to Keep Individuals Cool During Extreme Heat Events

Submitted by: Sushant Suresh Bhuvad

For the Degree of: Doctor of Philosophy

at The Hong Kong Polytechnic University in July 2025.

New temperature highs were recorded throughout 2024 as a record-breaking and deadly heat wave swept across the Americas, Africa, Europe, and Asia. These extreme heat waves have a direct negative impact on human health, causing exhaustion, heatstroke, and even fatalities. The simplest cooling solution against these heat events is air conditioning. However, it is energy-intensive and not universally available, especially for vulnerable people. Furthermore, the increased use of air conditioning creates a vicious cycle, as it contributes to global warming in the long term. Therefore, there is an urgent need to identify sustainable, affordable, and widely accessible cooling strategies to protect individuals from extreme heat events.

Various sustainable and accessible cooling methods, such as electric fans, cold water ingestion, foot immersion, leg immersion, and self-dousing, can help mitigate the adverse impacts of extreme heat. Among these strategies, electric fans are a widely adopted method. However, existing heat wave guidelines have often discouraged fan use. However, recent research suggests that guidelines may have overlooked the evaporative cooling potential of fans. Nonetheless, previous investigations have primarily examined the physiological responses associated with table fans. However, the air movement produced by both table fans and ceiling

fans may influence the occupants' physiological and perceptual responses differently. Hence, our first study focused on evaluating the effectiveness of no-fan, table-fan, and ceiling-fan scenarios during heat waves through an experimental approach. We conducted 2-hour controlled human trials in a climate chamber set to typical heatwave conditions (air temperature 41°C and relative humidity 35 %), involving 16 healthy young adults. We found that both fan types delayed thermoregulatory and cardiovascular strain relative to the no-fan scenario. Notably, table fans delivered better physiological relief compared to ceiling fans, implying that table fans are preferable during heat waves. Furthermore, we examined varying airflow rates for table fans and found that higher fan speeds further reduced physiological strain and better overall comfort under the tested conditions.

Although laboratory trials provide valuable insights into the effectiveness of fans during heat waves, they cannot represent how prolonged extreme heat affects the human body, given participant safety and ethical constraints. Therefore, to better inform public health decisions, we further evaluated the effectiveness and thresholds of electric fans across various physical activity levels for young adults during prolonged extreme heat events using a thermoregulation model. First, we modified the thermoregulation model by updating the hydration, sweating, and vasodilation processes. Further, moderate hyperthermia onset charts are presented across various fan speeds and activity levels to assess fan performance. Under moderate environmental conditions (40 °C and 50% RH), fan use effectively delayed hyperthermia onset, particularly at lower physical activity levels (PAR)-1.2 and higher fan speeds. In these scenarios, increased sweat evaporation due to higher fan speeds outweighed sensible heat gain, thus reducing overall heat stress. However, under extreme conditions—such as temperatures exceeding 46 °C and relative humidity above 60%—the benefits of fans diminished significantly, accelerating the onset of hyperthermia. In such environments, higher fan speeds worsened conditions as increased air movement amplified sensible heat gain from the

environment, outweighing the evaporative cooling benefits. For instance, at 50 °C and 40% RH, increasing fan speed from 0.8 m/s to 3.0 m/s reduced the hyperthermia onset time further, demonstrating the detrimental effect of high fan speeds under these extreme conditions. Results showed that fans are beneficial up to 42 °C and 10–20% RH at light activity (1.2 PAR) but become trivial or detrimental at higher temperatures and humidity, particularly under elevated activity. Overall, our findings suggest that fans effectively reduce thermal strain in moderate heat and humidity but may prove less helpful—or even harmful—in extreme scenarios, especially at elevated activity levels and fan speeds. Hence, we recommend that future health guidelines clearly define thresholds for temperature, humidity, fan speed, and physical activity when advising fan use during heat waves.

Electric fan use can become detrimental and may rapidly increase core body temperature in extreme heat environments. Therefore, we investigated alternate sustainable water-based cooling strategies, including foot immersion, leg immersion, and self-dousing, using a further modification of the thermoregulatory model. The model systematically examined the effects of foot immersion and leg immersion at different water temperatures over a 30-minute immersion session with a 15-minute time break. For dousing, the area of water application was varied to optimize the cooling approach and minimize thermo-physiological strain in hot environments. Our results indicated that leg immersion provided a significant core temperature reduction, lowering it by approximately 0.3–0.7 °C compared to no cooling approach. Foot immersion and self-dousing offered moderate cooling, with the effectiveness of dousing dependent on the body surface area exposed. The maximum temperature reduction achieved by foot immersion compared to no cooling was around 0.3 °C. In hot and humid climates, self-dousing was less effective due to reduced evaporation rates. These findings emphasize that water immersion and self-dousing can serve as valuable cooling strategies. In particular, leg immersion emerges as a simple, sustainable, and highly promising method for mitigating severe heat stress.

LIST OF PUBLICATIONS

Journal Publications

- **Sushant Suresh Bhuvad**, Ruoyu You, and Qingyan Chen. Assessment of Sustainable and Accessible Water-Based Cooling Interventions During Heat Events Through Thermoregulation Modeling, Building and Environment, (2025): 113639. https://doi.org/10.1016/j.buildenv.2025.113639

- **Sushant Suresh Bhuvad**, Ruoyu You, and Qingyan Chen. Evaluation of physiological and thermal comfort effectiveness of ceiling fan and table fan during a heat wave, Energy and Buildings, 322 (2024): 114706. https://doi.org/10.1016/j.enbuild.2024.114706

- **Sushant Suresh Bhuvad,** Ruoyu You, and Qingyan Chen. Electric Fans Effectiveness and Thresholds for Healthy Young Adults During Prolonged Heatwaves: Updated Thermoregulation Modeling, Energy and Buildings, revised version under review.

Conferences Publications

- **Sushant Suresh Bhuvad**, Ruoyu You, and Qingyan Chen. Effect of Fan Air Movement on Occupants Physiological and Perceptual Response During Heat Wave: Experimental Approach. Lecture Notes in Civil Engineering. CLIMA 2025-Decarbonized, healthy, and energy-conscious buildings in future climates. Politecnico Di Milano, Italy.

ACKNOWLEDGEMENTS

First and foremost, I would like to sincerely thank my supervisors, Prof. Qingyan Chen and Prof. Ruoyu You, for their mentoring, support, and encouragement throughout my PhD journey. They not only provided valuable research guidance but also instilled in me the ability to approach problems analytically and explore issues at a deeper level. Their willingness to listen, offer thoughtful advice, and share both professional insights and personal experiences has greatly influenced my perspective on research. Their constructive feedback and the time they generously devoted to reviewing my work have been instrumental in enhancing the quality and depth of my research output.

I sincerely thank the Hong Kong Jockey Club Charities Trust for funding this project. Special thanks to Emily for her consistent help with administrative tasks. I am grateful to Prof. Ollie Jay, Prof. Morris, and the broader heat and health research community for shaping the direction of my PhD. I also thank Prof. Udayraj for his continual inspiration, and Warden Prof. Allen and Joyce Cheung for warmly welcoming me into the Wuhua Hall family.

I am thankful to my department for providing the facilities and resources essential to my research. A special thanks to my "research family," including Dr. Prateek Singh, Dr. Wang Feng, Shan, Hamdoon, Houzhi, Shikang, and Bingyang. They made my research journey more enjoyable. I also deeply appreciate my close friends Ikhtedar, Ankit, Amit, Shubham, Rajnish, Omkar, Siddharth, Qin, Dharma, and Lam for their encouragement and for sharing many moments of joy and stress.

Lastly, I am deeply grateful to my mother, father, sister, adorable niece, and my girlfriend. Their unconditional love, constant encouragement, and belief in me have been my greatest strength. I truly could not have come this far without them.

TABLE OF CONTENTS

LIST OF TABLES

LIST OF FIGURES

NOMENCLATURE

Abbreviations

BSA	Body Surface Area (m^2)
CFD	Computational Fluid Dynamics
CLDS	Cold sensor signal
DILAT	Vasodilation signal
LR	Lewis Ratio
PAR	Physical Activity Ratio
RH	Relative Humidity
SKINS	Sweating distribution coefficient
SL	Sweat loss as a percentage of body weight
SWEAT	Sweating signal
WRMS	Warm sensor signal

Variables

α, β, γ	Thresholds and sensitivity coefficients
$AG_{sweat(i)}$	Aging factor for sweating
B	Segment-specific constant in hc-v relationship
$Cap_{(j(i))}$	Specific heat capacity of tissue layer (J/kg·K)
$c_{p,water}$	Specific heat of water ($J \cdot kg^{-1} \cdot K^{-1}$)
C	Convective heat transfer (W)

$D_{\{j\text{-}j'\}(i)}$	Conductive heat loss between layers (W)
$D_{water–air}$	Diffusion coefficient ($m^2 \cdot s^{-1}$)
$E_{(j(i))}$	Evaporative heat loss (W)
E_{sw}	Sweating evaporative heat-loss (W)
E_{max}	Maximum evaporative heat-loss (W)
$E_{water(i)}$	Evaporative heat loss due to external water (W)
$Err_{(cr[0])}$	Error signal from head core (°C)
$Err_{(sk(i))}$	Error signal from skin sensor (°C)
f_{cl}	Clothing area factor
h_c	Convective coefficient ($W \cdot m^{-2} \cdot K^{-1}$)
h_{et}	Total evaporative coefficient of heat transfer ($W \cdot m^{-2} \cdot K^{-1}$)
h_m	Mass transfer coefficient ($m \cdot s^{-1}$)
h_t	Total sensible coefficient of heat transfer ($W \cdot m^{-2} \cdot K^{-1}$)
i_{cl}	Clothing vapor permeation efficiency
I_{cl}	Clothing vapor resistance
L_v	Latent heat of vaporization ($J \cdot kg^{-1}$)
M_{base}, M_{work}	Basal metabolism, external work heat generation (W)
M_{shiv}, M_{nst}	Shivering and non-shivering thermogenesis (W)
Pa	Ambient water vapor pressure (Pa)
P_{sks}	Saturated vapor pressure at skin (Pa)
$Q_{(j(i))}$	Metabolic heat production (W)
$R_{(j(i))}$	Radiative heat transfer (W)

$RES_{(j(i))}$	Heat transfer by respiration (W)
Sh	Sherwood number
SKINS(i)	Coefficient of sweating distribution
t	Time (s)
$T_{[0]}$	Current core head temperature (°C)
$T_{o(i)}$	Operative or ambient temperature (°C)
$T_{(j(i))}$	Temperature of body tissue layer (°C)
$T_{setpt[0]}$	Set-point core head temperature (°C)
$T_{sk(i)}$	Local skin temperature (°C)
v	Air velocity (m/s)
$w_{(i)}$	Total skin wettedness
$w_{sweat(i)}$	Wettedness due to sweat
$w_{water(i)}$	Wettedness due to water
ΔT	Temperature difference (°C)
μair	Air viscosity (Pa·s)
ρair	Air density ($kg \cdot m^{-3}$)
ω	Skin wettedness (dimensionless)

Subscripts

i	Body segment
j	Tissue layer
j′	Adjacent tissue layer

(0)	Head core
cl	Clothing
cr	Core layer
et	Evaporative transfer
max	Maximum or limiting value
sk	Skin layer
sw	Sweating-related
sweat	Related to sweat evaporation
water	Related to applied water

CHAPTER 1. INTRODUCTION

1.1 Background and significance

According to the World Meteorological Organization (WMO) and World Health Organization (WHO) (WMO & WHO, 2015), a heat wave is unusually hot and dry or hot and humid weather for a period of at least 2-3 days that usually has a negative noticeable impact on human and natural systems. The definition of heat waves is not universally standardized, as the impact of heat events depends on various factors. This intense heat event also places an additional burden on different sectors, such as the energy and water sectors. For example, during the 2015 heat wave in Pakistan (Masood et al., 2015), a sudden increment in peak electricity demand caused a blackout, which eventually crippled the water supply system that increased dehydration and heatstroke cases. These heat events are mainly associated with acute pathophysiological disorders such as heatstroke, adverse cardiovascular events, kidney injury, etc. (see Figure 1.1) (Ballester et al., 2023; Hobbhahn et al., 2019; Watts et al., 2019). Furthermore, Mora et al. (Mora et al., 2017) review study shows at least 27 pathways that link heat waves to serious human health issues. To ensure consistency in this study, typical, moderate, and extreme heatwave conditions are defined operationally based on climatological evidence and experimental feasibility. Typical heatwave conditions were defined as approximately 41 °C air temperature with 35% relative humidity (RH), representing observed pre-monsoon conditions in Indian cities such as Ahmedabad and Indore. Moderate conditions correspond to 35–40 °C with 40–55% RH, where fan use remains beneficial, while extreme conditions were defined as ≥45–46 °C and/or RH ≥60%, under which evaporative cooling becomes limited and heat storage may increase. These operational definitions provide a consistent framework for interpreting the experimental and modeling results across diverse climatic contexts (WHO,

2018; WMO, 2019; IPCC, 2021; Sherwood & Huber, 2010). The impact of hot weather is a serious concern, especially for the vulnerable sectors that include the elderly, low-income, homeless, pre-existing health conditions and socially isolated populations (Vaidyanathan et al., 2019). Further, especially in economically disadvantaged countries, young adults are also increasingly exposed to extreme heat due to lack of access to cooling infrastructure and high metabolic workloads in labor-intensive settings.

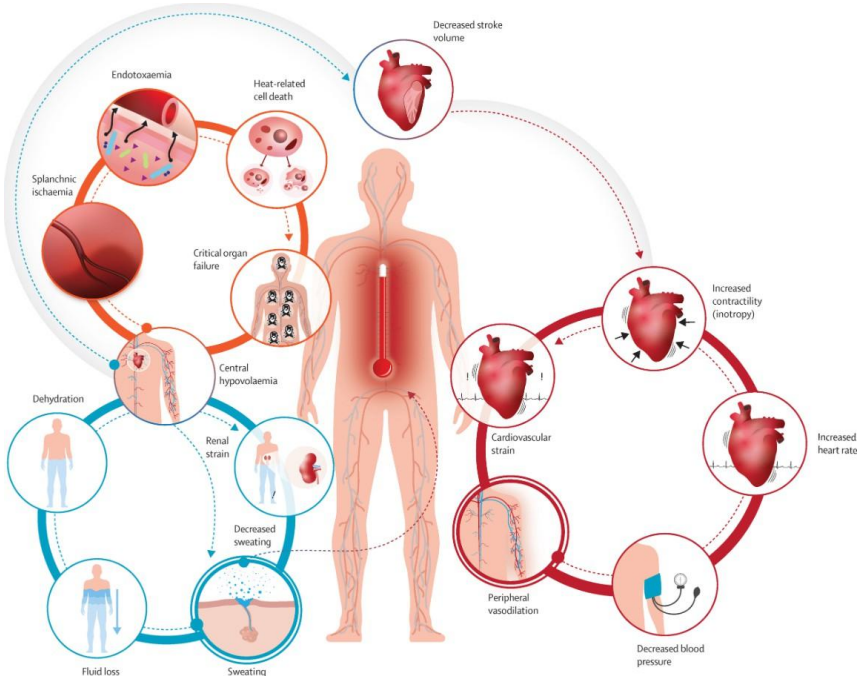

Figure 1.1. Overview of the physiological pathways associated with human heat strain. (Ebi et al., 2021)

Heat events represent a leading cause of weather-related deaths in economically developed nations. Countries with adequate death reporting systems show a significant increase in mortality due to heatwaves (see Figure 1.2) (World Disasters Report, 2020; Wang et al., 2023; Schinasi et al., 2023; Kanti et al., 2022). The 2003 heatwave in Europe and the 2010 heatwave in Russia (Robine et al., 2008; Staff Writers, 2011) killed more than 70,000 and 56,000 people, respectively. Similar, severe impact, with many deaths reported in North America and California during the heat events. According to Mora et al. (Mora et al., 2017), elevated heat-

related mortality was observed in 164 cities across 36 countries between 1980 and 2014. During the summer of 2022, an estimated 61,672 excess deaths occurred in Europe (Ballester et al., 2023). As per Intergovernmental Panel on Climate Change (IPCC-2021) and Mora et al. (Mora et al., 2017) study, heat wave frequency, intensity, and duration will likely increase in the future, and the adverse impact of heat waves on health will likely worsen globally (see Figure 1.3). Hence, human health is a measured concern during extreme heat waves.

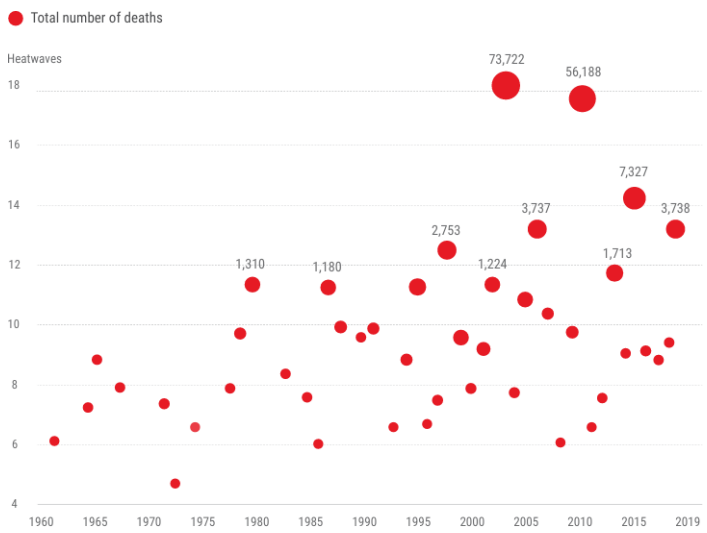

Figure 1.2. Number of heatwave-related deaths from 1960 to 2019. (World Disasters Report, 2020).

The simplest solution to prevent the adverse health impact of heat waves is to increase the use of air conditioning systems. Nonetheless, as per IEA 2016 (IEA, 2018) estimation, 2.8 billion people resided in the hottest parts of the world, and only 8% of them had air conditioners. Further, except in the U.S. and Japan, most households in developed countries also don't have air conditioning systems (Sherman, Lin, & McElroy, 2022). For example, in the U.K., only 5 % of households are equipped with air conditioning systems (AECOM, Delta-EE, & University of Exeter, 2021). In reality, most vulnerable populations don't have access to air conditioning

systems or even electricity. In addition, the increased use of air conditioning against heat stress is a vicious cycle as more air conditioning practices increase greenhouse gas emissions, contributing to the global warming effect in the long term, which will further increase the intensity and frequency of extreme heat events. Therefore, to keep individuals cool during extreme heat events, the identification of sustainable and accessible cooling strategies should be the top priority. However, developing such strategies requires a detailed understanding of human thermoregulation.

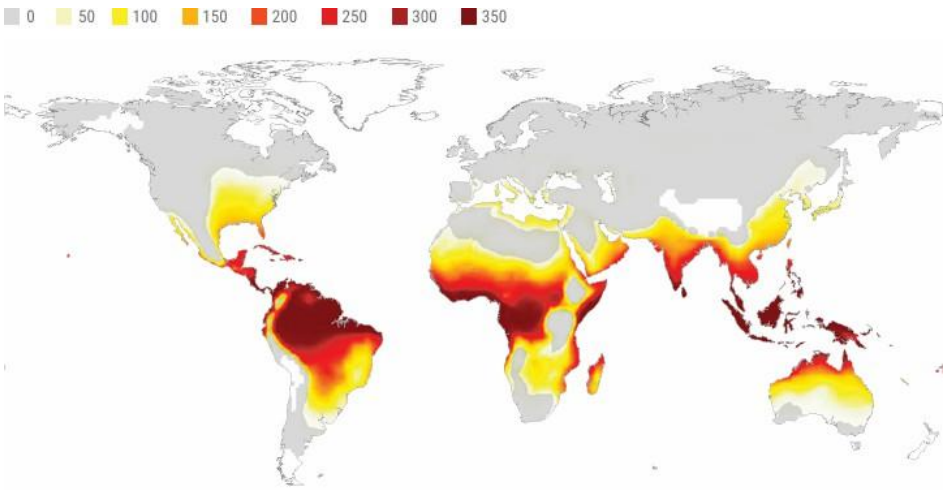

Figure 1.3. Projected annual number of days exceeding potentially deadly heat levels by 2100. (Mora et al., 2017)

The complex mechanisms of human thermoregulation enable the body to maintain its core temperature within a narrow and acceptable range, even under conditions of extreme heat or cold. This control system carefully modifies the rates of heat generation and dissipation to try maintain constant interior temperature, which is an essential requirement for cellular activity and protection from harm (Parsons, 2014). The human body's careful balance between internal heat generation and dissipation allows it to maintain a core-body temperature of about 37°C throughout times of rest (Havenith et al., 1999). However, exposure to harsh environmental factors, such heat waves, can cause the thermoregulatory system to reach its limits (Kingma et

al., 2014). In intensely hot settings, adequate heat dissipation to the environment allows for the maintenance of body temperature within the range of 37±0.5°C (from 36.5°C to 37.5°C), while insufficient heat loss results in hyperthermia. Therefore, researchers used both experimental and mathematical methods to understand human thermoregulation during extreme heat waves. These methods include human trials, thermal manikin trials, and numerical modeling, which are further used to evaluate effective strategies to mitigate human thermal stress.

The experimental method with human participants provides invaluable real-world insights to examine the heat strain and different sustainable and accessible cooling strategies during heat waves. These trials involve participants in designated tasks or activities within a controlled environmental climate condition, which is maintained using a climate chamber. During these trials, participants' physiological parameters were monitored, including skin temperature, core body temperature, and sweat rate etc. Further, the perceptual responses, such as thermal sensation thermal comfort, and skin wetness sensation of the participants are evaluated using a paper questionnaire. This method gives more realistic data to evaluate the heat strain and effectiveness of cooling strategies, and it empowers designers to make informed decisions regarding the strategy against heat waves. Nonetheless, human trials need a substantial sample size to ensure statistical robustness. The perceptual response may be affected and depend upon the participant's experience of such an environment. Also, experimental approach is costly, and the participants' response may be affected due to individual variability among participants. Moreover, the impact of long-duration extreme heat wave on the human body cannot be studied using an experimental approach due to ethical constrain.

Thermoregulation models serve as mathematical representations of the complex thermo-physiological process occurring within the body under different environmental scenarios (Schellen et al., 2013). These models evaluate the physiological parameters under both steady and transient conditions by evaluating body heat transfer with the environment (Mur akami,

Kato, & Zeng, 2000). These models play a crucial role in devising appropriate techniques for individuals facing extreme scenarios across diverse fields. Thermoregulation model consists of both passive and active elements, capturing the complex interactions between internal body heat transfer and its exchange with the external environment. The passive component focuses on simulating internal heat transfer and external exchange through mechanisms like conduction, convection, evaporation, and respiration etc. Meanwhile, the active component represents the body's regulatory responses, including processes such as vasodilation, vasoconstriction, sweating, and shivering, which help maintain thermal balance (Cheng, Niu, & Gao, 2012). Crucially, the passive system is under the control of the active system, ensuring temperature regulation in response to varying environmental conditions (Ivanov, 2006). This model offers a rapid, cost-effective, and efficacious means of predicting the performance of different cooling strategies. Nonetheless, existing thermoregulation models cannot accurately predict the human response in hot environments. Therefore, further modifications are required to enhance the predictive accuracy of the model in estimating skin temperature, core temperature, and internal heat storage. In addition, a comprehensive understanding of human thermoregulation in the context of climate change and adaptation to hot environments, such as heat waves, can inform public health policies and support the development of effective, sustainable, and accessible interventions.

1.2 Thesis Outline

Chapter 1 introduces the escalating global challenge of heatwaves driven by human-induced climate change, emphasizing the urgent need to protect vulnerable populations from severe heat stress. It highlights the limitations and environmental consequences associated with air conditioning, demonstrating the critical importance of identifying sustainable, affordable, and accessible cooling strategies to keep individuals safe during extreme heat events. This chapter

clearly defines the primary objectives of the thesis, establishes the research scope, and outlines the structure and content of the subsequent chapters.

Chapter 2 reviews existing literature relevant to sustainable and accessible cooling strategies for extreme heat events. This includes an in-depth examination of cooling interventions such as electric fans, foot immersion, leg immersion, dousing, and their physiological and perceptual impacts on humans. Additionally, the chapter critically evaluates previous thermoregulation models, emphasizing their strengths, limitations, and suitability for evaluating cooling methods. The chapter concludes by identifying significant knowledge gaps in the effectiveness and practical thresholds for these cooling strategies under different environmental and physiological conditions.

Chapter 3 investigates the physiological and thermal comfort impacts of ceiling fans and table fans under simulated heatwave conditions through controlled human trials. The methodology describes participant selection, experimental procedures, physiological measurements, and perceptual assessments. The chapter discusses the experimental results, focusing on how each fan type influences physiological strain and perceived thermal comfort. It concludes by comparing fan effectiveness with no fan scenario, highlighting the performance of ceiling and table fans, and identifying critical implications for public health recommendations.

Chapter 4 presents a comprehensive thermoregulation modeling study evaluating the performance and thresholds of electric fan usage under prolonged extreme heat exposure. The chapter first details the development and validation of the updated thermoregulatory model, including modifications related to hydration, sweating response, and vasodilation. Subsequent sections systematically explore the impact of varying fan speeds, environmental conditions, and physical activity levels on hyperthermia onset. Results from simulations identify specific

conditions under which fans provide effective cooling and scenarios where their use becomes detrimental, thus establishing clear thresholds for public health guidance.

Chapter 5 examines alternative, sustainable cooling interventions—foot immersion, leg immersion, and dousing—using an modified thermoregulatory modeling approach. The methodology outlines model modifications to incorporate water-based cooling, specifies environmental scenarios representative of real-world heatwaves in Indian cities, and describes various conditions tested (e.g., water temperature, immersion durations, dousing area). The chapter presents and analyzes results indicating the effectiveness of each method. The implications of these findings are thoroughly discussed, emphasizing the applicability of these strategies in settings where electrical resources are limited or unavailable.

Finally, Chapter 6 summarizes the main conclusions of the thesis, synthesizing insights from the experimental and modeling studies. It outlines the contributions to existing knowledge, emphasizing the practical implications for public health policy and heatwave preparedness strategies. The chapter also provides clear recommendations for future research directions, specifically advocating further investigations involving diverse demographic groups (e.g., elderly, pregnant women, and individuals with chronic conditions) to enhance the generalizability and robustness of the proposed cooling guidelines

CHAPTER 2. LITERATURE REVIEW

The intensifying frequency, duration, and severity of global heatwaves have posed unprecedented challenges to human health. These heat events are exacerbated by anthropogenic climate change and are predicted to become more severe in coming decades. While air conditioning remains the most effective cooling strategy, its high energy demand, limited accessibility in vulnerable regions, and contribution to greenhouse gas emissions necessitate alternative, sustainable, and accessible cooling strategies. This chapter systematically reviews the literature on such strategies, with an emphasis on electric fans and water-based methods including foot immersion, leg immersion, and self-dousing. In addition, we explore thermoregulation models that simulate physiological responses under extreme heat to complement experimental findings and bridge gaps in knowledge.

2.1 Electric Fans as Sustainable and Accessible Cooling Strategies

Cooling strategies such as electric fans, evaporative coolers, ice towels, cold water ingestion, and self-dousing can be used in hot environments. Among these approaches, ice towels, and cold water ingestion can effectively reduce the overall body temperature by increasing the evaporative and conduction losses from the body (Hailes, Cuddy, Cochrane, & Ruby, 2016; Schranner et al., 2017; Morris et al., 2019). However, these methods are laborious, time intensive, and require a sustained supply of clean water/ice (Jay et al., 2021). Meanwhile, evaporative coolers can be beneficial as they reduce the air temperature by forcing air through wet membranes (Jay et al., 2021). However, this method is less effective in hot and humid climates, entails a high capital cost, and requires a water supply (Jay et al., 2021). In contrast to the above cooling methods, electric fans are the most common in households and offices (Selkirk, McLellan, & Wong, 2004). An IEA report (IEA, 2018) estimated that 55% of all

households globally have at least one fan. Fans increase air movement, enhancing the convective and evaporative heat transfer between the occupants and the ambient environment. Overall, fans are an energy-saving, cost-effective and readily available cooling method, and may be an effective strategy for cooling during heat waves.

Numerous studies have investigated the impact of electric fans on occupants' overall thermal comfort in warm environments (Scheatzle, Wu, & Yellott, 1989; Zhai et al., 2013; Arens, Turner, Zhang, & Paliaga, 2009; De Dear, 1998). For example, Scheatzle et al. (Scheatzle, Wu, & Yellott, 1989) examined the influence of ceiling fans on the thermal comfort of occupants under a temperature range of 25°C to 35 °C and humidity of 24% to 73%. They concluded that ceiling fans improve thermal comfort compared to still air (no fan) when the humidity is below 50%. Zhai et al. (Zhai et al., 2013) studied a personally controlled table fan under environmental temperatures of 26°C, 28°C and 30°C with relative humidity levels of 60% and 80%. They found that up to 30 °C and 60% R.H., the air movement did not cause discomfort. Furthermore, studies by Zhai et al. (Zhai et al., 2013) and Arens et al. (Arens, Turner, Zhang, & Paliaga, 2009) concluded that the air flow patterns in both table-fan (horizontal air movement) and ceiling-fan (vertical air movement) cases significantly affected subjects' overall thermal comfort. These studies (Scheatzle, Wu, & Yellott, 1989; Zhai et al., 2013; Arens, Turner, Zhang, & Paliaga, 2009; De Dear, 1998) have shown that fans are effective at increasing the thermal satisfaction of occupants in a warm environment. In contrast, many health guidelines discourage fan use during heat events, such as guidelines published by WMO (WMO, 2015) , WHO (WHO, 2018), Ready.gov (a national public service campaign of the U.S. Government) (Ready.gov, 2020), and the Centers for Disease Control and Prevention (CDC) (CDC, 2012). For instance, WHO (WHO, 2018) states that if the dry bulb temperature (t_{db}) is higher than 35 °C, fans can make an individual hotter, and "fans should be discouraged unless they are bringing in significantly cooler air." A possible reason for such a conclusion is

the risk of accelerating the sensible heat gain. This heat gain can increase the body's core temperature, one of the main reasons for heat-related illness. However, the above guidelines do not consider fans' important evaporative cooling effect, which can assist in delaying the increment in body temperature. In addition, as we know, the air movement produced by table fans and ceiling fans influences the perceptual response of occupants. Hence, a detailed investigation is needed before accepting or discouraging table and ceiling fan use during heat events.

Previous studies have used mathematical approaches to understand the effectiveness of fans under extreme heat exposure (Jay et al., 2015; Morris et al., 2021; Tartarini et al., 2022). For example, Jay et al. (Jay et al., 2015) and Morrios et al. (Morris et al., 2021) developed a simplified heat balance model to understand the use of table fans under various environmental conditions. They concluded that fans at an air speed of 4.5 m/s provide slight advantages compared to fan-off conditions, at temperatures up to 51.1 °C for young adults and 48.1 °C for the elderly and at R.H. of 10 %. Tartarini et al. (Tartarini et al., 2022) used the energy balance model to calculate humidity-dependent temperature thresholds for fan use. They found that fans are detrimental when the dry bulb temperature (t_{db}) exceeds 43.5 °C and air speed exceeds 0.8 m/s. However, the above studies did not describe the detail thermoregulation of the human body during heat events. Therefore, the applicability of these types of models needs to be validated with more experimental evidence (Tartarini et al., 2022). The accuracy and reliability of the present model must improve before it can be used to understand fan effects during heat wave conditions.

Experimental methods are more reliable than mathematical approaches for studying the effectiveness of fans during heat events. Several laboratory studies have investigated the benefits of fans during heat events by maintaining a constant dry air temperature and varying the humidity (Ravanelli et al., 2015; Gagnon et al., 2016). For instance, Ravanelli et al.

(Ravanelli et al., 2015) exposed eight healthy male volunteers to no-fan and table-fan conditions at 36 °C and 42 °C while varying the R.H. every 7.5 minutes from 25% to 95% and from 20% to 70%, respectively. They found that the table fan helped to prevent an elevation in heart rate and the core temperature of the body compared to fan-off conditions up to 50% R.H. for t_{db} of 42 °C and 80 % R.H. for t_{db} of 36 °C. Furthermore, Gagnon et al. (Gagnon et al., 2016) examined the physiological response of young and aged participants under table-fan and no-fan conditions at a temperature of 42 °C. During the trials, the R.H. was initially kept constant at 30% for around 30 minutes; it was then increased by 2% every 5 minutes until it reached 70%. They observed that fan use was detrimental in the case of elderly people, whereas the changes in core temperature and heart rate in young participants were delayed with table-fan use compared to the no-fan condition. In the above laboratory studies, participants were exposed to varying humidity conditions in the course of a single trial. However, it is always recommended that the air temperature and humidity remain constant during physiological parameter studies (Lei, Lan, & Wang, 2023). Morris et al. (Morris et al., 2019) monitored the physiological response of 12 healthy male participants for 2 hours under fixed environmental conditions to further understand the effect of a table fan. They studied very hot and dry (47 °C; 10% RH) and hot and humid (40 °C; 50% RH) conditions and concluded that fan use is not advisable in the very hot and dry conditions, as the greater air movement produced by the fan only increases the convective heat gain from the surroundings without improving the sweat evaporative heat loss. Moreover, the study only considered male participants. It is always better to consider both male and female participants, as thermoregulatory behavior differs between sexes. Meanwhile, Cramer et al. (Cramer et al., 2020) studied the physiological response of elderly adults under wetted clothing conditions with and without a table fan in hot and moderately humid conditions (42 °C; 50% RH). They concluded that water-soaked t-shirts with fan operation were neither harmful nor beneficial compared to wetted t-shirts without fan

condition but wetted-t-shirts in combination with fan operation augmented sweat losses. Although all the above experimental studies provided great insight into a fan's effectiveness during heat waves. However, the number of experimental studies in the literature related to the effects of table fans and ceiling fans during heat exposure is limited. Furthermore, previous studies mainly focused on physiological parameters; the perceptual responses, such as thermal and skin wetness sensations, were not examined. Hence, further efforts should be made to evaluate the effectiveness of table- and ceiling-fan air movement on occupants' physiological and perceptual responses during extreme heat events.

2.2 Impact of Water-Based Cooling Strategies on Occupants

Human-induced climate change has led to longer, and more intense heatwaves worldwide (Alexander et al., 2007; Saman et al., 2013). In 2024, record-breaking temperatures were reported globally as a severe heatwave affected the Americas, Africa, Europe, and Asia (Dickie, 2024). These extreme heatwaves pose a serious threat to human health, often leading to exhaustion, heatstroke, and death. The 2003-European heatwave (Robine et al., 2008), which caused over 70,000 preventable deaths, highlights the deadly impact of such events. Air conditioning is the most effective cooling solution during heatwaves. However, it is energy-intensive and not accessible to vulnerable populations, such as low-income households, increasing the risk of heat-related deaths and worsening social inequalities (Jay et al., 2021; IEA, 2018). For example, only 8% of households in India have air conditioning, leaving a large portion of the population exposed to extreme heat (Santamouris et al., 2015). Rising air conditioner usage has also outpaced improvements in electrical infrastructure (Jay et al., 2021). This has led to power outages, which further increase health risks during heatwaves. During the 2015 heatwave in Pakistan (Masood, Majid, Sohail, Zia, & Raza, 2015), a surge in electricity demand caused a blackout that eventually increasing cases of heat related medical

events. Therefore, there is an urgent need to identify sustainable, affordable, and widely accessible cooling strategies to protect individuals from extreme heat events.

Various sustainable and accessible cooling methods, such as electric fans, evaporative coolers, cold water ingestion, foot immersion, leg immersion, and dousing, can help reduce the effects of heatwaves. Among these, electric fans are effective only up to a certain temperature beyond that, fan use can become harmful by rapidly increasing core body temperature (Jay et al., 2021; Bhuvad, You, & Chen, 2024). Additionally, both electric fans and evaporative coolers require continuous power supply. However, many countries don't have stable power supply. As an alternative, cold water ingestion, foot immersion, leg immersion, and dousing, which do not rely on electricity, are practical options especially during power outages if there is sufficient water available (Jay et al., 2021). While drinking water is essential for maintaining hydration during heat exposure (Montain, Sawka, Latzka, & Valeri, 1998; Semenza et al., 1996), recent studies suggest that cold water ingestion is not effective in reducing heat strain. The heat loss to the ingested cold fluid is offset by a decrease in evaporative heat loss caused by a lower sweat rate (Morris, Bain, Cramer, & Jay, 2014; Morris, Coombs, & Jay, 2016). In contrast, foot immersion and leg immersion can be efficient strategy for reducing core temperature and lowering thermal strain under heat stress primarily due to the significantly higher thermal conductivity of water, which is nearly 25 times greater than that of air (DeGroot, Gallimore, Thompson, & Kenefick, 2013). Additionally, when the body experiences elevated core temperatures, cutaneous blood flow in the extremities such as foot, and leg increases substantially, further facilitating heat transfer from the body to the surrounding water (DeGroot, Gallimore, Thompson, & Kenefick, 2013). Moreover, submerging the lower limbs in cool water enables greater heat dissipation due to larger surface-to-volume ratio of the limbs (Grahn, Dillon, & Heller, 2009). In addition, this method is also practical, as it allows the hands to remain free. Further, dousing where water is applied directly to the skin through spraying or

sponging the water to enhance evaporative cooling can be a possible cooling strategy against heat stress (Morris & Jay, 2016). Moreover, similar to water immersion, the application of water to the skin surface reduces skin temperature, which helps widen the core-to-skin temperature gradient, thereby enhancing heat transfer and promoting body cooling. Therefore, further understanding of foot immersion, leg immersion, and dousing needed to find the best possible and sustainable cooling interventions against heat waves.

Some researchers through experimental approach examined the heat loss caused by cooling the immersion and dousing (Morris & Jay, 2016; Livingstone, Nolan, & Keefe, 1995) (House, 1998; Hagobian, Jacobs, Kiratli, & Friedlander, 2004; Morris, Gruss, Lempert, et al., 2019; Cramer, Huang, Moralez, et al., 2020; Song, Wang, & Zhang, 2019; Anderson, Bellenger, Chaseling, & Chalmers, 2024; McDermott, Casa, O'Connor, et al., 2009). For instance, Livingstone et al. (Livingstone, Nolan, & Keefe, 1995) conducted an experimental study to assess the heat removal efficiency of leg immersion under hot environmental conditions. The study included six active young male military participants (25.2 ± 2.1 years; 175.0 ± 7.7 cm; 72.3 ± 10.9 kg) who were exposed to a controlled climate chamber maintained at 35 °C and 50% relative humidity. Each subject remained seated for 120 minutes, during which both legs were immersed to a depth of 25 cm in water for 20 minutes. The experiment was repeated across five separate trials using water at 10 °C, 15 °C, 20 °C, 25 °C, and 30 °C. The results demonstrated that at 10 °C, the heat loss was approximately 151 ± 15 W, while at 30 °C, it dropped to 55 ± 5 W. They concluded that immersion in colder water can significantly enhance heat dissipation from the body, and reduce skin temperature and core temperature. These findings indicate that immersion, particularly in cooler water, could be an effective countermeasure to delay the onset of thermal strain and potentially extend operational endurance in heat-stressed environments. Similarly, House et al. (House, 1998) evaluated the cooling potential of foot immersion following exercise-induced heat strain. In this study,

participants underwent a 20-minute foot immersion in 10 °C water post-exercise. The findings indicated a substantial decline in core temperature, with an average reduction of approximately 1 °C during the immersion period. This result highlights the efficiency of cold-water foot immersion in rapidly lowering core body temperature, making it a practical cooling intervention following physical activity in hot environments. Hagobian et al. (Hagobian, Jacobs, Kiratli, & Friedlander, 2004) investigated the effects of foot immersion as a cooling intervention during exercise in the heat. Six subjects performed arm cranking at 66% of their maximum capacity in an environmental chamber maintained at 31.8 °C and 26% relative humidity for 45 minutes. The results demonstrated that heat extraction via the feet effectively reduced tympanic temperature during exertional heat stress. These findings suggest that foot immersion may serve as a practical and targeted strategy to regulate core temperature, particularly in physically active individuals exposed to hot environments. Furthermore, Morris et al. (Morris, Gruss, Lempert, et al., 2019) examined the physiological effects of a dousing intervention during prolonged exposure to extreme heat. In their study, participants were instructed to apply 22 °C water to the face, chest, arms, back, and legs using a sponge whenever they began to feel warm. Each trial lasted 120 minutes and was performed under both hot-humid (40 °C, 50% RH) and very hot-dry (47 °C, 10% RH) conditions. The dousing strategy significantly reduced heart rate, sweat production, and thermal discomfort across both environments. These results highlight the potential of dousing to alleviate thermal strain during extreme heat exposure. Further, Song et al. (Song, Wang, & Zhang, 2019) conducted a 90-minute trial with ten young male participants exposed to 43 °C air temperature and 57 % relative humidity, where participants were intermittently doused with tap water every 30 minutes. Their results showed that this simple intervention significantly reduced both core and mean skin temperatures. These findings demonstrate that foot immersion, leg immersion and dousing can effectively mitigate thermal strain under heatwave conditions and may serve as a

practical and ecologically valid cooling strategy. Such methods are especially useful for seated individuals in vulnerable groups, contributing to improved thermal safety. While experimental studies have provided valuable insights into the effectiveness of water immersion and dousing strategies during heatwaves, they are generally limited to short durations and controlled environments due to participants' safety, and ethical considerations. Nonetheless, heatwaves are more dynamic, and climate change has further intensified the frequency and severity of heatwaves, making real-world scenarios more extreme. For instance, the 2021 Canadian heatwave recorded indoor temperatures above 35 °C for more than 8 hours, while in parts of Asia, temperatures of 46–47 °C with low humidity have persisted for 6–8 hours (Vaughan, 2021; Wang, Deng, Lei, Wang, & Wang, 2023). Therefore, given such prolonged exposure conditions, human thermoregulatory modeling offers a practical and ethical alternative to human testing.

2.3 Thermoregulation model

Another approach to assess the effects of extreme heat on the body is through thermoregulation modeling. This method first utilizes a heat transfer model to calculate key physiological parameters, including skin temperature, core temperature etc. These physiological outputs are then used to predict thermal sensation or an equivalent comfort temperature. When modeling human physiological responses, the heat transfer process can be further detailed by incorporating anatomical features, leading to the classification of models into single-segment and multi-segment categories. Figure 2.1 illustrates the various types of thermoregulation and thermal comfort models.

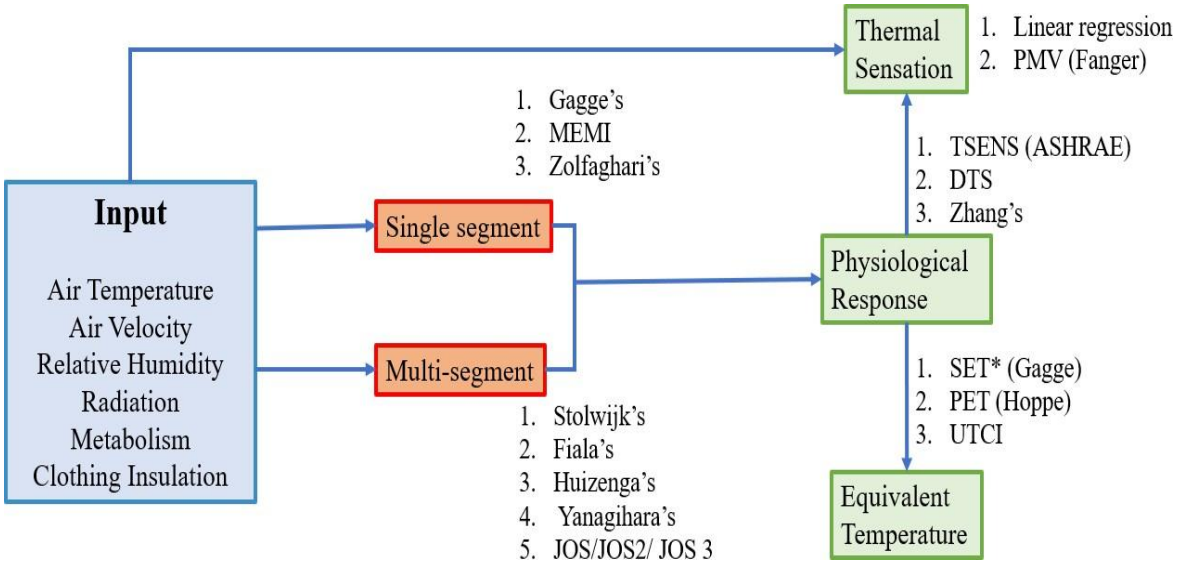

Figure 2.1. Classification of singel and multi-segment thermoregulation models and comfort models.

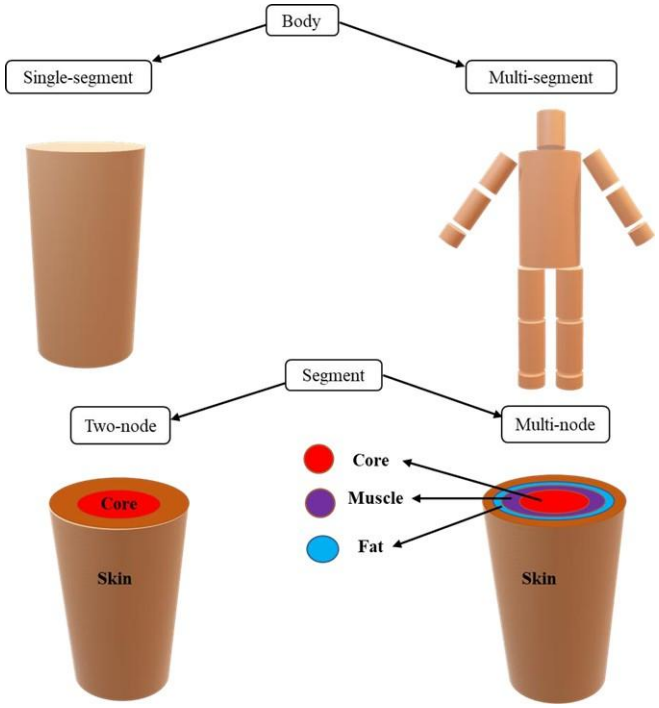

Figure 2.2. A schematic illustration of the segmentation and nodal structure applied in thermoregulation models.

In the single-segment modeling approach (see Figure 2.2), the human body is considered as a uniform system, with its thermal and physiological properties averaged across the entire body. This simplification allows for the formulation of an overall heat balance equation between the body and a uniformly distributed ambient environment. Several classical models fall under this category, including Gagge's model (Gagge, 1971), the Munich-Energy-Balance Model for Individuals (MEMI) developed by Höppe in 1993 (Höppe, 1993), and the model introduced by Zolfaghari and Maerefat in 2010 (Zolfaghari & Maerefat, 2010). Gagge's model, in particular, conceptualizes the human body using two thermal compartments: the core and the skin. Heat generated by metabolic processes in the core is transferred to the skin layer via conductive mechanisms and blood perfusion. From the skin, this heat is subsequently dissipated to the surrounding environment primarily via convection, evaporation, radiation, and other thermoregulatory mechanisms. This model establishes a simplified yet effective representation of thermal interactions between internal body processes and external environmental conditions, facilitating the calculation of steady-state and transient heat exchanges (see Figure 2.3).

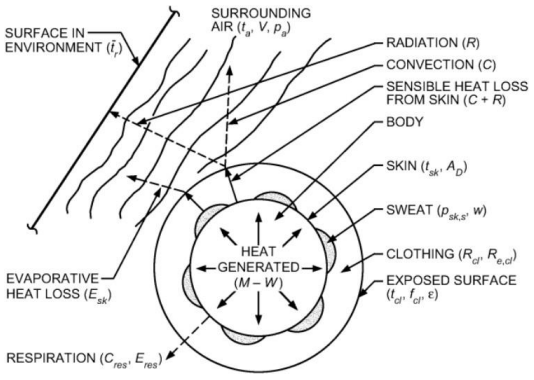

Figure 2.3. Two-node Gagge thermoregulation model. (Gagge, 1971)

$$M + \Delta\mathrm{M} - \mathrm{W} = Q_c + E_{res} + (\mathrm{K} + m_{bl}c_{bl})(T_{cr} - T_{sk}) + m_{cr}c_{cr}\frac{dT_{cr}}{dt} \qquad (2.1)$$

$$(\mathrm{K} + m_{bl}c_{bl})(T_{cr} - T_{sk}) = E_{res} + E_{diff} + \mathrm{C} + \mathrm{R} + m_{sk}c_{sk}\frac{dT_{sk}}{dt} \qquad (2.2)$$

In the provided equation set, where ΔM represents additional metabolism resulting from shivering (W/m^2). Q_c and E_{res} denote convective heat transfer and evaporative heat loss from respiration (W/m^2), respectively. K denotes the skin and core compartments conductive coefficient ($W/m^2/K$), m_{bl} represents blood-mass flow rate per unit body-surface area (in $kg/m^2/s$), c_{bl} signifies the specific-heat of blood (J/kg/K). Further, the core and skin temperatures are denoted by T_{cr} and T_{sk} (^oC), respectively. The masses of the core and skin compartments are represented by m_{cr} and m_{sk} (kg), and their corresponding specific heat capacities are c_{cr} and c_{sk} (J/kg/K). The variable t indicates time in seconds. Additionally, E_{rsw} accounts for the evaporative loss due to sweating (W/m^2), and E_{dif} represents the evaporative loss through skin diffusion (W/m^2). By solving Equations (2.1) and (2.2), the time-dependent variations of core temperature (T_{cr}) and skin temperature (T_{sk}) can be determined. Furthermore, skin wetness levels can be evaluated based on the calculated values of E_{rsw} and E_{dif}.

In addition to passive heat transfer between the skin and core compartments, as well as between the skin compartment and the environment, Gagge's two-node model incorporates various thermoregulatory parameters such as sweating, vasoconstriction, and dilation etc. This model facilitates the computation of transient changes in body temperature. Further, the thermoregulation model is improved using inclusion of physiological processes in the single-segment model. It also permits temporary analysis. Nevertheless, by portraying the human body as if it were made up of just two or three concentric nodes, the model greatly simplifies the process of heat transfer. Human physiological response calculations become inaccurate as a result of this reduction. Moreover, the model is inappropriate for use in non-uniform thermal settings because it is single-segment.

To address the limitations associated with above models and to facilitate the assessment of thermoregulation in spatially non-uniform thermal environments, it becomes critical to

accurately quantify heat transfer within individual body segments. This necessitates a more detailed anatomical and physiological representation of the human body. The foundation for this approach was laid by Stolwijk (1971), who introduced the first multi-segment thermoregulation model. Building upon this framework, subsequent researchers such as Fiala et al. (2001), Huizenga et al. (2001), and Ferreira and Yanagihara (2009) introduced significant refinements to improve the physiological accuracy and predictive capabilities of these models. These multi-segment models are fundamentally established on the bioheat transfer formulation proposed by Pennes (1948), which governs the heat transport within biological tissues (refer to Equation 2.3).

$$\rho C \frac{\partial T}{\partial T} = \nabla.(k\nabla T) + q_m + \omega_{bl}\rho_{bl}c_{bl}(T_{bla} - \mathrm{T}) \tag{2.3}$$

Stolwijk's groundbreaking contribution introduced the first multi-segment thermoregulation model, in which the human body was represented as a composition of six cylindrical segments corresponding to the head, torso, arms, hands, legs, and feet. Each segment was internally structured with four concentric tissue layers corresponding to anatomical regions: core, muscle, fat, and skin. Collectively, this multilayered configuration produced 24 thermal nodes, and the inclusion of an additional node to represent circulating blood brought the total to 25 nodes, as demonstrated in Figure 2.4. In addition to proposing the body construction, Stolwijk introduced equations governing the control of thermoregulation processes.

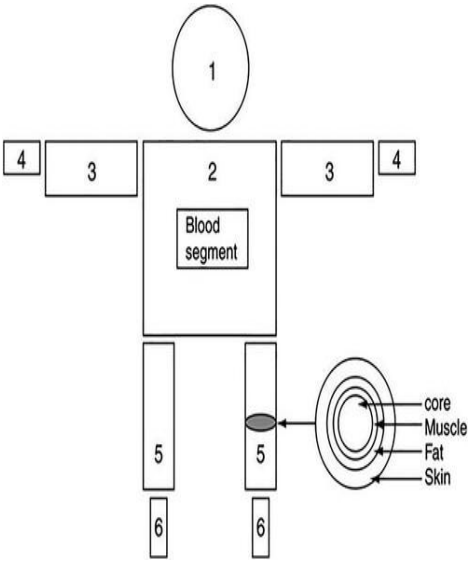

Figure 2.4. Schematic of anatomical segmentation of Stolwijk thermoregulatory human-model (Stolwijk, 1971).

While Stolwijk's model (Stolwijk, 1971) marked a pivotal development in the evolution of multi-segment thermoregulatory frameworks, it presents several notable limitations. The model's formulation was based on a restricted dataset, incorporated the assumption of a constant blood temperature, and treated radiative and convective heat exchanges between the human-body and the surrounding environment as invariant. Despite these simplifications, Stolwijk's framework has provided the basis for a range of subsequent enhancements in multi-segment human heat transfer modeling, including the notable developments by Fiala et al. (Fiala, Lomas, & Stohrer, 2001), Huizenga et al. (Huizenga, Zhang, & Arens, 2001), and Ferreira and Yanagihara (Ferreira & Yanagihara, 2009).

Fiala et al. (Fiala, Lomas, & Stohrer, 2001) pioneered the development of the multi-segment model, building upon Stolwijk's model. This model subdivided the human body into ten geometric segments—such as the head, face, neck, shoulders, thorax, abdomen, arms, hands, legs, and feet—using cylindrical or spherical representations. Each of these segments was further stratified into four or five concentric tissue layers to capture key anatomical structures,

including the brain, lungs, skeletal components, musculature, visceral organs, adipose tissue, and skin (as depicted in Figure 2.5).

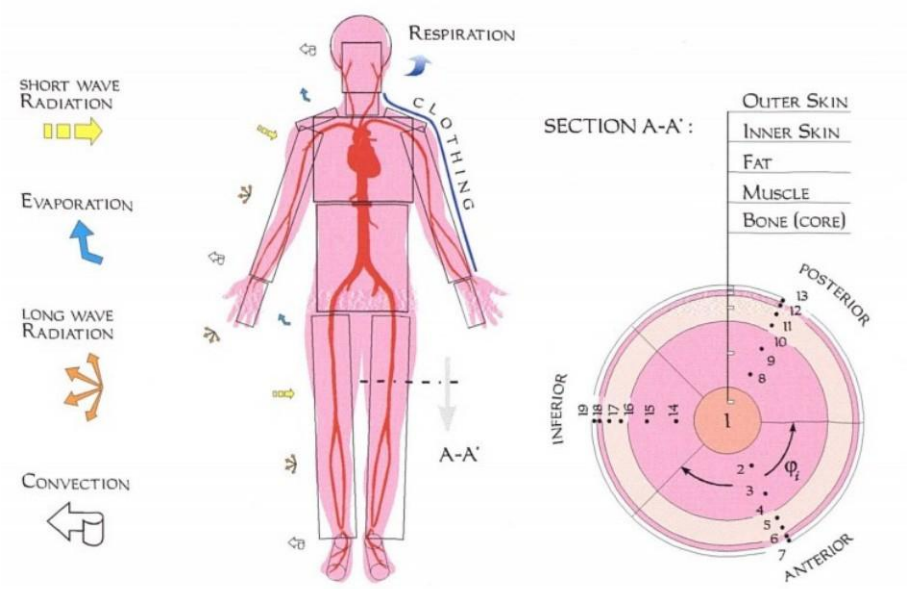

Figure 2.5. Illustrates the segmentation and structural configuration of the human body as conceptualized in Fiala's thermoregulation model (Fiala, Lomas, & Stohrer, 2001).

Fiala's model introduced major advancements in the representation of human thermoregulation by incorporating statistically derived control equations for physiological responses such as shivering, sweating, vasoconstriction, and vasodilation, based on extensive experimental data. This model identified mean skin temperature, core body temperature, and the rate of skin temperature change as critical factors regulating these thermoregulatory responses. Despite these improvements, the model has certain drawbacks, including its inability to simulate the reduction of arterial blood temperature in the extremities, neglect of localized variations in clothing insulation, and exclusion of conductive heat transfer effects in angular directions.

Huizenga et al. (Huizenga, Zhang, & Arens, 2001) further advanced the multi-segment model originally conceived by Stolwijk. These improvements encompassed a more sophisticated representation of blood circulation, precise definitions of convective and radiative heat transfer

coefficients tailored to individual body segments, and the addition of a dedicated clothing node to simulate thermal interactions between the body and clothing layers. Huizenga's model provides the capability to simulate a flexible number of body segments; however, the initial version utilized 16 segments to represent the human anatomy, including the head, chest, back, pelvis, upper and lower arms, hands, thighs, lower legs, and feet on both sides of the body, as illustrated in Figure 2.6 Despite this structural adaptability, a key limitation of the model is the absence of improvements in the thermoregulatory control system, which is essential for accurately assessing overall thermoregulation and comfort in varying environmental conditions.

Figure 2.6. Schematic illustration of the human segmentation used in Huizenga's thermo-physiological model. (Huizenga, Zhang, & Arens, 2001).

In the JOS-3 model (Takahashi et al., 2021), which is an advancement of JOS-2 (Kobayashi & Tanabe, 2013) and the earlier JOS model (Tanabe et al., 2002), the calculation of parameters such as the rate of change in total body surface area, body mass, and total basal metabolic rate (BMR) is first performed at the whole-body level and subsequently distributed to individual body segments. The JOS-3 model extends the principles established by Stolwijk's model and

incorporates improvements from JOS-2 to provide more detailed and accurate estimations of human thermoregulatory responses. JOS-3 model comprises 85 nodes delineated as follows: one central blood, seventeen artery, seventeen vein, twelve superficial veins, seventeen core, two muscle, two fat, and seventeen skin nodes. The body is segmented into 17 distinct regions (see Figure 2.7). Artery and vein blood pools reside centrally within the core layer, while the superficial vein pool lies within the skin layer. The JOS-3 model introduces the concept of arteriovenous anastomosis (AVA) blood flow within the hand and foot segments, representing a direct connection between arteries and the superficial venous network. This model assumes that blood arriving from multiple upstream pathways is completely mixed before it is delivered to the downstream tissues, ensuring uniformity in the thermal and physiological conditions of the blood supplied to these regions.

In the JOS-3 model (Takahashi et al., 2021), the head and pelvis regions are uniquely structured with four distinct layers to enhance prediction accuracy. While the head anatomically lacks conventional muscle and fat layers, these layers are conceptually introduced in the model as thermal layers to simplify thermal calculations. Despite being artificial representations, they are labeled as muscle and fat layers for computational convenience. The distribution of fat within the model is determined based on the individual's overall body fat percentage and is incorporated into the calculation of thermal conductance. Additionally, the model accounts for sex differences when calculating basal metabolic rate, and age-related effects are considered in adjusting the shivering threshold, sweat response, and basal blood flow calculations. The total body mass rate is determined using a set of predictive equations based on an individual's height, weight, age, and sex. This overall value is then refined through distribution fractions to determine localized physiological properties. Key physiological parameters influenced by individual variability include surface area, thermal conductance, heat capacity, basal blood flow, metabolic rate, and thermoregulatory thresholds for shivering and sweating. However,

JOS-3 requires the definition of set-point temperatures representing thermal neutrality, from which the thermoregulatory system determines deviations to initiate appropriate physiological responses. Although these set-points can theoretically be personalized for each individual, the current implementation remains based solely on simulation rather than experimental validation.

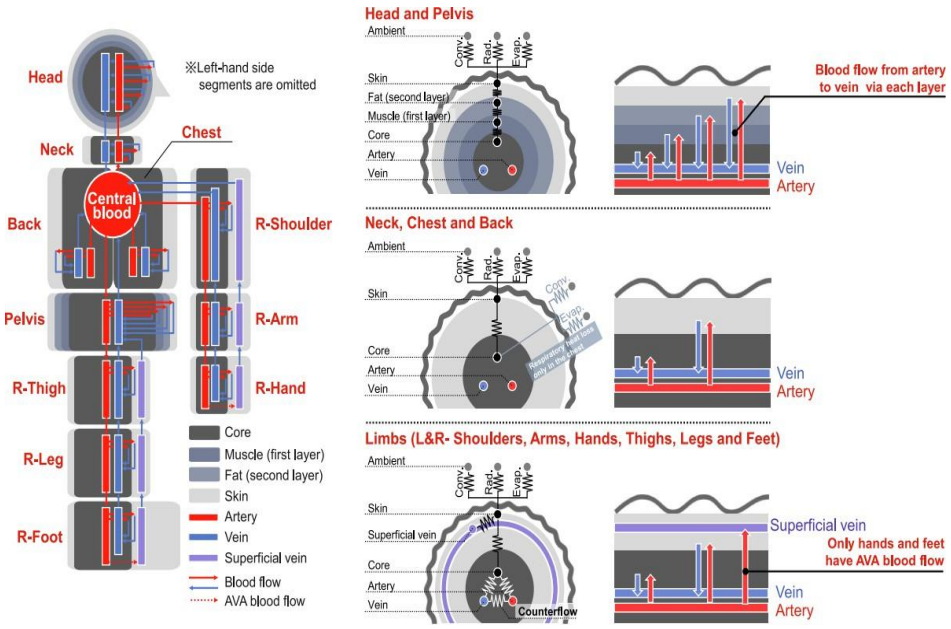

Figure 2.7. Representation the structural configuration of the human body as represented in the JOS-3 model (Takahashi et al., 2021).

The multi-segment model, as discussed earlier, significantly improves the accuracy of heat transfer estimations by evaluating heat exchange across individual body segments and is well-suited for transient and non-uniform thermal environments. It also provides a more detailed representation of physiological processes. However, existing multi-segment models often neglect critical factors such as the control of sweating mechanisms, which play a vital role in thermoregulation under hot environmental conditions. In addition, these models lack the capability to assess heat transfer responses among specific demographic groups, including young adults, healthy elderly individuals, and elderly individuals on medication, both with and without the use of cooling interventions. Another important limitation is the inability of these

models to predict occupant hydration levels, a key consideration during prolonged exposure to extreme heat. Consequently, there is a pressing need for further research to advance our understanding of human thermoregulation under extreme heat events, such as heatwaves, and to develop models that can accurately capture these critical physiological responses.

2.4 Conclusions

According to the literature review conducted in this chapter, the following tasks are proposed in this study:

(1) To evaluate the effectiveness of ceiling fans and table fans during heatwave conditions through controlled human trials. This involves examining physiological responses along with comfort. The goal is to determine which fan type provides better thermal relief and reduces heat strain.

(2) Investigate the thresholds and limitations of electric fan use for young adults during prolonged heatwave exposure using a modified thermoregulation model. In this context, the model was enhanced by incorporating hydration-dependent set-point temperatures, sweating, and vasodilation responses. This allows the identification of safe-use thresholds for electric fans across varying combinations of temperature, humidity, fan speed, and physical activity levels.

(3) Assess the physiological effectiveness of simple water-based cooling interventions—specifically foot immersion, leg immersion, and dousing through thermoregulation modeling. Simulations were conducted using meteorological data from Indian cities representing hot-dry, warm-humid, and composite climates. These interventions were compared based on their ability to reduce core and skin temperatures, delay the onset of hyperthermia, and provide stable thermal relief during extreme heatwave conditions.

CHAPTER 3. EVALUATION OF PHYSIOLOGICAL AND THERMAL COMFORT EFFECTIVENESS OF CEILING FAN AND TABLE FAN DURING A HEAT WAVE

This chapter presents an experimental investigation into the physiological and perceptual responses of individuals exposed to extreme heatwave conditions under different electric fan scenarios. The study aims to evaluate and compare the effectiveness of no-fan, table-fan, and ceiling-fan conditions in mitigating heat stress. Sixteen healthy young participants were recruited, and controlled human trials were conducted inside a climate chamber set to simulate typical heatwave conditions (41 ± 0.5 °C, 35 ± 2% RH). Key physiological indicators, including local and mean skin temperature, core temperature, heart rate, and sweat production rate, were continuously monitored. Additionally, perceptual responses—thermal sensation, comfort, and skin wetness—were assessed using standardized questionnaires. This chapter also outlines the experimental setup, participant selection criteria, instrumentation, and statistical procedures adopted to interpret the results. The outcomes contribute to understanding the comparative performance of fan-based cooling and provide insights to guide public health recommendations during extreme heat events.

3.1 Methodology

Physiological and perceptual responses are crucial in avoiding thermal stress-related health issues such as heatstroke or hypothermia during heat events. These parameters help individuals recognize the effectiveness of a cooling method in preventing severe health consequences. Therefore, in the present study, physiological parameters and perceptual responses were collected from selected healthy participants during the trials. This section discusses the instruments used to measure physiological parameters and perceptual questionnaire. Furthermore, criteria for statistical analysis are presented as needed to interpret the physiological and perceptual collected data and generalize the results for a broader population. The climate chamber facilities, test setup for fan-off, table-fan, and ceiling-fan scenarios, and trial procedure are also described. Prior to experimentation, ethical clearance was received from The Hong Kong Polytechnic University Human Ethics Research Board (application number: HSEARS20230228009) for data collection from the participants.

3.1.1 Participants

We performed power calculation by implementing an α of 0.05, a β of 0.20, and an effect size of 0.65 in a G*Power 3 software (Heinrich-Heine-Universität Düsseldorf, Germany). This calculation shows that 16 participants would be enough to detect a statistical difference of comparable magnitude. Further, in previous studies also, groups of at least eight participants (equal numbers of male and female) were recruited to identify effective cooling strategies during heat waves (Zhai et al., 2013; Cramer et al., 2020). Therefore, in the present study, we planned to recruit 16 volunteers, of whom 8 were male and 8 were female. It is always recommended that the participants' age, body surface area, body mass index, physical fitness, and medical history be homogeneous, as these factors can independently influence physiological parameters and thermal comfort votes (Selkirk and McLellan, 2001). Therefore,

during recruitment, we checked all the volunteers' basic information, such as age, weight, height, daily exercise and medical history. For the present study, we selected university students of Chinese ethnicity with homogeneous anthropometric characteristics and good health conditions. Table 3.1 presents the selected participants' anthropometric information. Furthermore, to maintain research integrity, written consent was obtained from all participants after they were informed about the nature of the study and associated discomforts.

Table 3.1. Characteristics of participants.

Sex	Sample size	Mean age	Height (m)	Weight (kg)	Body surface area (m^2)	BMI (kg/m^2)
Male	8	22.13 ± 1.73	1.71 ± 0.05	64.9 ± 4.53	1.75 ± 0.05	22.4 ± 1.7
Female	8	21.38 ± 1.51	1.61 ± 0.04	49.81 ± 6.06	1.50 ± 0.01	20.3 ± 1.2

3.1.2 Physiological parameters and survey questions

The negative effects of heat events on humans are mainly heatstroke, adverse cardiovascular events, kidney injury, etc., which are directly linked to physiological parameters such as skin temperature, core temperature, heart rate, and sweat production rate. Therefore, as shown in Figure 3.1 (a), ten small, wireless, portable thermocouples (i-Button DS1923-F5 sensors with a range of -20 to 85 °C and resolution of 0.0625 °C) were used to measure the local skin temperatures at intervals of 10 seconds. Researchers (Li et al., 2018) traditionally select the forehead, chest, scapula, upper arm, forearm, hand, abdomen, lumbar, thigh, and calf skin for measurements of local skin temperature (see Figure 3.1(d)). Thus, in the present study, sensors were attached to these body parts using medical adhesive tape. Although temperatures were recorded at ten sites, only six representative locations (forehead, chest, forearm, abdomen, thigh, and calf) were reported to avoid redundancy, as scapula and lumbar exhibited similar trends to chest and abdomen. For calculating the mean skin temperatures, the standard 8-point

weighting system proposed by Ramanathan (1964) was applied. The heart rate was measured at intervals of 1 second using a Polar H10 heart rate sensor, which straps to the chest (Figure 3.1 (b)). The CORE device estimates internal temperature via dual-heat-flux technology, providing a continuous, non-invasive measurement of deep body temperature while compensating for ambient influences. The sensor contains two thermistors that measure differential heat flux between the skin surface and the environment, from which an energy balance equation is solved to estimate the internal temperature of central body tissues and organs. This "core temperature" reflects the thermoregulatory state of the body and serves as a key indicator of thermal and cardiovascular strain. The device has been validated against ingestible telemetric pill sensors, demonstrating comparable accuracy within ±0.1 °C under various thermal conditions. The core temperature was measured using a non-invasive device (CORE; accuracy: ±0.1 °C) at 1-minute intervals (Figure 3.1 (c)). In addition, tympanic temperature was intermittently (in every 5 minutes) measured using an infrared ear thermometer (Braun ThermoScan, Germany) as a supportive reference however we did not found any differences between core temperature. Figure 3.1(d) illustrates all the skin-sensor, heart-rate and core-sensor sites on the body during the trials. Furthermore, as displayed in Figure 3.1(e), each participant's weight was measured with a scale (range: 0 to 150 kg; accuracy: ±2 g) before and after the trial, and this weight was then used to determine the sweat production rate. For the present scale, the uncertainty (Cheuvront and Kenefick, 2017) ranges from 0.40%-0.46%, and it is within acceptable limits.

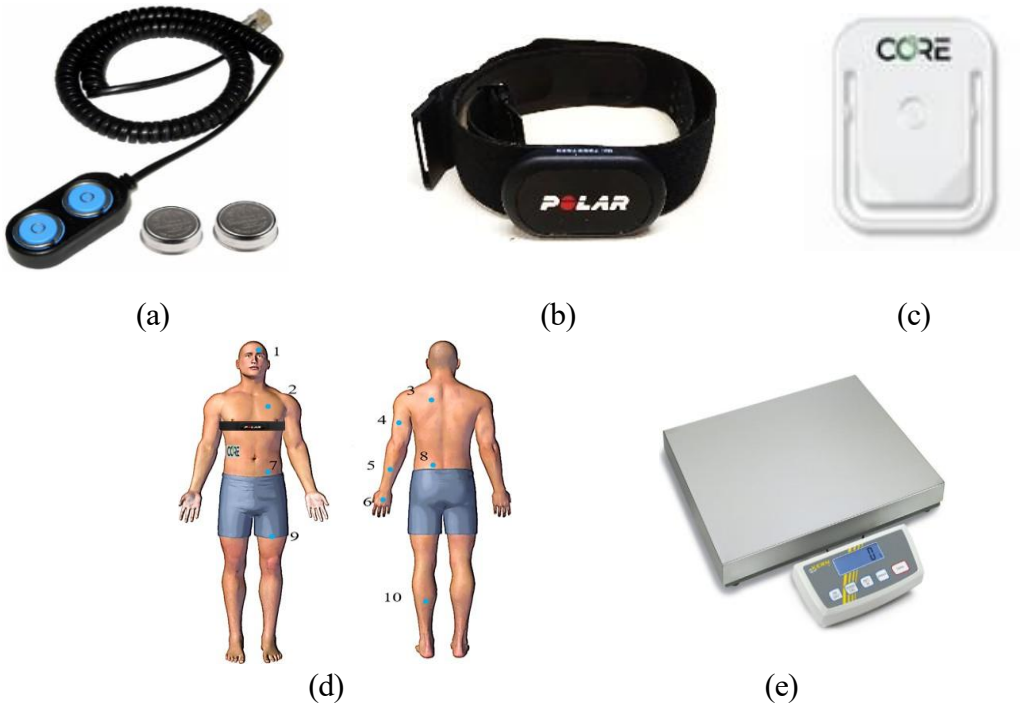

Figure 3.1. Physiological measurements: (a) i-Button thermocouples to measure skin temperatures (source-(iButtonLink, 2023)); (b) polar chest strap to measure heart rate; (c) CORE sensor (source- (CoreBodyTemp, 2023); (d) sensor measurement sites; (e) weighing scale (source- (Kern-Sohn, 2023)).

In addition to physiological parameters, the perceptual responses of the participants were evaluated using a paper questionnaire, which further contributed to understanding individuals' overall well-being. The most common perceptual response measures are thermal sensation and thermal comfort, which reveal discriminative and affective perception details, respectively. Furthermore, during heat events, sweating is a typical response for maintaining body temperature; hence, understanding the skin wetness sensation is necessary. Thus, the questionnaire in our study was comprised of the above three primary inquiries. The thermal sensation scale was based on a modified 9-point rating scale (Yang et al., 2020), which is an extension of the normal ASHRAE (ASHRAE, 2004) seven-point thermal sensation scale and

ranges from -4 (very cold) to +4 (very hot). The range of the thermal comfort scale was from 0 (comfortable) to +4 (extremely uncomfortable), which is a 5-point rating scale (Wang et al., 2023). A 4-point rating scale was utilized to record the skin wetness sensation, with the range of 0 [normal] to +3 [very wet]). The thermal sensation, thermal comfort and skin wetness sensation scales are displayed in detail in Table 3.2. During each trial, the participants were instructed to answer the questionnaire on paper at 10-minute intervals.

Table 3.2. Rating scales used on questionnaire to collect overall responses of participants.

Rating scale	Thermal sensation	Rating scale	Thermal comfort	Rating scale	Skin wetness sensation
-4	Very cold	0	Comfortable	0	Normal
-3	Cold				
-2	Cool	1	Slightly uncomfortable	1	Slightly wet
-1	Slightly Cool				
0	Neutral	2	Uncomfortable		
1	Slightly Warm			2	Wet
2	Warm	3	Very uncomfortable		
3	Hot				
4	Very Hot	4	Extremely uncomfortable	3	Very wet

After all the data had been collected from the participants, a statistical analysis was performed for use in interpreting the physiological and perceptual data. This is the standard procedure employed by researchers to examine the data in thermoregulation and thermal comfort studies in order to generalize the results to a broader population (Zhai et al., 2013; Ravanelli et al.,

2015; Gagnon et al., 2016). A two-way repeated measure analysis of variance (ANOVA) [conditions (fan off, table fan and ceiling fan) x time (i.e., 10 sec, 1 min or 10 min interval)] was conducted using SPSS software. The paired-samples t-test were performed at every time interval if ANOVA analyses detected a significant effect. The $p < 0.05$ was set as a significant level.

3.1.3 Chamber facilities and test conditions

We conducted human trials in a climate chamber that controlled the temperature and relative humidity. For the trials, the chamber [dimensions: 3.9 m *x* 3.8 m *x* 2.6 m] (Figure 3.2 (a)) was maintained at 41.0 ± 0.5 °C and R.H. of 35± 2 %, which mimic the typical heat wave conditions (Morris et al., 2021; Wang et al., 2023). We used temperature and humidity sensors installed in the chamber to monitor the air temperature and humidity. Furthermore, RS-WS Y4 sensors (temperature accuracy: ±0.1 °C; humidity accuracy: ±1 %) were placed near the participant at heights of 0.7 m, 1.1 m, and 1.7 m (ASHRAE, 2004; ISO, 1998) for measurement of the air temperature and humidity (see Figure 3.2 (a)) near the participant.

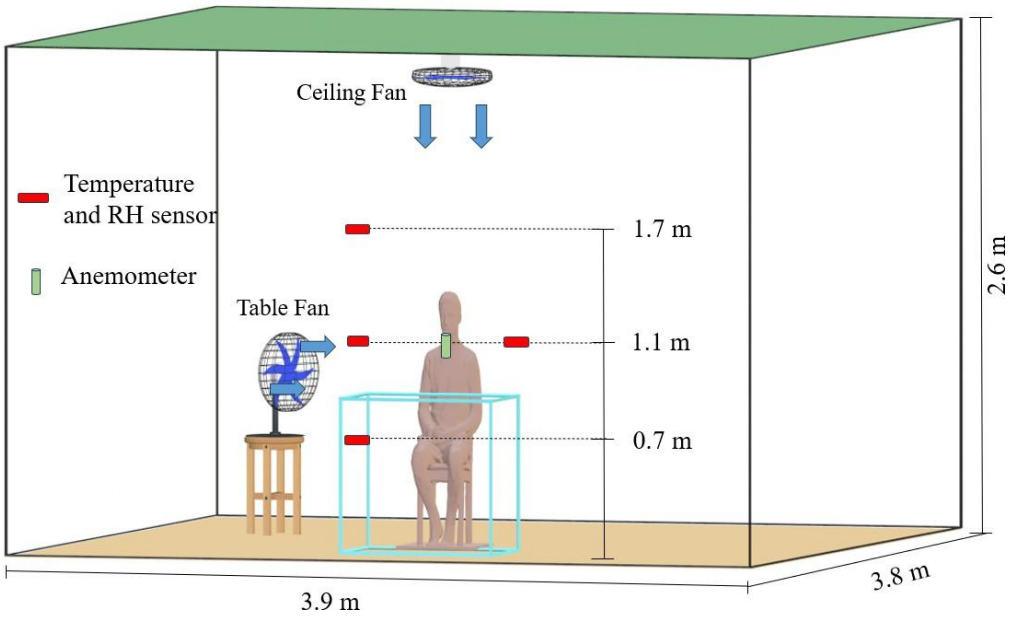

(a)

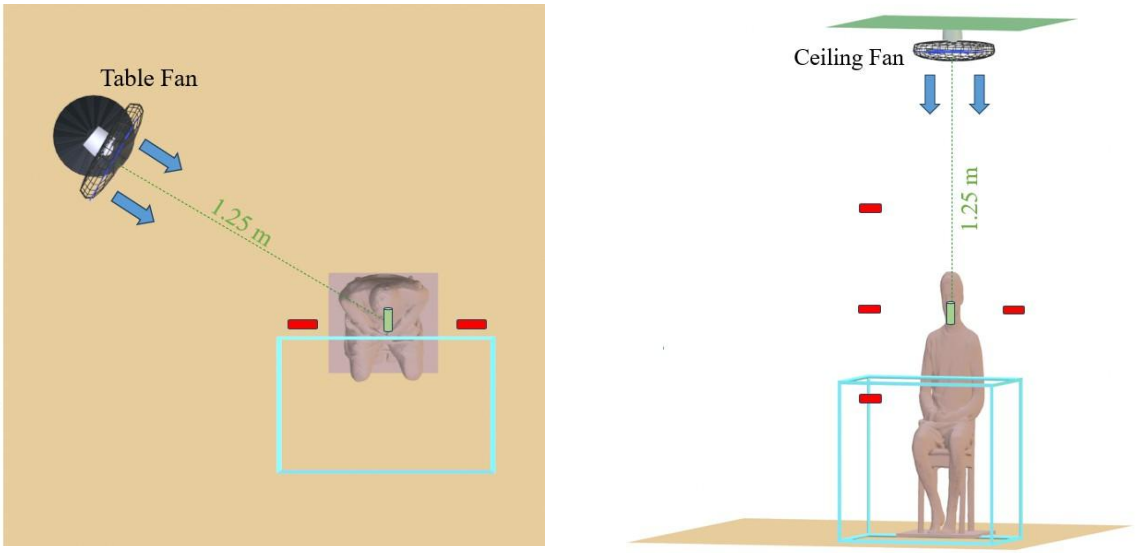

(b) (c)

Figure 3.2. Schematic diagrams of experimental layout: (a) climate chamber (b) table-fan scenario, and (c) ceiling-fan scenario.

Three types of experimental trials, including the fan-off, table-fan, and ceiling-fan scenarios (see Table 3.3) were conducted in the climate chamber. For the table-fan trials, a 12-inch fan was placed in a location that was 1.25 m diagonally behind the participant (Jay et al., 2019; Vellei et al., 2023) (see Figure 3.2(b)). A similar-sized fan was installed on the chamber ceiling for the ceiling-fan trials, and was also placed at 1.25 m from the participant (see Figure 3.2(c)). Note that we also wanted to ensure that similar air speed was generated near the participants in both the table-fan and ceiling-fan scenarios. For this purpose, as demonstrated in Figure 3.2 (a)-(c), the anemometer was placed at a location 1.25 m from both fan positions and at a height of 1.1 m (ASHRAE, 2004; ISO, 1998; Jay et al., 2019; Vellei et al., 2023) from the ground. The air speed was measured prior to the human experimental trials (without a participant) using a Testo omni-direction hot sphere anemometer (range: 0-5 m/s, accuracy: 0.03 m/s or 4% of

reading). The measured mean air speeds in the no-fan, table-fan and ceiling-fan trials were 0.11 m/s, 1.76 m/s and 1.68 m/s, respectively.

Table 3.3. Different environmental and electric-fan parameters.

Cases	**Case 1**	**Case 2**	**Case 3**	**Case 4**
Type	No fan	Low table fan speed	Ceiling fan	High table fan speed
Air temperature (°C)	41.0 ± 0.5°C			
Relative humidity (%)	35 ± 2 %			
Fan position	-	Fixed	Fixed	Fixed
Mean air speed near participants (m/s)	0.11	1.76	1.68	2.40

3.1.4 Trial procedure

The standard exposure time of human trials to identify the effectiveness of different cooling strategies during heat waves is 1.5 to 2 hours (Ravanelli et al., 2015; Gagnon et al., 2016; Morris et al., 2019; Cramer et al., 2020). Therefore, the participants were exposed to each test scenario for 2 hours in this study. The trials were performed from May to October 2023, during which time the ambient temperature in Hong Kong was warmer. The trial procedure, which was approved by the ethical research board of the university, followed the standard procedure which has traditionally been used in thermoregulation and thermal comfort experimental studies (Zhai et al., 2013; Ravanelli et al., 2015; Gagnon et al., 2016; Morris et al., 2019; Cramer et al., 2020). Participants were advised to avoid consuming caffeine or alcohol or performing heavy strenuous activities within 24 hours before the start of each trial. They were also asked to maintain proper sleep schedules and a similar diet the day before and on the day

of the trial. The test procedure was divided into two phases. The test began with a preparation phase. As shown in Figure 3.3 (a), the chamber temperature increased from the typical ambient temperature (~24.0 °C) to 46.2 °C in about 110 minutes with the use of a chamber load-generating unit and two heater systems. After that, the generating unit was shut down, and then we waited another 90 minutes for the temperature to stabilize at 41.0 ± 0.5 °C. As shown in Figure 3.3(b), the humidity dropped from a typical room humidity level to around 35± 2%. Achieving the stabilized temperature and humidity level took approximately 3 hours and 20 minutes. After that, the second phase (trial phase) began.

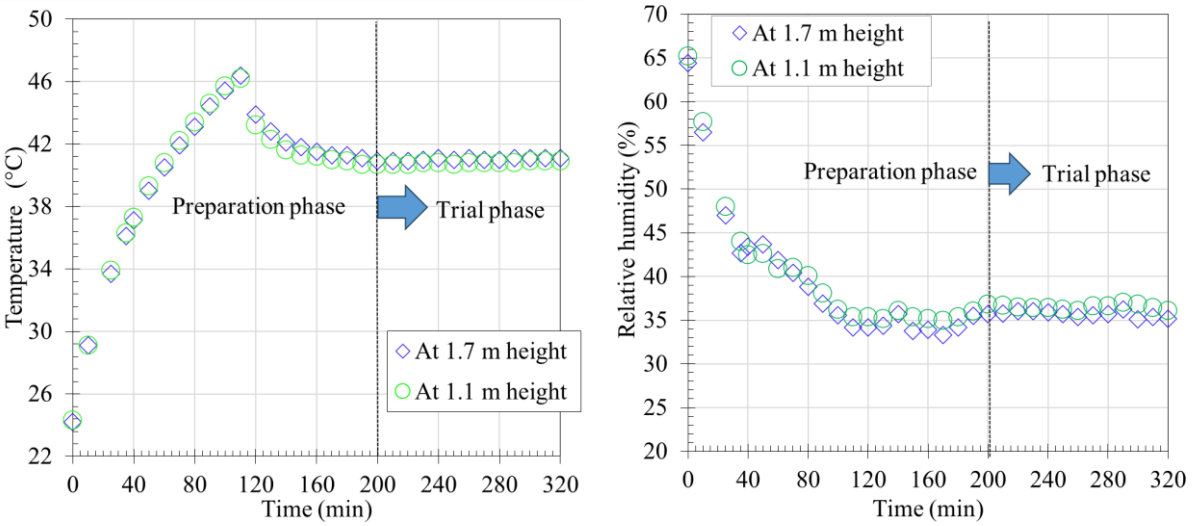

(a) (b)

Figure 3.3. Climate chamber (a) temperature and (b) humidity variation under no-fan, table-fan and ceiling-fan conditions (where the results represent only one trial)

For the trial, participants were asked to wear summer clothing consisting of a short-sleeved t-shirt, short pants, briefs and slippers. The outfit's clothing insulation and permeability index were around 0.4 clo and 0.38, respectively (ASHRAE, 2004). All the participants arrived 45 minutes before the trial phase started. During the 45-minute period, they sat in a room maintained at 23.5 ± 0.5 °C. This period ensured that the participants reached thermal neutrality, which is crucial for maintaining consistent and reliable results. Typically, thermal

neutrality is achieved when the participants' core temperature is approximately 36.9 °C, their thermal sensation and thermal comfort are at a neutral level, and there is no sensible sweating (Lei et al., 2023). During this phase, various sensors were placed on the participants to measure the physiological parameters. In the second phase (trial phase), the participants each entered the climate chamber and sat in a chair; they were exposed to one of the test conditions for 2 hours. During this phase, participants did computer work or reading and answered the survey questions at 10-minute intervals. Participants' weight was measured before and after the trial phase, and this information was further used to evaluate their sweating rate. Figure 3.4 provides a photographic view of the experimental trials. A trial was terminated if one or more of the following conditions were met (Lei et al., 2023): (a) the participant's core temperature reached 39.0 °C; (b) the heart rate (H.R.) exceeded 90% or 95% of the maximum H.R.; (c) the participant felt any heat-related health symptoms; (d) the participant wanted to quit for any reason; (e) the participant completed the trial.

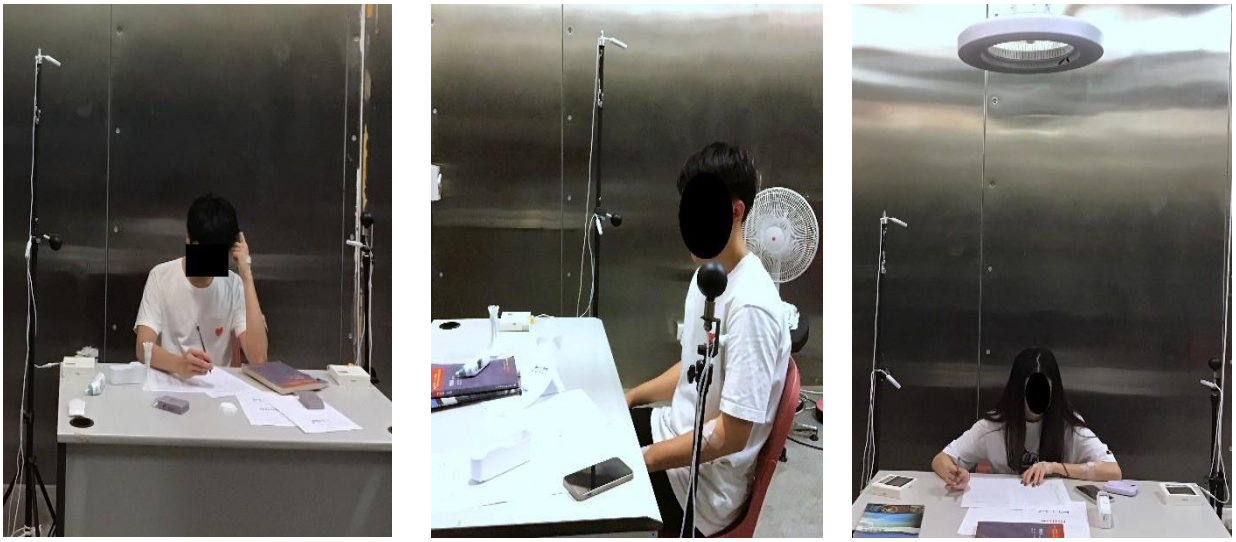

(a) No Fan (b) Table Fan (c) Ceiling Fan

Figure 3.4. Photographic view of the experimental trials.

3.2 Results

The effectiveness of the no-fan, table-fan and ceiling-fan conditions during a heat wave can be assessed using thermo-physiological parameters such as skin and core temperature. Furthermore, the heart rate and sweat production rates provide elucidation of any other physiological strain on the body. Therefore, in the present section, we discuss the effectiveness of no-fan, table-fan and ceiling-fan conditions during a heat wave using the above physiological parameters. Finally, the perceptual responses of the participants were reported and analyzed to understand the occupants' overall behavior during a heat wave. In the present study, all participants exposed to heat wave conditions successfully completed a trial under fan-off, table-fan, and ceiling-fan conditions. Presentation of data for individual participants would be difficult for readers to understand. Furthermore, we found no significant ($P > 0.05$) difference between male and female participants collected data in any similar condition. Hence, we have expressed the results as a mean ± standard deviation of all the participants.

3.2.1 Local skin temperature

For clarity, only six representative sites (forehead, chest, forearm, abdomen, anterior thigh, and anterior calf) are reported, as scapula showed similar trends to chest, and lumbar to abdomen. In the no-fan condition, the baseline temperatures (start of trial) of the forehead, chest, forearm, abdomen, anterior thigh, and anterior calf were 33.2 ± 1.1 °C, 33.4 ± 1.4 °C, 31.5 ± 1.4 °C, 33.4 ± 1.5 °C, 31.2 ± 1.0 °C, and 30.7 ± 1.4 °C, respectively. Figure 3.5(a) shows the skin temperature variation in the upper body parts (forehead, chest and forearm) in the no-fan trial. During the first 20 minutes, there was a sharp rise in local skin temperatures because the participants moved to the trial phase (chamber at 41.0 ± 0.5 °C) from a preparation phase (room at 23.5 ± 0.5 °C). This move triggered the body's thermoregulatory processes. We observed faster stabilization of forehead temperature than of other local skin temperatures. The high

density of blood vessels near the skin, greater surface area, and faster onset of sweating compared to other body parts (Arens and Zhang, 2006) contributed to the faster adjustment of the forehead temperature. During the 120-minute trial, the forehead temperature increased by 4.5 °C, from 33.2 ± 1.1 °C to 37.7 ± 0.3 °C. We observed that the chest temperature rose by around 3.4 °C from the baseline temperature (33.4 ± 1.4 °C). This change was the smallest because the chest has greater body surface area, which helps to dissipate heat efficiently. The elevation in forearm skin temperature (6.2 °C) was significantly higher as the forearm was directly exposed to the surroundings and had less surface area (Arens and Zhang, 2006) . By the end of the trial (120th minute), the reported forearm temperature was 37.8 ± 0.4 °C.

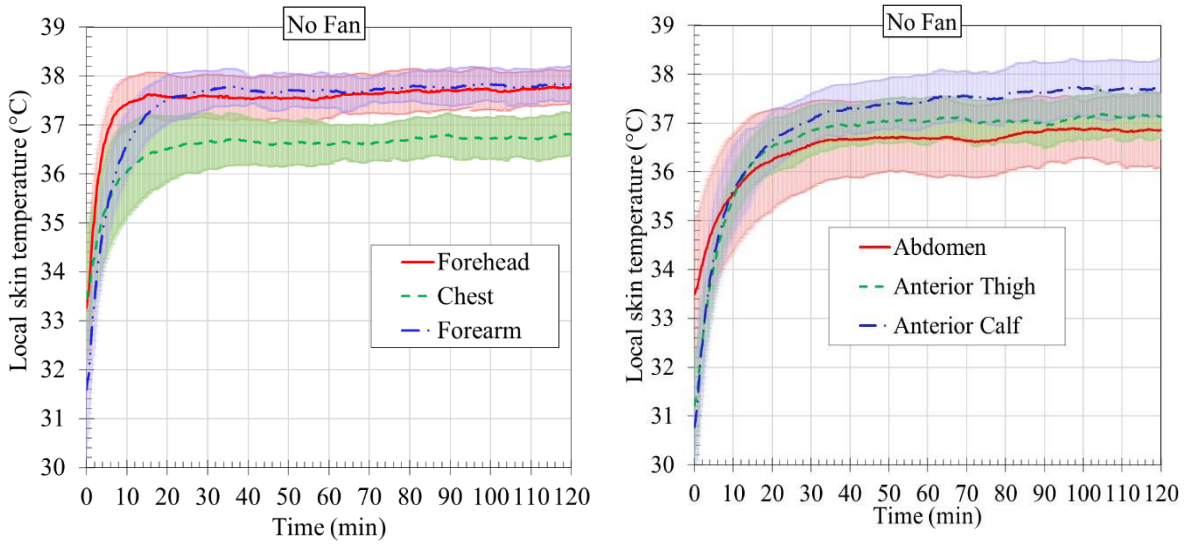

(a) (b)

Figure 3.5. Variation in local skin temperature in no-fan condition: (a) forehead, chest, and forearm; (b) abdomen, anterior thigh, and anterior calf.

Figure 3.5(b) presents the variation in the abdomen, anterior thigh, and anterior calf skin temperatures in the no-fan trial. Compared with the upper body parts, the lower body parts took a longer time (approximately 40 minutes) to stabilize. The increases in the thigh and calf temperatures were similar for the first 20 minutes, but subsequently the calf temperature

became higher than that of the thigh. The reason for this difference was that the anterior thigh has a higher vasodilation function and greater surface area, which enhances the sensible heat transfer from the body. The rise in abdomen temperature was similar to that of the chest regions, as both these body parts are near vital organs. By the end of the heat-exposure period, the abdomen, anterior thigh and anterior calf temperatures had increased to 36.8 ± 0.7 °C, 37.1 ± 0.4 °C and 37.7 ± 0.5 °C, respectively. To keep this paper concise, the results for the table-fan and ceiling-fan cases are provided in Appendix A (see Figure A 1 and Figure A 2). The baseline local skin temperatures in the table-fan and ceiling-fan cases did not differ from those in the no-fan case. Furthermore, similar local skin temperature variations were observed in both fan cases compared with the no-fan case. It was observed that the local skin temperatures in all the scenarios increased steeply initially and achieved a new equilibrium, after which they increased slowly. The highest local skin temperatures generally occurred at the end of the trial.

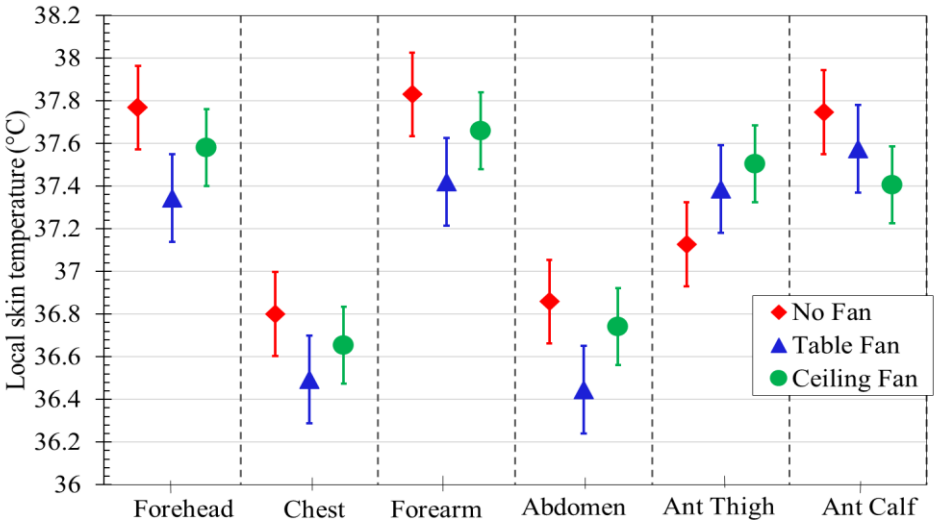

Figure 3.6. Local skin temperature with no fan, table fan and ceiling fan at the end of heat exposure.

Figure 3.6 presents the local skin temperatures at the end of heat exposure (120th minute) for the no-fan, table-fan and ceiling-fan scenarios. We observed that the local skin temperatures were lower ($p < 0.05$) in both fan cases than in the no-fan case, with the exception of the anterior

thigh temperature. The reason for the above observation may have been that the stronger air circulation in both fan cases promoted sweat evaporative cooling, which eventually helped to lower local skin temperatures. In contrast, for the anteior thigh, as the thigh has fewer sweat glands and stronger vasodilation regulatory mechanisms, the higher air speed in the fan scenarios may have increased negative dry heat loss (from the surrounding environment to the anterior thigh) compared to sweat evaporation (see Figure 3.6 and Figure A 3). Therefore, the overall heat transfer was reversed, which increased the anterior thigh temperature. The table fan and ceiling fan lowered the upper body skin temperature (including the forehead, chest, and forearm) compared to the fan-off scenario by approximately 0.3–0.4 °C and 0.1–0.2 °C, respectively. The reason may have been that the ceiling fan pushed down the hot air that had gathered near the ceiling, as we observed higher surrounding air temperature at a height of 1.7 m in the ceiling-fan case (41.2 ± 0.3 °C) than in the table-fan case (40.7 ± 0.2 °C). This hot air circulation increased the negative dry heat loss (from the surroundings to the body). Hence, the ceiling fan was less effective than the table fan. The exception to the above observation was the anterior calf temperature, which was lower with the ceiling fan (37.4 ± 0.4 °C) than with the table fan (37.5 ± 0.5 °C).

3.2.2 Mean skin temperature

To understand the overall thermal state of the body, this study employed the mean skin temperature ($T_{sk,mean}$), calculated using the following 8-point formula [Li et al., 2018]:

$$T_{sk,mean} = 0.07\,(T_{forehead} + T_{upper\,arm} + T_{forearm}) + 0.175\,(T_{chest} + T_{scapula}) + 0.05\,T_{hand} + 0.19\,T_{anterior\ thigh} + 0.2\,T_{anterior\ calf} \quad (3.1)$$

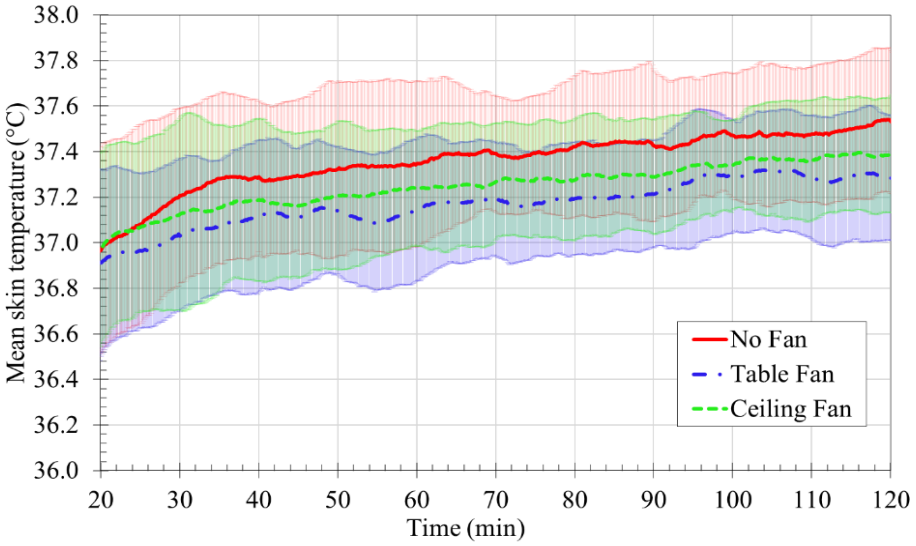

Figure 3.7. Comparison of mean skin temperature in the no-fan, table-fan, and ceiling-fan cases.

Note that there were sharp rises in local skin temperatures during the first 20 minutes in all three scenarios, and then the body achieved a new equilibrium (see Figure 3.5 and Figure A 4). Therefore, we focused on the variation in the mean skin temperature (Figure 3.7) from the 20th minute under the fan-off, table-fan, and ceiling-fan conditions in order to better compare the different trials. We found that the mean skin temperatures at the 20th minute in the no-fan (37.0 ± 0.5 °C), table-fan (36.9 ± 0.4 °C) and ceiling-fan (37.0 ± 0.4°C) cases were similar. From the 45th minute until the end of the trial, a significant temperature difference ($p < 0.05$) was observed in both fan cases compared to no fan. The maximum reductions reported under table-fan and ceiling-fan conditions compared to no fan were 0.3 °C and 0.2 °C, respectively. This finding indicates that the air circulation with both the table fan and the ceiling fan enhanced heat transfer from the body to the surrounding environment. Furthermore, we found that there was no significant temperature difference between the table-fan and ceiling-fan scenarios. Nonetheless, the lowest mean skin temperature was observed with the table fan. At the end of the heat-exposure period, the reported mean skin temperatures with no fan, table fan and ceiling fan were 37.5 ± 0.3 °C, 37.3 ± 0.3 °C 37.4 ± 0.4 °C, respectively.

3.2.3 Core temperature

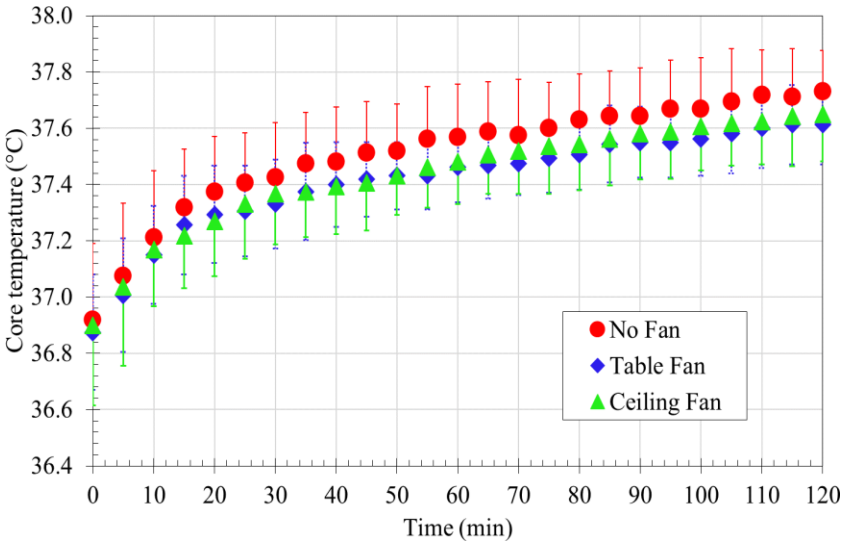

Figure 3.8. Comparison of core temperature in the no-fan, table-fan, and ceiling-fan cases.

Figure 3.8 presents the core temperature variation in the no-fan, table-fan, and ceiling-fan cases. The (start of trial) baseline core temperatures were similar among the different scenarios, at around 36.9 ± 0.2 °C. The core temperature remained lower throughout the trial in both the fan cases compared to the no-fan scenario, and this finding demonstrates that table and ceiling fans are beneficial at 41 °C and 35% R.H. There was no significant ($P > 0.05$) core temperature difference between the table-fan and ceiling-fan scenarios throughout the trial. The maximum core temperatures noted at the end of the trial in all the cases were 37.7 ± 0.1 °C, 37.6 ± 0.1 °C, and 37.6 ± 0.2 °C in the no-fan, table-fan and ceiling-fan cases, respectively. Furthermore, we observed that the core temperature increased slowly and steadily throughout the trials, irrespective of the fan or no-fan scenario (see Figure 3.8 and Figure A 5). This means that although the fan increases the evaporative heat transfer and produces a lower core temperature than no fan, there was still a limit to the increase in evaporative heat loss when a fan was used. Hence, fans may not be helpful for long durations during heat waves.

3.2.4 Heart rate and sweat production rate

Figure 3.9 (a) shows the average heart rate in the no-fan, table-fan, and ceiling-fan trials. The baseline heart rate did not differ among the trials (no fan: 76 ± 6 bpm; table fan:74 ± 8 bpm; ceiling fan: 76 ± 6 bpm). Compared to a neutral environment, the heart rate increases during a heat wave in all cases because of a change in sensible heat loss (greater blood circulation near the skin and enhanced vasodilation function). The average heart rate during the trial was highest (98 ± 5 bpm) in the no-fan condition because of the increased body temperature. The body resisted this increase in temperature and tried to maintain the body temperature steady by increasing the sensible heat loss, which required a higher blood flow rate and heart rate. Fan use significantly reduced the heart rate ($P < 0.05$) compared to the fan-off scenario, because in the fan case, the body enhanced the heat transfer by sweat evaporative cooling. The average heart rate was 86 ± 5 bpm for the table-fan trial and 91 ± 4 bpm for the ceiling-fan trial. The difference in the average heart rate between the table fan and ceiling fan may have been due to differences in upper body skin temperature, which was 0.1–0.2 °C lower with the table fan than with the ceiling fan. The smallest change in heart rate was observed in the table-fan case (Figure 3.9 (a) and Figure A 6 (a)).

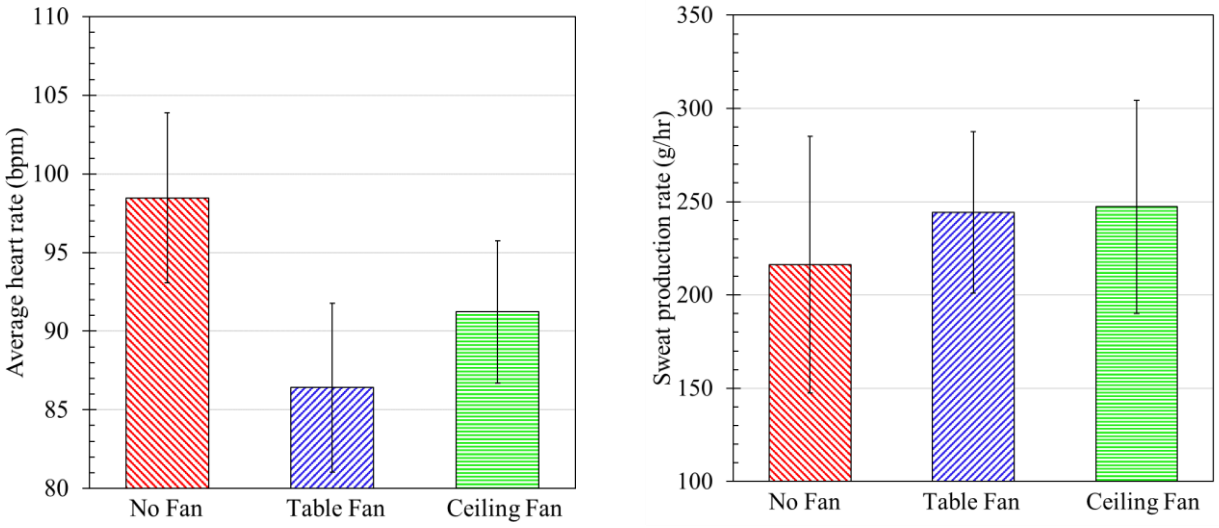

(a) (b)

Figure 3.9. Comparison of (a) average heart rate and (b) sweat production rate in no-fan, table-fan, and ceiling-fan trials.

A fan provides marginal benefits compared to the no-fan scenario by promoting latent heat loss due to sweat evaporation. However, this greater evaporation can potentially increase the sweat production rate, which in turn can elevate the physiological strain on the body, for example, in the form of dehydration (WHO, 2018). Hence, the effect of fan use on the sweat production rate is discussed here. To calculate the total sweat production (SW_p), the following equation is used (Li et al., 2018):

$$SW_{\mathrm{p}} = W_{\mathrm{pre-trial}} - W_{\mathrm{post-trial}} \tag{3.2}$$

where $W_{pre\text{-}trial}\ (g)$ is the body weight at the start of the trial, and $W_{post\text{-}trial}\ (g)$ is the body weight at the end of the trial.

Furthermore, the sweat production rate (g/hr) is calculated using equation (3.3).

$$SW_{\mathrm{p}} = \frac{SW_{\mathrm{p}}}{\Delta t} \tag{3.3}$$

Here, Δt (hr) is the total trial duration.

The mean of the 16 participants' sweat production rates in the fan-off, table-fan and ceiling-fan scenarios is presented in Figure 3.9(b). The sweat production rates under the present simulated heat wave exposure with no fan, table fan and ceiling fan were 216.3 ± 68.7 g/hr, 244.3 ± 43.3 g/hr and 247.3 ± 57.1 g/hr, respectively. The fans enhanced the evaporation of sweat from the skin; hence, the sweat production rate increased in both fan cases (see Figure 3.9(b) and Figure A 6(b)). However, the change was less than 35 g/hr (~35 ml/hr), for which a person can compensate by drinking an extra cup (250 ml) of water every 7 hours. No significant difference in sweat production rate was found between table- and ceiling-fan conditions ($p > 0.05$).

3.2.5 Perceptual response

Figure 3.10 displays the participants' thermal sensation responses at the end of heat exposure with no fan, table fan and ceiling fan. It should be noted that the baseline (start of trial) thermal sensation votes were similar in all the conditions. The highest mean thermal sensation vote was observed in the no-fan case and was equal to +3.45 (between hot and very hot). The highest and lowest thermal sensation votes reported in the fan-off case were +4 (very hot) and +3.2 (between warm and hot), respectively. The mean thermal sensation levels were significantly lower ($p < 0.05$) in the table and ceiling fan conditions. This shows that increasing air movement, irrespective of the fan type, helps to better the thermal sensation level compared to the no-fan condition (see Figure A 7). Furthermore, the difference in mean thermal sensation levels with the table fan (+2.5) and ceiling fan (+2.65) was not significant ($p > 0.05$).

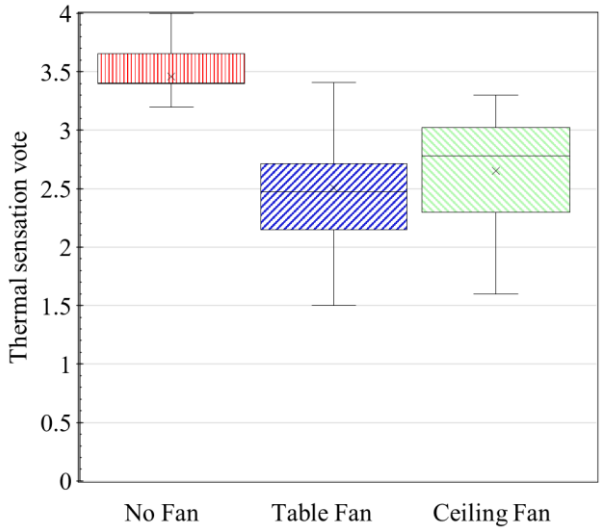

Figure 3.10. Comparison of body thermal sensation votes among the no-fan, table-fan and ceiling-fan conditions at the end of heat exposure.

The overall thermal comfort votes at the end of the trial in different conditions are shown in Figure 3.11. It was found that there was a significant improvement ($p < 0.05$) in overall thermal comfort response in the table-fan and ceiling-fan conditions compared to the fan-off condition. For the no-fan condition, the mean, highest and lowest thermal comfort responses reported were +3.09 (very uncomfortable), +3.8 (close to extremely uncomfortable) and +2.3 (between uncomfortable and very uncomfortable), respectively. The mean votes in the table- and ceiling-fan scenarios were +2.0 (uncomfortable) and +2.5 (between uncomfortable and very uncomfortable), respectively. The table fan provides greater thermal comfort than the ceiling fan ($p < 0.05$). The highest thermal comfort responses observed with the table and ceiling fans were +3.2 and +3.3, respectively. The lowest overall thermal comfort responses reported were +1.2 and +1.6 for the table and ceiling fan trials, respectively.

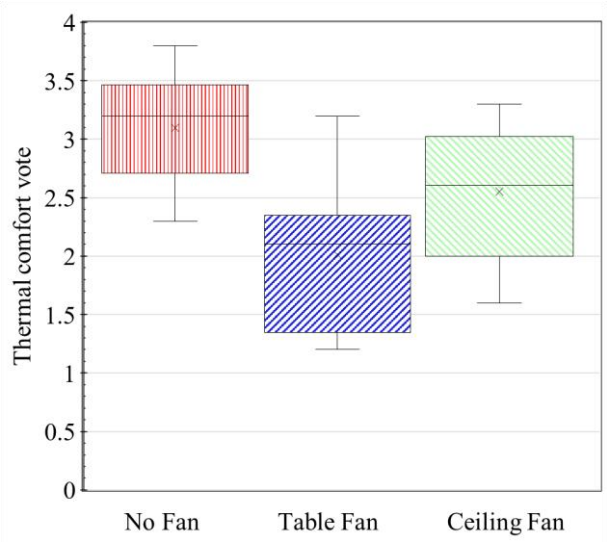

Figure 3.11. Comparison of body thermal comfort votes among the no-fan, table-fan and ceiling-fan conditions at the end of heat exposure.

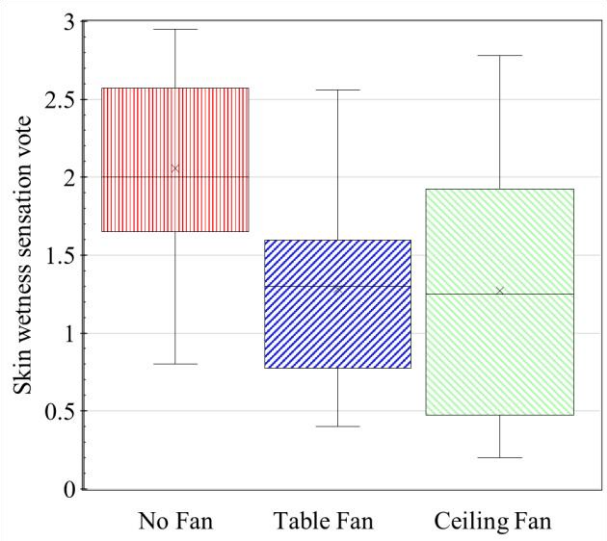

Figure 3.12. Comparison of body skin wetness votes among the no-fan, table-fan and ceiling-fan conditions at the end of heat exposure.

The skin wetness sensation under no-fan, table-fan, and ceiling-fan conditions at the end of the trial is shown in Figure 3.12. Compared to both of the fan scenarios, the mean skin wetness sensation was higher in the no-fan scenario. For the no-fan case, the mean skin wetness sensation was equal to 2.05 (wet). In the no-fan condition, there was no forced air movement.

Therefore, the surface area of sweat had to increase in order to evaporate the generated sweat faster, which eventually increased the sensation of skin wetness. The highest and lowest skin wetness votes reported by participants in the no-fan case were +2.95 and +0.8, respectively. In the table- and ceiling-fan conditions, no difference ($p > 0.05$) was observed in mean skin wetness sensation. The highest skin wetness votes noted for table and ceiling fan were +2.56 and +2.78, respectively. The lowest skin wetness sensations observed were +0.4 and +0.2 for the table-fan and ceiling-fan trials, respectively.

3.3 Discussion and limitations

This experimental study aimed to evaluate the physiological and perceptual effectiveness of three distinct cooling conditions—no fan, table fan, and ceiling fan—during simulated extreme heat wave exposure. Controlled trials were carried out in a climate chamber maintained at a high thermal load of 41.0 ± 0.5 °C and 35 ± 2% relative humidity, which mimics real-world heatwave conditions found in tropical and subtropical regions. Sixteen healthy young adult participants (eight male and eight female) underwent a 2-hour exposure under each scenario, during which critical physiological markers and subjective responses were monitored.

The results clearly demonstrate that the use of electric fans which include table and ceiling types, significantly enhances evaporative heat transfer from the human body. This improvement manifests as a delay in the rise of mean skin temperature, core body temperature, and heart rate, indicating lower thermoregulatory and cardiovascular strain compared to the no-fan condition. The table fan, in particular, showed marginally better performance in reducing upper body skin temperature and improving overall comfort compared to the ceiling fan. This could be attributed to its directional airflow targeting the upper torso, where thermal sensitivity is high and where major thermoregulatory receptors are located. The physiological outcomes presented a consistent pattern across parameters. Mean skin temperature showed the

clearest benefit, with final values 0.3 °C lower in the table-fan trial and 0.2 °C lower in the ceiling-fan trial compared to no-fan. Core temperature reductions were more modest, not exceeding 0.1 °C, but nonetheless followed the same direction. Cardiovascular responses were also alleviated, as average heart rate fell from 98 bpm in the no-fan condition to 86 bpm with the table fan and 91 bpm with the ceiling fan. In contrast, sweat production rates increased by about 35 g/h with both fan types compared to no-fan, indicating greater evaporative cooling but also a slightly higher hydration requirement. Together, these findings suggest that the main benefit of fans lies in lowering cardiovascular strain through improved evaporative heat transfer, with only a small trade-off of increased sweat loss.

Subjective responses closely aligned with these physiological effects. At the end of exposure, thermal sensation was better from +3.45 (between hot and very hot) in the no-fan condition to +2.5 with the table fan and +2.65 with the ceiling fan. Thermal comfort followed a similar pattern, shifting from +3.09 (very uncomfortable) without a fan to +2.0 (uncomfortable) with the table fan and +2.5 (between uncomfortable and very uncomfortable) with the ceiling fan. Skin-wetness sensation was also lower in the fan conditions compared with no-fan, consistent with higher sweat evaporation and reduced wetted area on the skin. These results indicate that reductions in skin temperature and heart rate were reflected in better perception of heat strain. However, it should be emphasized that thermal sensation in all cases remained in the “hot” range, demonstrating that fans only partially mitigate discomfort under such extreme conditions.

Local variations in cooling also help explain the relative performance of table and ceiling fans. Upper-body sites such as the forehead, chest, and forearm experienced greater reductions in skin temperature with the table fan (≈0.3–0.4 °C lower than no-fan), consistent with its directed airflow toward these regions. By contrast, the anterior thigh was warmer in the fan cases, likely due to fewer sweat glands, stronger vasodilatory heat delivery, and less favorable convective

exchange. The ceiling fan also circulated hotter ceiling air (41.2 °C measured at 1.7 m vs. 40.7 °C with the table fan), which reduced its cooling effectiveness relative to the table fan. From a public health perspective, these findings have practical implications. As climate change exacerbates the frequency and intensity of heatwaves, electric fans offer a relatively low-cost and energy-efficient cooling solution, especially in regions where access to air conditioning is limited. This study strengthens the evidence base that fan usage should be reconsidered in heatwave health advisories, especially under moderate to high, but not extreme, environmental conditions.

Nonetheless, several limitations must be acknowledged in the current study. First, the sample size was relatively small and comprised only young, healthy university students. This population may not represent vulnerable groups such as older adults, children, pregnant women, or individuals with underlying health conditions, who are typically more susceptible to heat stress. Their thermoregulatory responses could differ significantly, thus limiting the generalizability of our findings. For example, Gagnon et al. (2016) reported that fan use at 42 °C and 50% RH increased heart rate by approximately 15 bpm in older adults compared to young adults, reflecting impaired sweating and vasodilation with age. Similarly, Wolf et al. (2023) demonstrated that the critical environmental limits at which older adults can no longer maintain heat balance occur at lower temperature–humidity thresholds than in young adults. In contrast, children exhibit higher rises in core temperature and heart rate under comparable heat exposure due to a greater surface-area-to-mass ratio and immature sweating mechanisms (Smith et al., 2019; Notley et al., 2020). These findings highlight that the thresholds identified in this thesis for young adults likely underestimate risks for vulnerable groups and reinforce the need for tailored fan-use guidelines across age categories. Second, all participants were non-acclimatized to prolonged extreme heat exposure, which might have influenced both their physiological and perceptual responses. Heat acclimatization is known to alter sweat rate,

cardiovascular function, and thermal tolerance. Future studies should explore how acclimatized populations respond differently to fan use under similar conditions. Third, the study tested only a few fan speed, whereas in real-world scenarios, fan speed and direction can be adjusted. The physiological effects and perceptual responses could vary significantly with different fan velocities and air circulation patterns. Investigating a range of fan speeds would provide a more nuanced understanding of optimal operational settings for heat mitigation. Additionally, trials were conducted over a relatively short duration (2 hours), which, while sufficient to evaluate acute physiological responses, may not capture the cumulative effects of prolonged exposure across several hours or days. Our findings showed a steady rise in physiological strain over time in all scenarios, suggesting that fan-based cooling might have diminishing returns during extended heatwave events.

Lastly, the spatial layout and airflow distribution of the chamber might differ from real residential settings, and external variables like airflow obstruction, and fan angle could influence fan effectiveness. Therefore, complementary field studies in real homes or shelters would be valuable in validating these results under practical conditions. In conclusion, this study underscores the benefits of electric fan usage, particularly table fans, as a feasible intervention for mitigating heat stress. However, their limitations under extreme environmental loads and for specific populations must be acknowledged. Further research is essential to refine fan guidelines, account for user diversity, and develop comprehensive cooling strategies that balance accessibility, effectiveness, and energy sustainability.

3.4 Summary

This chapter presented a comprehensive experimental investigation aimed at evaluating the effectiveness of electric fans in mitigating heat strain during simulated extreme heatwave conditions. The study focused on comparing three cooling scenarios: no fan, table fan, and

ceiling fan, to understand their relative performance in promoting thermal comfort and reducing physiological stress. Sixteen healthy young adults participated in the trials, which were conducted in a controlled climate chamber set to replicate severe heatwave conditions (air temperature of 41.0 ± 0.5 °C and relative humidity of 35 ± 2%) for a duration of two hours. The data collected included physiological responses such as local skin temperature, mean skin temperature, core body temperature, heart rate, and sweat production, as well as perceptual responses like thermal sensation, thermal comfort, and skin wetness.

Prior to the trials, participants were screened for uniformity in anthropometric parameters and health status to ensure consistency in results. Ethical approval was obtained, and participants gave informed consent. The measurement setup included thermocouples placed at ten body locations, a non-invasive core temperature sensor, a chest-worn heart rate monitor, and a weighing scale to determine sweat loss. Subjective feedback was collected through structured questionnaires using standardized rating scales for thermal sensation, comfort, and wetness. Air velocities generated by the fans were measured to confirm uniformity across fan conditions, ensuring valid comparisons.

Results indicated that both fan types delayed the onset of thermoregulatory and cardiovascular strain compared to the no-fan condition. Specifically, table fans provided slightly better cooling performance in terms of lower local and mean skin temperatures, reduced heart rate, and better perceptual responses. Notable findings included reductions in mean skin temperature by 0.3 °C with table fans and 0.2 °C with ceiling fans compared to the no-fan scenario. Core temperatures were consistently lower in the fan scenarios, although increases over time suggested that fan use alone may not suffice for prolonged exposures. Heart rates followed a similar trend, being highest in the no-fan scenario and lowest with the table fan.

Perceptual responses corroborated the physiological findings. Thermal sensation and thermal comfort ratings were significantly better in fan conditions. Table fans resulted in the lowest discomfort ratings, likely due to more effective sweat evaporation and better air circulation near the skin. Skin wetness sensation was also perceived to be lower in fan trials. While both fans increased sweat production, the rates remained within physiologically manageable limits and could be counterbalanced by moderate hydration practices.

The experimental setup was robust, with air temperature and humidity monitored at multiple heights to account for spatial variations. The experimental design also ensured that all participants underwent each condition, making it a within-subject study and enhancing the reliability of comparisons. However, the study was limited to young, healthy individuals. Further investigations with broader demographic groups are needed to generalize the findings.

Overall, this chapter offers detailed empirical evidence that supports the use of electric fans, particularly table fans, as effective and sustainable cooling strategies during heatwaves. The findings have practical implications for public health policy and climate-resilient design, especially in low-resource settings where air conditioning is not viable. By quantifying the physiological and perceptual benefits of fan use under controlled conditions, the study provides a foundational reference for developing evidence-based heat mitigation guidelines. The results advocate for incorporating fan use recommendations into public advisories, especially during moderate heatwaves, to enhance thermal safety and comfort in vulnerable populations.

CHAPTER 4. ELECTRIC FANS EFFECTIVENESS AND THRESHOLDS FOR HEALTHY YOUNG ADULTS DURING PROLONGED HEATWAVES: UPDATED THERMOREGULATION MODELING

Building upon the experimental findings presented in Chapter 3, which highlighted the physiological and perceptual responses of young adults to different electric fan scenarios during extreme heatwave conditions, Chapter 4 advances this investigation through numerical modeling. While the human trials provided critical empirical insights into the effectiveness of fan-based cooling strategies, they were inherently limited by ethical, logistical, and physiological constraints, particularly in exploring prolonged exposures, severe environmental extremes, and varied physical activity levels. To overcome these limitations and extend the applicability of the findings, this chapter employs a modified JOS-3 multi-segment thermoregulatory model. The modeling framework allows for a detailed simulation of human physiological responses under diverse real-world scenarios, enabling a comprehensive evaluation of electric fan effectiveness across a broader range of conditions that could not be safely replicated in experimental settings. This chapter presents a comprehensive thermoregulatory modeling investigation aimed at evaluating the effectiveness of electric fan use during prolonged heatwave conditions. Using a modified JOS-3 multi-segment model, this study simulates physiological responses under extreme heat environments by accounting for hydration depended set point temperature, change in set point temperature value, linear and exponential sweat signal and hydration dependent vasodilation signal. The model simulates a

range of heat event conditions that involved various extreme environmental conditions, different fan speeds, and physical activity levels.

The objectives of this chapter include (i) constructing and validating a segment-wise thermoregulatory model that incorporates hydration depended set point temperature, linear and exponential sweat signal and vasodilation signal; (ii) assessing the impact of ambient temperature, humidity, and air movement on thermal strain; and (iii) generating threshold charts that identify the operational range within which electric fans are beneficial or detrimental. By quantifying moderate hyperthermia onset (core temperature ≥ 38 °C), this study aims to provide actionable insights into safe fan use, helping public health stakeholders and vulnerable populations manage heat stress more effectively during severe and prolonged heatwave events.

4.1 Model description

Stolwijk's (Stolwijk, 1971) pioneering work introduced the first multi-segment thermoregulation model, comprising 25 nodes across six body segments (head, trunk, arms, hands, legs, and feet). Each segment was characterized by four concentric layers: core, muscle, fat, and skin. Stolwijk also developed governing equations for thermoregulatory processes. However, the model had limitations, such as assuming constant convection and radiation between the body and environment. Subsequent models, including Tanabe's (Tanabe et al., 2002), Fiala's (Fiala, Lomas, & Stohrer, 2001; Fiala et al., 2012), Huizenga's (Huizenga, Zhang, & Arens, 2001), ThermoSEM (Kingma et al., 2012), JOS-2 (Kobayashi et al., 2013), and JOS-3 (Takahashi et al., 2021), addressed the previous shortcomings. Among these models, JOS-3 (Takahashi et al., 2021) is widely recognized for its detailed representation of human thermal responses, its incorporation of improved shivering thermogenesis, and its non-shivering thermogenesis control approach. Therefore, we chose the JOS-3 model as the basis

for constructing a modified thermoregulation model, which serves as an initial step in evaluating electric fan thresholds during prolonged heatwaves using thermoregulation modeling. This section begins by explaining numerical solution methodology and the formulation of the thermoregulation model. Next, the generalized heat balance equation is introduced to calculate body heat transfer. Finally, the modifications made to the thermoregulation model, specifically related to hydration, set-point temperatures, and the sweating and vasodilation response, are described.

4.1.1 Overview of thermoregulation model setup

To simulate the present model, the computation program was written using the MATLAB software. Figure 4.1 displays the flow chart for evaluation of the human body temperature using the thermoregulation model in a hot environment. The calculation program for thermoregulatory simulation during a heat wave comprises six primary modules: an input module that includes parameters such as air temperature, RH, air velocity, human geometry, time, and calculation of human body parameters, discretization of the computational mesh, application of boundary conditions, initiation and feedback of control signals, and computation of thermo-physiological responses.

Next, we constructed the multi-segment human body thermoregulation model, which is based on the JOS-3 model (Takahashi et al., 2021). We divided the entire body into 17 segments (see Figure 4.2 (a)), and each segment was further divided into two layers, the core and the skin. The exceptions were the head and pelvis segments, which each consisted of four layers (core, muscle, fat, and skin) to maintain adequate prediction accuracy for the human body (see Figure 4.2 (b)). Furthermore, the core layer of each segment had two blood vessels (artery and vein), and the limb segments also had a superficial vein in the skin segment. All the segments were modeled with cylindrical geometry except the head, which was modeled as a sphere. The

details of the body surface area and the heat capacity and heat conductivity of each segment were the same as those employed in the JOS-3 model (Takahashi et al., 2021).

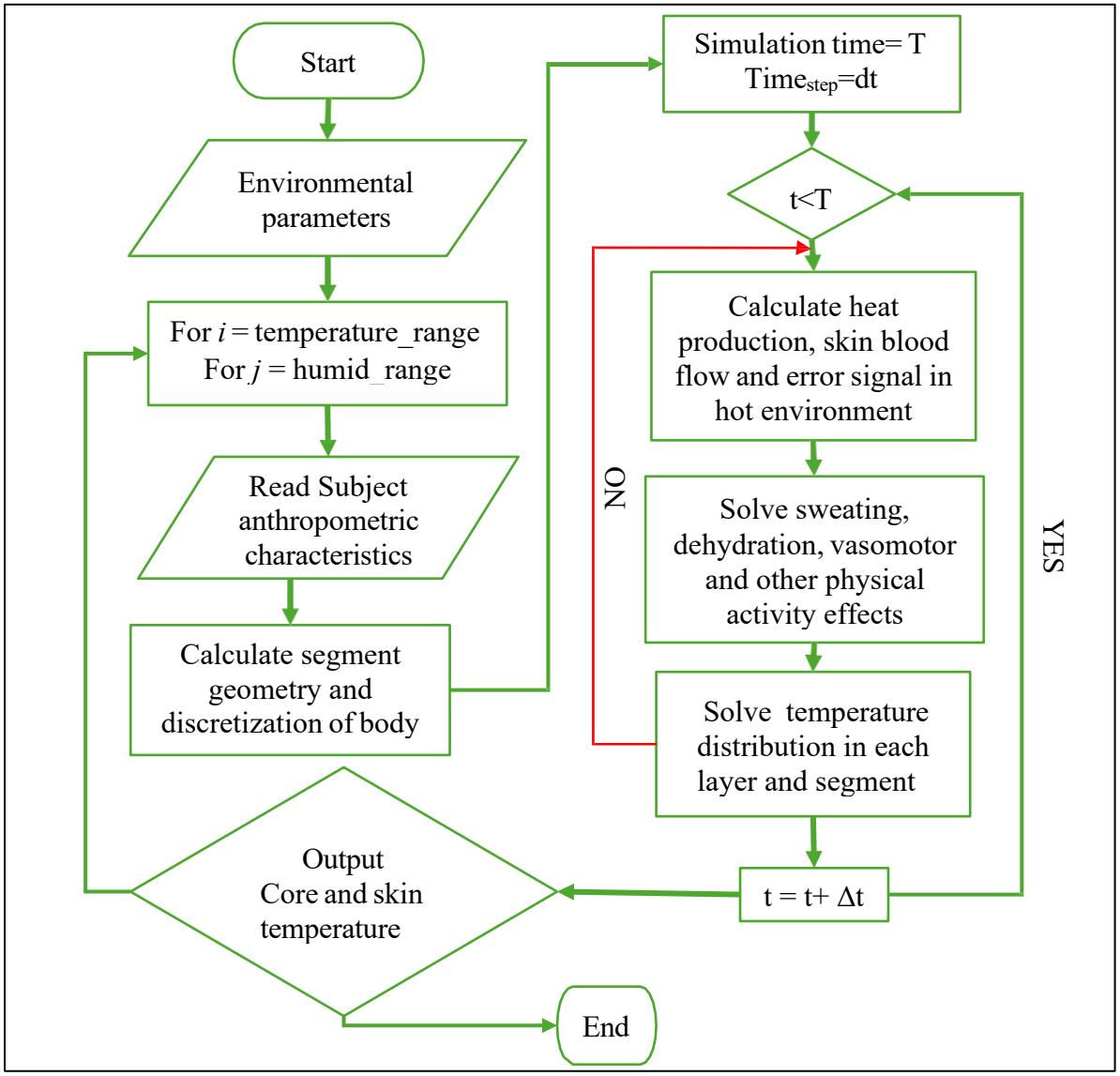

Figure 4.1. Flow chart for evaluation of human body temperature using the thermoregulation model in a hot environment.

To compute the heat transfer in the model the generalized heat balance equation is used (see equation (4.1)) (Takahashi et al., 2021):

$$C_{ap_{j(i)}} \frac{d}{dt}(T_{j(i)}) = Q_{j(i)} + B_{j(i)} - D_{j-j\&(i)} - C_i - R_i - E_i - RES \qquad (4.1)$$

where C_{ap} is the specific heat capacity of the body layer, T is the body-layer temperature, and t represents time. Meanwhile, B, Q, D, C, R, E and RES are the blood flow heat transfer, heat production, conduction heat transfer, convection heat transfer, radiation heat transfer, evaporation heat transfer and respiration heat transfer, respectively. Furthermore, the subscripts i, j and j' represent the segment, layer and adjacent body layer, respectively.

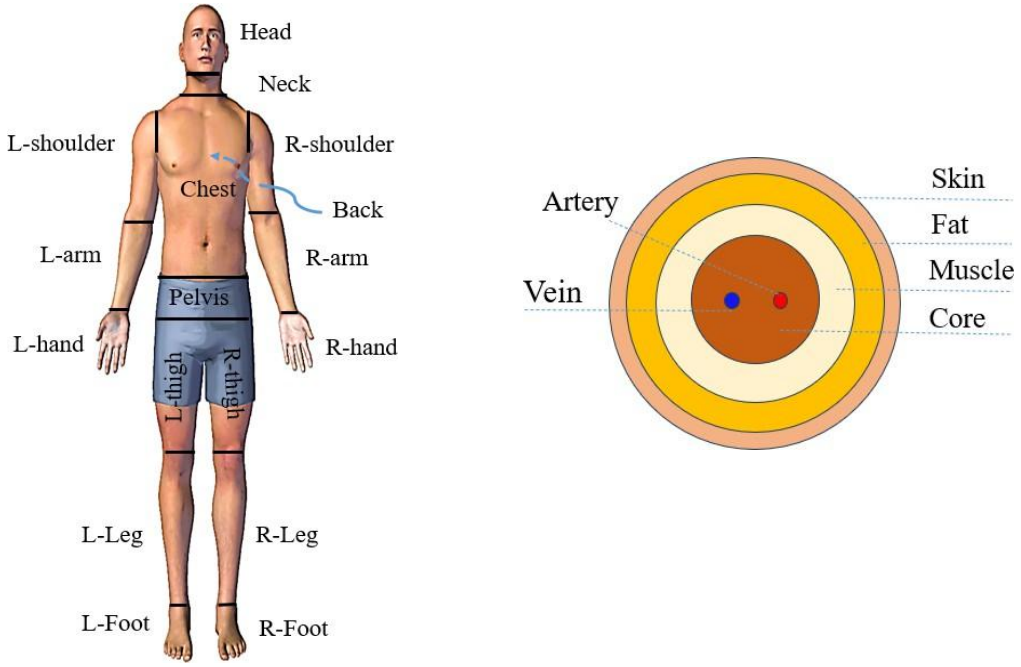

(a) (b)

Figure 4.2 Human thermoregulation model construction: (a) body division into 17 segments; (b) abdomen segment layer formulation.

Next, heat production in the body is evaluated using equation (4.2) (Takahashi et al., 2021),

$$Q_{j(i)} = M_{basej(i)} + M_{work(i)} + M_{shv(i)} + M_{nst(i)} \tag{4.2}$$

where Mbase, Mwork, Mshiv, and Mnst are heat production by basal metabolism, external work, shivering thermogenesis, and non-shivering thermogenesis, respectively. The overall metabolic rate is partially influenced by body temperature through the Q10 effect, with a sensitivity coefficient of 2 applied. At each time step of exposure, this was determined by

summing the basal metabolic rates of the individual body layers. A comprehensive description of heat production, heat transfer by blood circulation, conduction heat loss between body layers, and respiration calculations can be found in the JOS 3 and Fiala studies. In line with JOS-3 (Takahashi et al., 2021) and other established thermoregulation models, thermal characteristics of tissues (specific heat, conductivity, density) were assumed constant for each layer (core, muscle, fat, skin). Skin dryness primarily affects evaporative heat loss through the surface energy balance rather than conductive transport, which is determined mainly by fixed tissue composition.

The evaporation heat transfer (E) is calculated as (Takahashi et al., 2021),

$$E_{(i)} = w_{(i)} \times E_{\max\,(i)} \tag{4.3}$$

where, w is skin wittedness and E_{max} is maximum evaporative heat loss. The latter parameter is obtained by means of equation (4.4):

$$E_{\max\,(i)} = ((P_{sks(i)} - p_{a(i)}) \times h_{et(i)} \times BSA_{(i)} \tag{4.4}$$

where, P_{sks} and P_a are the saturated water vapor pressure at the skin and the water vapor pressure in the surroundings, respectively, and BSA is the body surface area.

Total evaporative heat transfer coefficient (h_{et}) can be obtained as:

$$h_{et(i)} = \frac{i_{cl(i)} \times L_R}{0.155\ I_{cl(i)} + \frac{i_{cl(i)}}{f_{cl}\, h_c}} \tag{4.5}$$

Here, i_{cl} and L_R are the clothing vapor permeation efficiency and the Lewis ratio, respectively, while f_{cl} and h_c are the clothing area factor and convective heat transfer coefficients (see equation (14)).

Sweating evaporative heat loss (E_{sw}) is computed as (Takahashi et al., 2021),

$$E_{sw(i)} = SKINS_{(i)} \times AGsweat_{(i)} \times SWEAT \times BSA_{ra} \times 2^{\frac{Err_{sk(i)}}{10}} \quad (4.6)$$

In the above equations, SKINS is the sweating distribution coefficient, SWEAT denotes the sweating signal, E_{rr} represents the error signal used to trigger thermoregulatory responses, and AG_{sweat} refers to the aging factor influencing the body's sweating mechanism.

The exchange of sensible heat between the skin surface and the external environment predominantly occurs through convective [$C\ (W/m^2)$] and radiation [$R\ (W/m^2)$] heat transfer mechanisms. This combined heat loss can be quantified using the formulation presented by Takahashi et al. (2021).

$$C_{(i)} + R_{(i)} = h_{t(i)}(T_{sk(i)} - T_{o(i)}).BSA_{(i)} \quad (4.7)$$

where h_t is the total heat transfer coefficient that calculated using the convective heat transfer coefficient (see equation (14)); T_{sk} is the local skin temperature; and T_o is the operative or ambient temperature.

4.1.2 Modified thermoregulatory model

In existing thermoregulation models, sensor signals such as vasodilation and sweating are activated based on fixed set-point temperatures. However, recent laboratory studies indicate that the set-point temperature are not fixed but operate within a physiological range that shifts depending on both thermal and non-thermal influence (Cabanac, 2006; Mekjavic, 2006; Montain, 1995). In particular, dehydration alters hypothalamic control through increased plasma osmolality and reduced plasma volume, which provide osmo- and baroreceptor inputs. These signals elevate the threshold core temperature for sweating and cutaneous vasodilation and reduce the sensitivity of these responses (Mekjavic, 2006; Gagnon & Kenny, 2012; Montain, 1995). As a result, for the same T_{core} and T_{skin}, a dehydrated individual produces less sweat and lower skin blood flow, conserving water and maintaining circulation but allowing

greater heat storage under hot conditions. This phenomenon reflects the concept of an "adjustable set-point," in which thermoeffector thresholds shift under stress rather than remaining constant (Mekjavic, 2006; Gagnon & Kenny, 2012; Montain, 1995). To capture this mechanism, the present model incorporates a dehydration-dependent shift in the head-core error signal, such that accumulated sweat loss progressively elevates the threshold for effector activation (see equations (4.8)–(4.9)). Hence, in the present model we have included the effect of hydration level over time on the above human physiological reactions by calculating the sweat loss (SL), i.e., the percentage of sweat lost by the body in relation to total body weight, as follows:

$$SL = \frac{Initial\ body\ weight - current\ \ body\ weight}{Initial\ body\ weight} = \frac{\int_0^t Sweat.dt}{Initial\ body\ weight} \quad (4.8)$$

The sweat loss data was further used to compute the sensor signals from the head core layer ($Err_{[0]}$) as expressed by equation (4.9) (Ivanov, 2006; Kobayashi & Tanabe, 2013);

$$Err_{cr[0]} = T_{[0]} - [T_{setpt[0]} + (\alpha \times SL)] \quad (4.9)$$

Here, $T_{[0]}$ and $T_{setpt[0]}$ represent the present temperature and head core temperature set point, respectively.

For accurate simulation of the sweating phenomenon, the temperature set point is adjusted. The set-point temperature of the head core was 37.46 °C in the JOS-3 (Kobayashi & Tanabe, 2013), but it dropped to 36.9 °C in the present model (Kobayashi & Tanabe, 2013). A lower temperature set point allows sweating to begin earlier, resulting in a response that aligns more closely with physical activity levels and environmental fluctuations. Furthermore, the threshold parameter (α) was set at 0.06 °C, and the sensitivity coefficient for sweating (β) was 0.068 $kg \cdot h^{-1} \cdot °C^{-1}$. The vasodilation threshold (γ) was also defined as 0.06 °C, following the findings of previous studies (Cabanac, 2006; Mekjavic, 2006; Montain, 1995). In contrast, the JOS-3 model used zero values for these parameters, indicating no threshold or sensitivity adjustment.

The sensor signal from the head core layer is used to compute the sweating (*SWEAT*) and vasodilation (*DILAT*) signal responses. In the JOS-3 model (Takahashi et al., 2021), single linear equation is used to represent the signal for sweating activation that caused a sudden drop in skin temperature due to the rapid onset of sweating in hot environmental conditions. To address this issue, modifications have been introduced in the present model to improve the sweating signal. Instead of using a single linear equation, the modified model incorporates a combination of linear and exponential equations. Now, the sweating slope signal is more gradual and realistic as the sweating slope signal is reduces, and thus better reflecting the natural process of sweat generation.

When $Err_{cr(1)} \leq 0.01$ and $WRMS \leq 0.4$, the signal for sweating activation (*SWEAT*) is:

$$SWEAT = (371.2 - \beta xSL)\ xErr_{cr(0)} + 33.64\ x\ (WRMS - CLDS) \quad (4.10)$$

Otherwise, the sweating signal is:

$$SWEAT = (371.2 - \beta xSL)\ xexp(Err_{cr(0)}) + 33.64\ x\ (WRMS - CLDS) \quad (4.11)$$

Furthermore, the vasodilation signal (*DILAT*) is expressed by equation (12),

$$DILAT = (100.5 - \gamma xSL)xErr_{cr(0)} + 6.4x(WRMS - CLDS) \quad (4.12)$$

Here, *WRMS* and *CLDS* are integrated warm and cold signals, respectively, and can be evaluated by different sensor signals for different body segments (Takahashi et al., 2021).

Next, skin wettedness (ω), indicating the body's capacity for sweat evaporation, is calculated as follows:

$$w_{(i)} = 0.06 + 0.94\ \frac{E_{sw(i)}}{E_{\max\ (i)}} \quad (4.13)$$

In the present model, a critical ω value of 0.85 was applied, enabling effective compensation for endogenous and exogenous heat loads. These parameters were derived from established data, including Connell et al. (Connell et al., 1924), to ensure physiological relevance.

The present model incorporates variations in convective heat transfer coefficients (h_c) across different segments under no-fan and fan scenarios by applying the formulation from de Dear et al. (De Dear et al., 1997), who conducted detailed measurements of convection heat loss in various segments inside a wind tunnel. They described the relationship between h_c and air velocity v (m/s) using the following equation (De Dear et al., 1997):

$$h_{c(i)} = Bv^n \tag{4.14}$$

Here, B and n are constant for each segment, in accordance with a study by de Dear et al. (De Dear et al., 1997). Further, radiative heat exchange coefficient (h_r) was calculated by:

$$h_r = 4\sigma\epsilon \frac{A_r}{A_d} \left(273.2 + \frac{T_{sk}+T_r}{2}\right)^3 \tag{4.15}$$

Here, σ=5.67x10^{-8} (W/m^{2}K^4) is the Stefan-Bolzmann constant, ε is the area-weighted emissivity of the clothed body surface and ε_r are the emission coefficients of the body surface, A_r is the effective radiative area of the body in m^2; A_D is the body surface area in m^2, T_{sk} and T_r are the temperatures of the body surface and mean radiant temperature which was assumed equal to ambient temperature (T_a,) respectively. This heat transfer coefficient is then used to compute the total heat transfer coefficient (h_t) and total evaporative heat transfer coefficient (h_{et}).

4.2 Validation

The present modified model was validated with various previous experimental studies that conducted in extreme hot environments to ensure model reliability and accuracy. First, the model was compared with a study by Bhuvad et al. (Bhuvad, You, & Chen, 2024), which evaluated physiological responses under no-fan and fan-assisted conditions. In that study, 16 participants were exposed to 41 °C air temperature and 35% relative humidity during 2-hour trials. The mean air speed was 0.11 m/s in the no-fan case and 1.76 m/s in a table fan case in the experiment. We incorporated these different air speeds into our model using equations (4.3)-(4.7) and equation (4.14). Figure 4.3(a) and Figure 4.3(b) provide comparisons of mean skin and core temperatures for the no-fan scenario, and the model-predicted results exhibit strong agreement with the experimental data. For core temperature in the no-fan case, the mean error (ME) was -0.046 °C, the mean absolute error (MAE) was 0.043 °C, and the root mean squared error (RMSE) was 0.047 °C, underscoring the model's precision in replicating thermal responses.

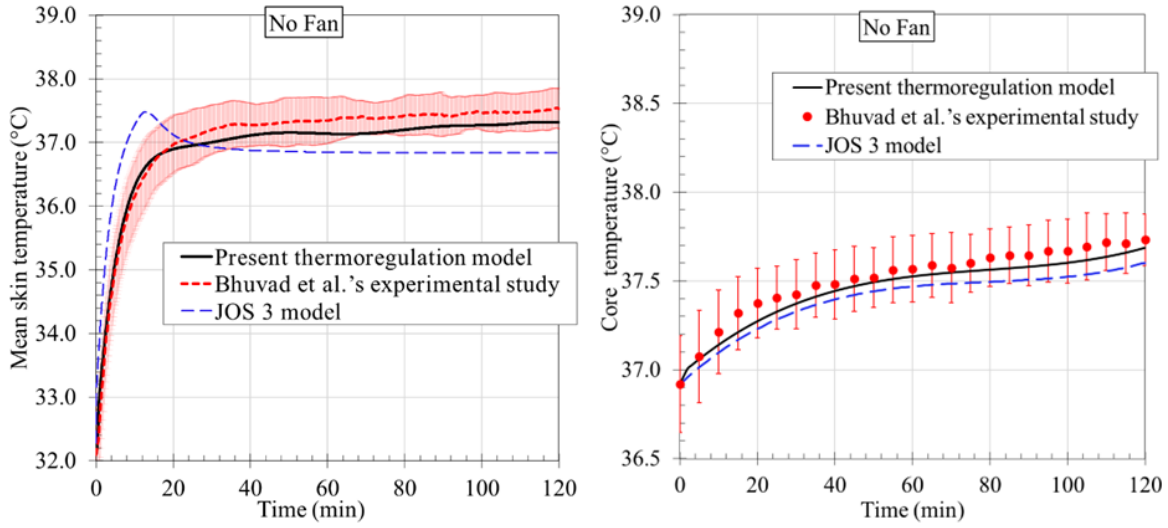

(a) (b)

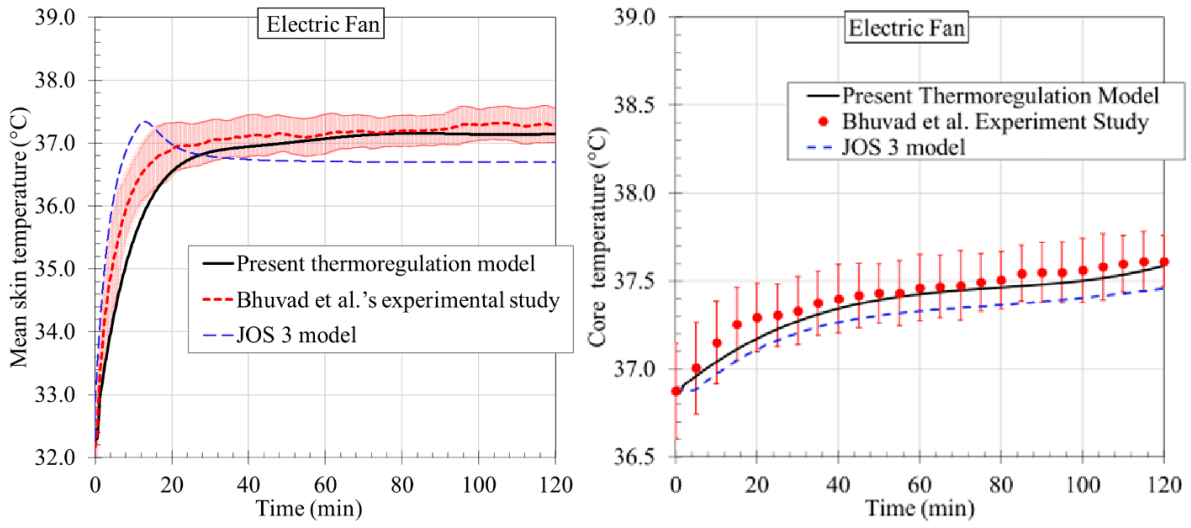

(c) (d)

Figure 4.3. Comparison of experimental study by Bhuvad et al. (Bhuvad, You, & Chen, 2024): with the present thermoregulatory and JOS 3 model: (a) mean skin temperature and (b) core temperature in no-fan case; and (c) mean skin temperature and (d) core temperature in fan case.

Additionally, the model was validated in the fan case (see Figure 4.3(c) and Figure 4.3(d)). It can be observed that there is good agreement between the result obtained from the present model and the experimental results. In both no-fan and fan conditions, the JOS 3 model was also evaluated and compared. The JOS 3 model tended to underpredict mean skin temperature, particularly in the initial transient phase, and also showed a consistent bias in underestimating core temperature. In contrast, the present model more accurately captured the thermo-physiological parameters, highlighting its improved predictive capability over the JOS 3 model.

The model was further validated with Gagnon et al.'s (Gagnon et al., 2016) experimental study, which was conducted under different heat event conditions (see Figure 4). Gagnon et al. (Gagnon et al., 2016) examined mean skin temperature and core temperature in a controlled environment. Nine young participants (mean age: 26 years) were exposed to 42 °C air

temperature, with relative humidity incrementally increasing from 30% to 70% in 2% steps every 5 minutes. Two test conditions were examined: without any cooling device and with an electric fan providing an air velocity of 4 m/s. The experimental results for mean skin temperature and core temperature were compared with predictions from both the present thermoregulation model and the JOS 3 model. Across all figures (see Figure 4.4 (a) and Figure 4.4 (b)), it is evident that the present model aligns more closely with the experimental data than the JOS 3 model. In the no-fan case, the present model captures the gradual increase in temperature with rising humidity and shows a maximum deviation of 0.56 °C for mean skin temperature and 0.2 °C for core temperature. In contrast, the JOS 3 model tends to slightly underestimate both parameters, particularly at higher humidity levels. In the fan-assisted condition, the present model continues to provide accurate predictions, reflecting the enhanced evaporative cooling effect due to increased air velocity. The JOS 3 model, although following the overall trend, underpredicts mean skin temperature and shows limited responsiveness to increasing humidity.

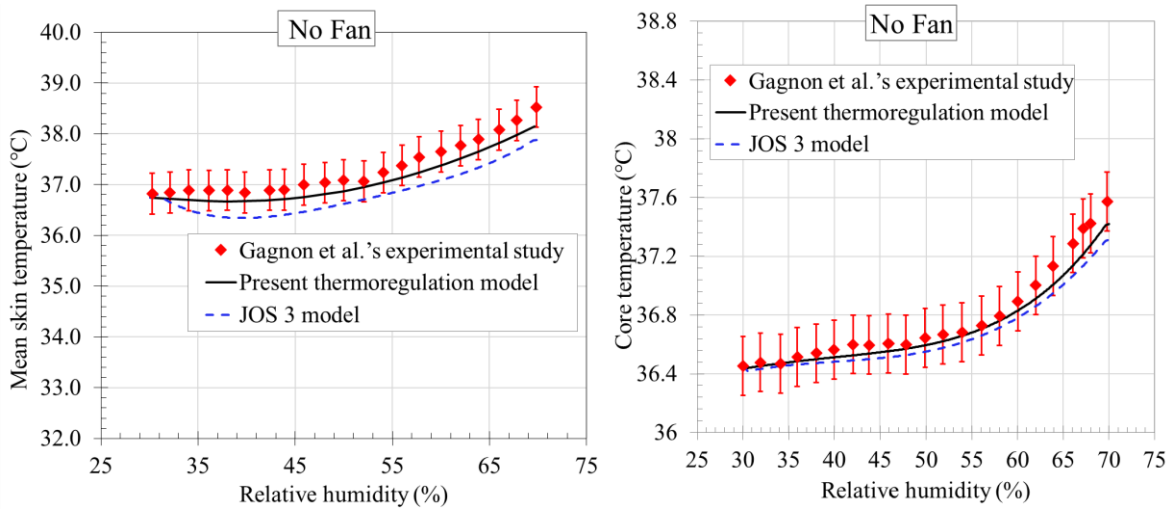

(a) (b)

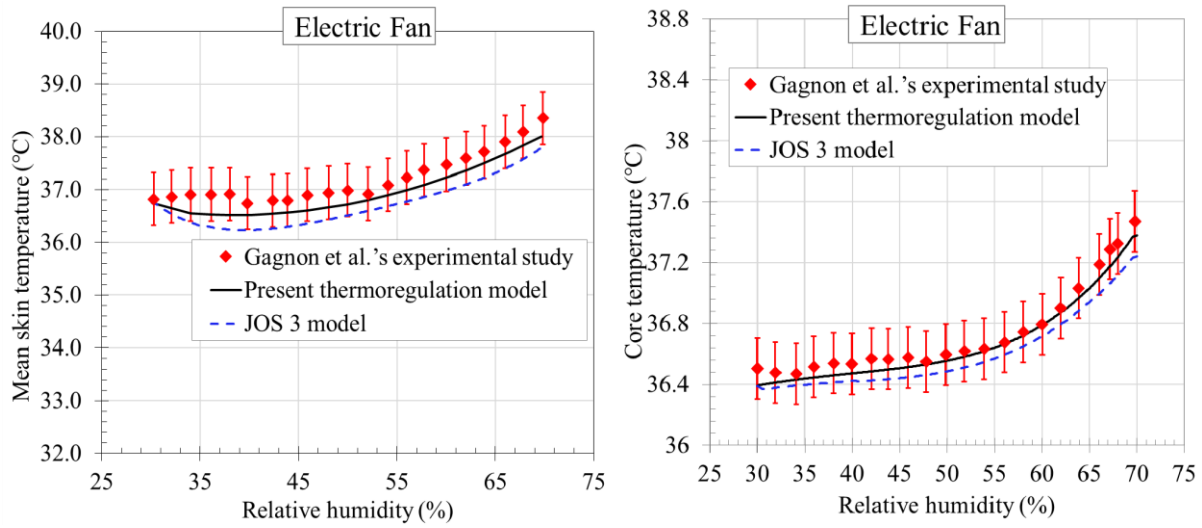

(c) (d)

Figure 4.4. Validation of the present modified model with the Gagnon et al.'s (Gagnon et al., 2016) experimental study and compared with JOS 3 model: (a) mean skin temperature and (b) core temperature in no-fan case; and (c) mean skin temperature and (d) core temperature in fan case.

Figure 4.5 shows the comparison of core temperature responses obtained from the present thermoregulation model with the experimental results reported by Beatty et al. (Beatty et al., 2015) under hot and humid conditions (35 °C air temperature and 60 % relative humidity). The experimental trials lasted for 135 minutes and involved a continuous physical workload of 400 Watts. The measured data under no-fan (air speed 0.5 m/s) and fan-assisted conditions (air speed 3 m/s) are used for model validation. In the no-fan case (Figure 4.5a), the model-predicted core temperature closely matches the experimental trend across all stages of the exercise. The predicted values capture the stepwise rise in temperature with each successive workload increment, with minimal over- or under-prediction. The JOS 3 model, although following the overall trend, tends to overpredict core temperature values in the latter half of the exposure duration, particularly beyond 75 minutes.

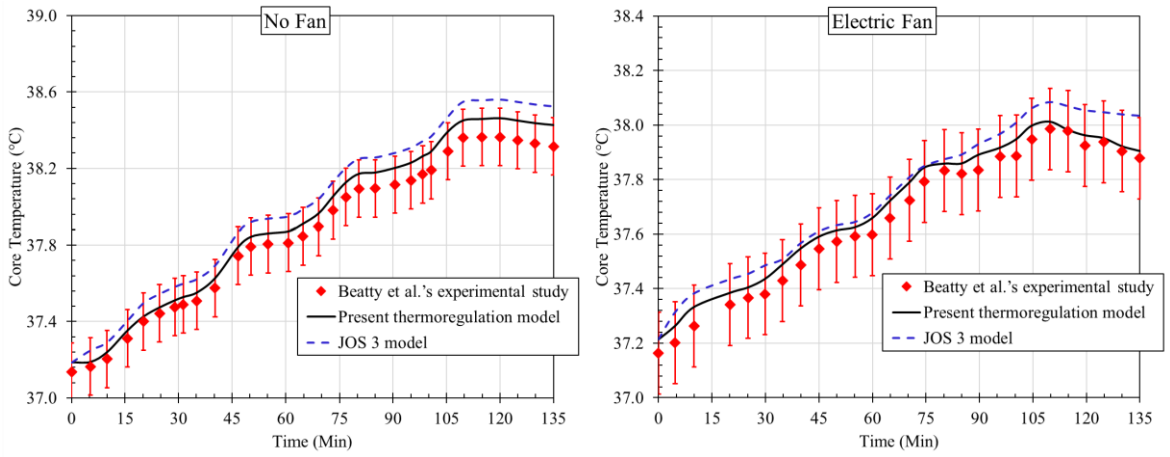

(a) (b)

Figure 4.5. Comparison of core temperature from Beatty et al.'s (Beatty et al., 2015) experimental study with the present thermoregulatory and JOS 3 model: (a) No fan and (b) fan cases.

In the fan-assisted case (Figure 4.5b), the measured core temperature shows a moderated increase compared to the no-fan condition due to enhanced convective cooling. The present model successfully reflects this moderated rise and tracks the variations observed across the full trial duration. In contrast, the JOS 3 model continues to show a linear increase in core temperature and fails to replicate the observed plateauing effect in the final phase. Overall, the present model effectively simulates the thermoregulatory response across both cases, while the JOS 3 model displays notable limitations in capturing the behaviours.

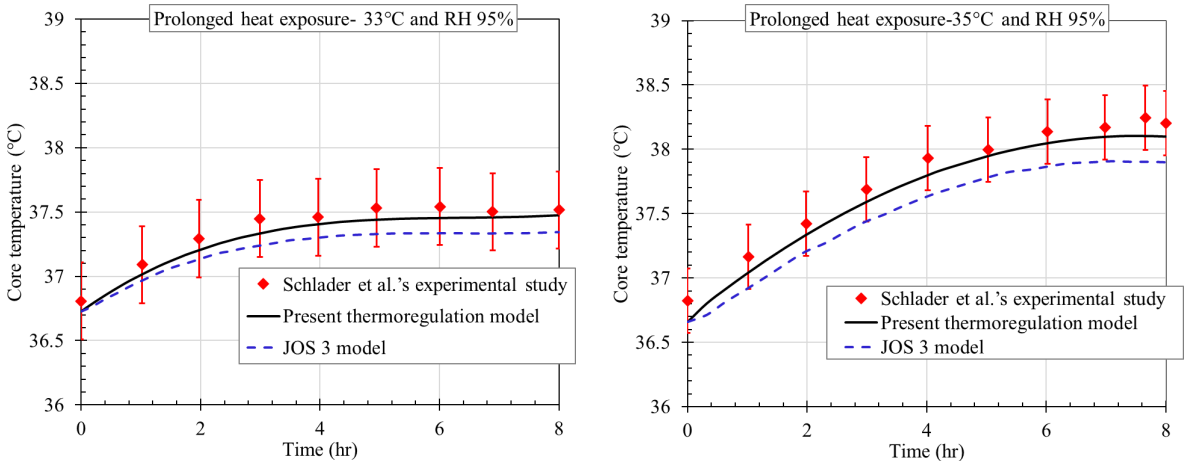

(a) (b)

Figure 4.6. Comparison of core temperature from Schlader et al.'s (Schlader et al., 2020) prolonged heat exposure experimental study with the results of the present model and JOS 3: (a) under 33 °C, RH 95%; and (b) under 35 °C, RH 95%.

The present model was further validated using an experimental study by Schlader et al. (Schlader et al., 2020), which analyzed core temperature responses in controlled hot and humid conditions under prolonged heat exposure. The study involved 15 participants, aged 23 years, who were exposed to ambient temperatures of 33 °C and 35 °C at a consistent relative humidity of 95% for 8 hours. Strong agreement can be seen in Figure 4.6 (a), with a root mean squared error (*RMSE*) of 0.02 °C, highlighting the model's accuracy. The maximum deviation from experimental results was 0.085 °C, demonstrating the reliability of the present model in replicating thermal responses in extreme hot environments for long durations (see Figure 4.6 (a) and Figure 4.6 (b)). In both cases, the present model successfully captures the gradual rise and saturation trend of core temperature across the 8-hour exposure. Overall, the present model reflects the thermoregulatory adaptation and delayed thermal equilibrium more accurately than the JOS 3 model. The ability of the present model to follow the time-dependent physiological response with minimal error reinforces its enhanced performance over existing modeling.

4.3 Case Study & Results

Climate change has increased the frequency and intensity of heat events, leading to prolonged extreme temperatures. For example, during the 2021 heatwave in Canada, indoor temperatures exceeded 42 °C for over 4 hours. Similarly, daytime temperatures of 46–47 °C with 10–20% RH have been recorded in Asian countries. To replicate such extreme events and capture the combined effects of temperature and humidity on human thermoregulation, a 5-hour heat exposure period was simulated across a range of ambient temperatures (35 °C to 55 °C) and relative humidity levels (10% to 90%). Although real-world exposures above 50 °C may not typically persist for extended durations, including such extreme conditions in the analysis is crucial for understanding potential future heatwave intensities under climate change scenarios. Further, moderate hyperthermia (core temperature between 38.0 °C and 39.0 °C) is associated with fatigue, mild confusion, and heightened heat stress, while severe hyperthermia (>39.0 °C) can cause dizziness, confusion, and heatstroke above 40.0 °C (Morris et al., 2021; Tartarini et al., 2022; Meade et al., 2024). We chose moderate hyperthermia as the key indicator because it reflects a critical threshold at which heat stress begins. Furthermore, we used 38 °C as the threshold for evaluating fan effectiveness in preventing unchecked hyperthermia, as it is also a commonly recommended upper limit for occupational heat exposure (Morris et al., 2021; Tartarini et al., 2022; Meade et al., 2024). Therefore, fans were considered effective if they maintained core temperatures below 38.0 °C and lower than no fan scenario, and detrimental if they accelerated temperature rise above this threshold or core temperature is higher in fan case. Additionally, simulations were stopped once the core temperature reached 39.5 °C, as this threshold indicates that the body is approaching dangerous levels of thermal strain and may require immediate cooling interventions or clinical support. This section presents the results of thermoregulation modeling to evaluate electric fans' effectiveness during extreme heat events. First, we discuss the effects of extreme environmental conditions on core temperature. Next,

the results are analyzed in terms of the effects of extreme air temperature and humidity on core temperature, the onset of moderate and severe hyperthermia, and the role of fan air movement. Finally, moderate hyperthermia onset charts are presented to provide insights into the conditions under which fans are beneficial or detrimental during prolonged heat exposure.

4.3.1 Effects of extreme environmental conditions on core temperature

To evaluate the impact of extreme heat environment conditions, we considered a hypothetical male subject aged 24 years, with a height of 1.73 m, a body mass of 71.5 kg, and a body surface area (BSA) of 1.85 m² (Meade et al., 2024). The subject was assumed to be in an indoor environment with a physical activity ratio (PAR) of 1.2 (sedentary behavior) and dressed in light summer clothing (0.4 clo insulation, 0.38 permeability index). The occupant was non-acclimatized to extreme heat, ensuring that the physiological responses represented those of a healthy, unadapted young individual (Morris et al., 2021; Tartarini et al., 2022; Meade et al., 2024). Figure 4.7a illustrates the effect of air temperature ranging from 35 °C to 50 °C on core temperature over time under relative humidity of 50% in a no-fan scenario. We found that as air temperature increases, the core temperature also rises. At air temperatures below 42 °C, the core temperature remains below the moderate hyperthermia threshold (38 °C) throughout the 5-hour exposure period, indicating manageable heat stress under these conditions. However, at air temperatures exceeding 44 °C, the core temperature reaches the severe hyperthermia threshold (39 °C) within 2 hours. This observation can be attributed to the body's reduced ability to dissipate heat as external temperatures approach or exceed the thermoneutral zone for sweat evaporation. Notably, at air temperatures of 46 °C and above, the core temperature rises sharply, surpassing the severe hyperthermia threshold within the first 4 hours of exposure. This rapid increase indicates that the body's thermoregulatory mechanisms are unable to cope with extreme heat, leading to a substantial risk of heatstroke. The steep rise in core temperature

at higher air temperatures is likely due to insufficient evaporative cooling, compounded by increased sensible heat gain from the surroundings due to the higher ambient temperature. Beyond 48 °C, the body's heat accumulation rate becomes critical, with severe hyperthermia observed in less than 2 hours, suggesting an extremely high likelihood of life-threatening heat-related illnesses such as heat stroke. These findings emphasize the critical impact of air temperature on thermal strain, particularly in the absence of active cooling measures such as electric fans or other sustainable cooling methods.

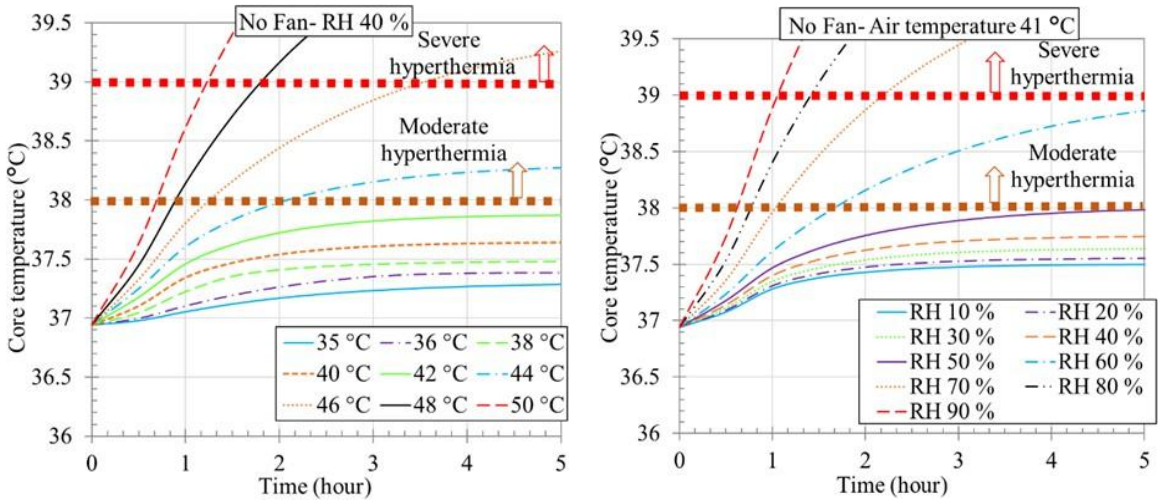

(a) (b)

Figure 4.7. Core temperature variation over time in no-fan condition during extreme heat events: (a) air temperature varies from 35 °C to 50 °C with fixed relative humidity of 40 %; (b) relative humidity varies from 10% to 90% with fixed air temperature of 41 °C.

Figure 4.7b demonstrates the variation in core temperature over time under no-fan conditions, with relative humidity (RH) ranging from 10% to 90% at an air temperature of 41 °C. At lower RH levels, such as 10% and 40%, the core temperature rises very gradually, remaining well below the moderate hyperthermia threshold (38 °C) even after 5 hours of exposure, indicating manageable thermal strain in low-humidity conditions. In contrast, at RH levels of 60% or higher, the core temperature reaches the moderate hyperthermia threshold in less than 2 hours,

highlighting the significantly increased risk of thermal stress as humidity rises. At even higher RH levels, specifically between 70% and 90%, the core temperature rapidly exceeds the severe hyperthermia threshold (39 °C) within the first few hours of exposure. This rapid increase suggests that the combination of high humidity and elevated air temperature severely limits the body's ability to dissipate heat through sweat evaporation, resulting in accelerated heat accumulation. These findings underscore the critical role of relative humidity in amplifying heat stress, particularly when the air temperature is high. The data indicate that high-humidity environments pose a severe risk of hyperthermia and heat-related illnesses within a short duration.

4.3.2 Effects of fan speed on core temperature

Different fan speeds were tested to determine their influence on core temperature. Four air movement scenarios were considered: no fan (0.1 m/s) and fan speeds of 0.8 m/s, 1.7 m/s, and 3.0 m/s, representing commercially available settings (Tartarini et al., 2022). The anthropometric characteristics of the subject and other experimental conditions were consistent with those described earlier. Figure 4.8a shows the effect of different air speeds on core temperature during heat exposure at an ambient temperature of 39 °C and relative humidity of 50%. As fan air speed increases, the core temperature decreases, indicating that the increase in fan speed enhanced evaporative cooling. In the no-fan scenario (air speed 0.1 m/s), the core temperature rises more sharply and stabilizes at a higher level than in the higher air speed cases in which the fan was used. This observation can be attributed to the reduced effectiveness of sweat evaporation at lower air velocities, leading to greater heat retention. At higher fan speeds (e.g., 1.7 m/s and 3 m/s), the core temperature stabilizes at significantly lower values. This is due to the fact that the increased air movement created by the fan enhances sweat evaporation and reduces total heat storage in the body. Although higher fan speeds increase sensible heat

gain from the surrounding environment, the enhanced evaporative cooling compensates for this increase, resulting in an overall reduction in heat strain. Furthermore, even though higher fan speed reduces the core temperature, the effect of fan speed on core temperature becomes less pronounced as the speed increases.

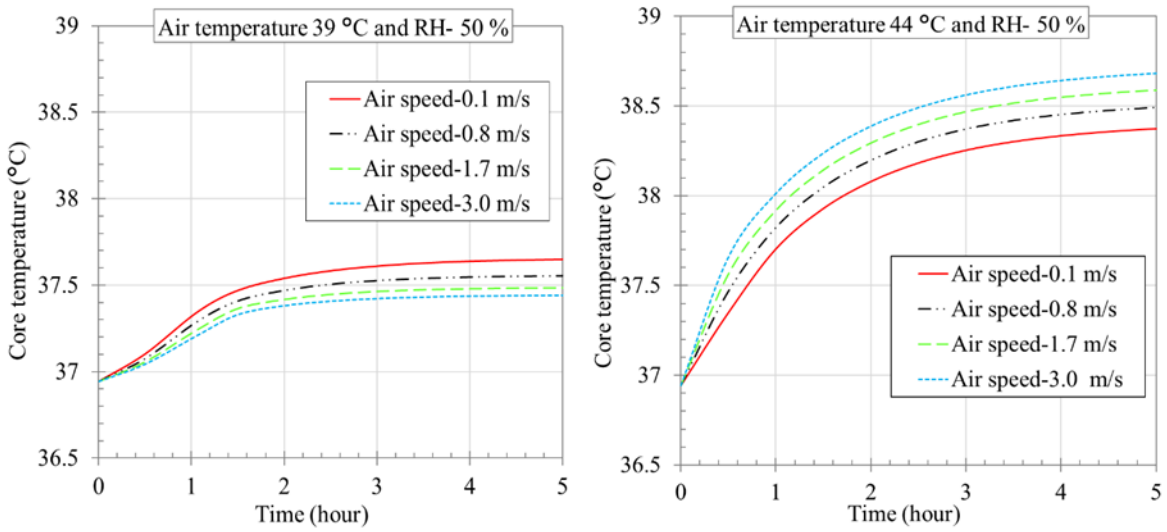

(a) (b)

Figure 4.8. Core temperature variation during heat exposure with no fan (0.1 m/s) and in different fan speed scenarios (0.8 m/s, 1.7 m/s, and 3.0 m/s): (a) air temperature of 39 °C and relative humidity environment 50 % (b) air temperature of 44 °C and relative humidity of 50%.

To keep this paper concise, results on whole-body sweat loss and evaporative heat loss from skin for no-fan and fan (0.8 m/s) cases are presented in Appendix B. These results show that sweat losses are not always lower when fans are used, as one might intuitively expect. In most temperature–humidity combinations, predicted sweat losses are slightly higher under still-air conditions compared to fan use at 0.8 m/s (see Table B1 and Table B2). Conversely, fan use leads to higher sweat losses when relative humidity is below 40% and ambient temperature exceeds 40 °C, as the additional sensible heat gain must be offset. Importantly, the maximum difference in sweat loss due to fan use is small (<35 mL/h) and easily compensated. By contrast,

evaporative heat loss at the skin surface is consistently higher with fan use (Table B3), which explains the lower core temperatures observed with fans despite small changes in total sweat loss. Figure 4.8b presents the core temperature variation over a 5-hour period under different air speeds (0.1 m/s, 0.8 m/s, 1.7 m/s, and 3.0 m/s) at an ambient temperature of 44 °C and 50% relative humidity. Unlike typical scenarios where higher air speed enhances cooling, Figure 8b shows an unusual trend: as the air speed increases, the core temperature stabilizes at progressively higher levels. This finding indicates that in such an extreme environment, fan use may be counterproductive. At the lowest air speed (0.1 m/s) (no fan scenario), the core temperature at the end of 5 hours is 38.37 °C. However, at higher air speeds, the core temperature exceeds the moderate hyperthermia threshold earlier and at the end of 5 hours, with the 3.0 m/s scenario exhibiting the highest core temperature at approximately 38.68 °C. This suggests that the increased air movement enhances sensible heat gain from the hot environment, outweighing the benefits of evaporative cooling. The observed trend can be attributed to the fact that at high ambient temperatures, airflow accelerates heat transfer from the environment to the skin. This reduces the net heat dissipation, as the skin absorbs more heat than it loses through evaporation. Consequently, increased airflow under such conditions intensifies thermal strain, leading to higher core temperatures. This finding highlights the critical threshold at which fan use transitions from being beneficial to being detrimental. Overall, these findings emphasize the need to optimize fan speed based on environmental conditions in order to achieve maximum cooling efficiency.

4.3.3 Moderate hyperthermia onset chart for electric fan use

Figure 4.9 displays the onset times for moderate hyperthermia (core temperature reaching 38.0 °C) across varying ambient temperatures and relative humidity levels under electric fan speed of 0.8 m/s and activity level of 1.2 PAR. Fan use is effective (green zone- FE) when Tc-fan <

38.0 °C and Tc-fan reduction relative to no-fan by ≥ 0.1 °C; trivial (yellow zone- FT) when Tc-fan < 38.0 °C with a reduction relative to no-fan < 0.1 °C; detrimental (orange zone- FD) when Tc-fan < 38.0 °C but exceeds no-fan; and detrimental (red zone) when Tc-fan > 38.0 °C and exceeds no-fan. Fans are effective (green zone) at lower ambient temperatures and moderate RH levels. For instance, at 40 °C and RH up to 40%, fans prevent core temperatures from exceeding the threshold for hyperthermia and also show lower values compared to no-fan. Similarly, at 35 °C, fans maintain safe core temperatures up to 80% RH. However, fan effect is trivial as reduction in core temperature compare to no fan is lower than 0.1 °C (at 43 °C with 10–30%). However, at extreme temperatures, such as 50 °C, fans become detrimental, with onset times for hyperthermia becoming significantly shorter. At 50 °C and 10% RH, the onset time is 1.14 hours, dropping dramatically to just 0.22 hour at 90% RH. This highlights the combined effect of high temperature and humidity in accelerating thermal strain, limiting the benefits of fan use. In conditions exceeding 46 °C with RH above 60%, hyperthermia onset times become critically short, often less than 0.5 hour. At 55 °C, regardless of RH, fans are unable to mitigate overheating effectively, as the onset of moderate hyperthermia is almost immediate (0.58 hour at 10% RH). This indicates the severe risks posed by extreme temperatures and humidity, where fan use alone is insufficient for cooling. Above 43 °C with 40% RH, fans fail to keep core temperatures below the hyperthermia threshold, transitioning into the detrimental (red zone) category. This demonstrates the limitations of fans under extreme environmental conditions and highlights the need for supplemental cooling methods, especially during prolonged heat waves. Furthermore, between 44 °C and 46 °C with 10–20% RH, although hyperthermia is not triggered, fan use is considered detrimental as the core temperature exceeds the no-fan condition by >0.1 °C. Overall, fans are beneficial up to 43 °C with 10–20% RH.

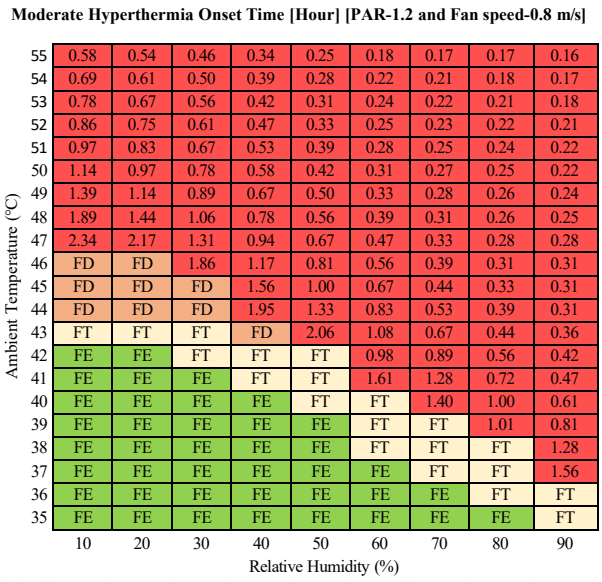

Figure 4.9. Moderate hyperthermia onset chart under various extreme environmental conditions under fan speed of 0.8 m/s and PAR of 1.2. Fan use is effective (green zone- FE) when Tc-fan < 38.0 °C and Tc-fan reduction relative to no-fan by ≥ 0.1 °C; trivial (yellow zone- FT) when Tc-fan < 38.0 °C with a reduction relative to no-fan < 0.1 °C; detrimental (orange zone- FD) when Tc-fan < 38.0 °C but exceeds no-fan; and detrimental (red zone) when Tc-fan > 38.0 °C and exceeds no-fan.

To keep this paper concise, the findings regarding the effects of different fan speeds are provided in Appendix B. Figure B 2 illustrates the onset of moderate hyperthermia under varying electric fan speeds (1.7 m/s and 3.0 m/s) across different ambient temperatures and relative humidity levels. At a fan speed of 1.7 m/s, the onset of moderate hyperthermia accelerates compared to a fan speed of 0.8 m/s (See Figure B 2(b)). For instance, at 45 °C and 50% RH, hyperthermia occurs within 0.86 hour at 1.7 m/s, compared to 1 hours at 0.8 m/s. Similarly, at 47 °C and 40% RH, the onset time drops from 0.94 hours at 0.8 m/s to 0.78 hour at 1.7 m/s. This trend can be attributed to higher sensible heat gain from the surrounding environment as fan speed increases. Enhancing air circulation at greater speeds reduces the effectiveness of sweat evaporation by increasing dry heat gain, which outweighs the benefits

of evaporative cooling. Consequently, higher fan speeds result in greater heat accumulation in the body, leading to a faster progression to moderate hyperthermia.

Meanwhile, at a fan speed of 3.0 m/s, the onset of hyperthermia further accelerates. For example, at 45 °C and 50% RH, hyperthermia begins within 0.75 hour (fan speed of 3.0 m/s) compared to 0.86 hour at 1.7 m/s. Similarly, at 50 °C and 40% RH, the onset drops to 0.44 hours at 3.0 m/s, compared to 0.50 hour at 1.7 m/s. This trend indicates that the additional air circulation at 3.0 m/s increases dry heat transfer from the environment to the body, completely outweighing the benefits of sweat evaporation, particularly at high temperatures and humidity levels. These findings underscore the need for caution when increasing fan speeds in severe heat, as higher air movement may exacerbate thermal strain rather than alleviate it. Overall, compared to a lower fan speed of 0.8 m/s, fan speeds of 1.7 and 3.0 m/s demonstrate reduced effectiveness in delaying hyperthermia onset, especially at extreme temperatures above 45 °C and RH levels exceeding 50%. However higher fan speeds provide a better cooling benefit (lower core temperature than no fan) below 43 °C and 10 % RH.

4.3.4 Moderate hyperthermia onset chart under various activity levels during electric fan use

To evaluate the impact of activity levels on core temperature under different fan speed during extreme heat events, physical activity levels were classified using the physical activity ratio (PAR): 1.2 for sedentary behavior, 1.8 for light tasks like standing, 2.8 for moderate activity (Walking slowly), and 3.8 for Walking quickly [[36], [55]]. This classification enabled an assessment of metabolic heat generation and its interaction with environmental heat stress. As illustrated in

Figure 4.10, the benefits of fan use are strongly influenced by physical activity ratio. At PAR-1.2 (Figure 4.9), fans are beneficial under specific conditions, maintaining safe core

temperatures at ambient temperatures up to 43 °C with RH levels below 10% compared to no fan. For example, at 41 °C and 30% RH, hyperthermia does not occur within the exposure period and also show lower core temperature compared to no fan, indicating effective heat dissipation through sweat evaporation. However, as the activity level increases to PAR-1.8 (

Figure 4.10a), the effectiveness of fan use is diminished considerably. At 41 °C and 50% RH, hyperthermia now occurs within 1.61 hours, compared to no risk at PAR-1.2. Similarly, at 43 °C and 40% RH, the onset of hyperthermia accelerates to 1.27 hours, reflecting the additional production of metabolic heat by higher activity, which amplifies thermal strain. Furthermore, fan is only effective up to 38 °C and 40% RH and above that fan usage is trivial till 41 °C and 30% RH. At PAR-2.8 (

Figure 4.10b), the safe zones for fan use are further diminished. Hyperthermia onset occurs within 0.79 hour at 41 °C and 50% RH, demonstrating that the fan becomes less effective in maintaining thermal balance as metabolic heat increases. Moreover, fan use is trivial and does not provide any significant advantage compared to the no-fan scenario at lower ambient temperatures and humidity such as 35 °C and 10% RH. At 43 °C and 40% RH, hyperthermia occurs within 0.79 hour, compared to 1.28 hours at PAR-1.8, underscoring the compounding effect of increased metabolic heat and environmental heat stress. At PAR-3.8 (

Figure 4.10c), the fan is no longer beneficial under most conditions. For instance, at 38 °C and 30% RH, hyperthermia occurs within 1.8 hours, while at 43 °C and 40% RH, it occurs in just 0.74 hour, compared to 1.28 hour at PAR-1.8. Even at less extreme ambient conditions, such as 36 °C and 40% RH, hyperthermia occurs within 1.71 hours at PAR-3.8, highlighting the limited efficacy of fans at high activity levels.

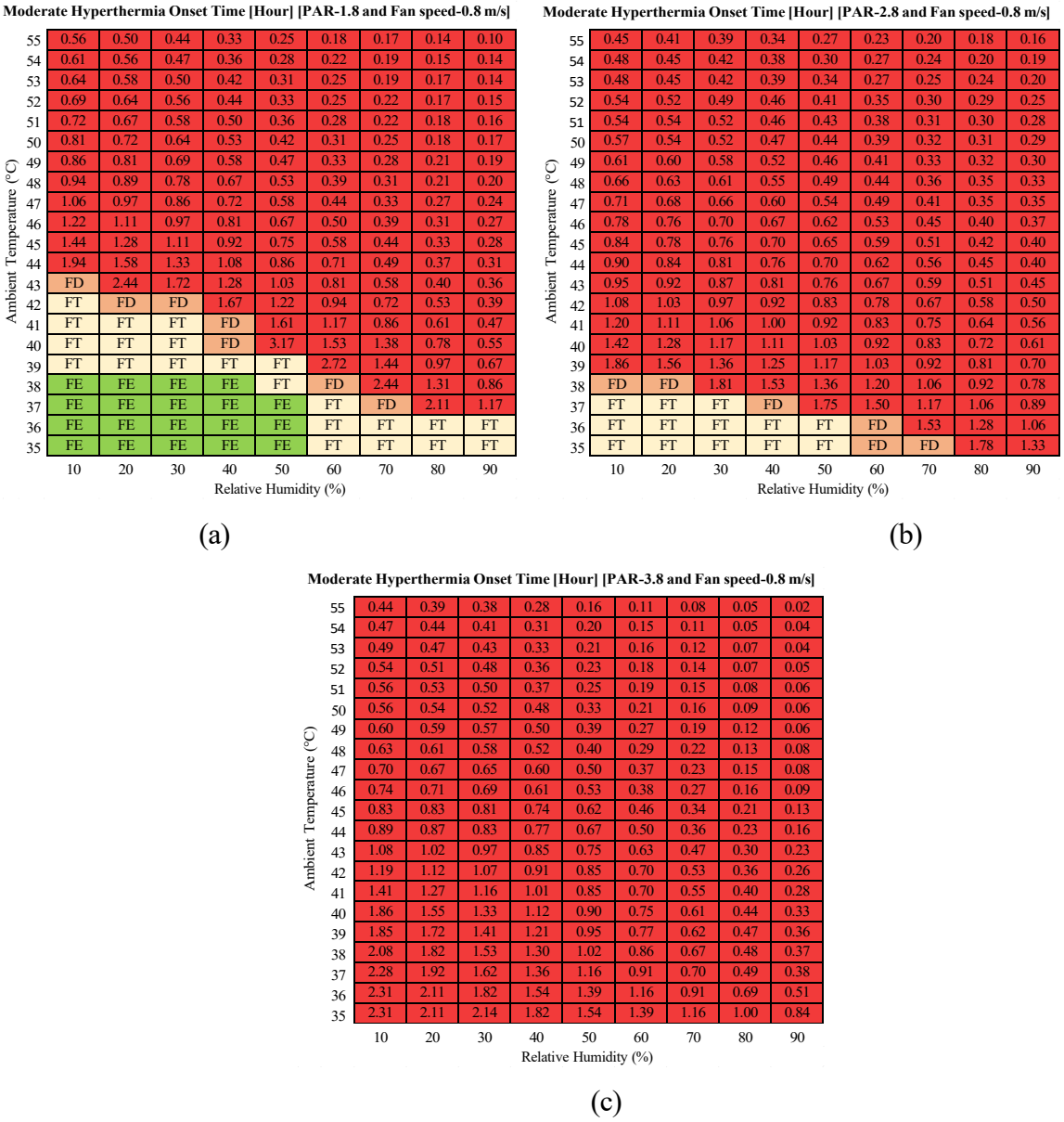

Figure 4.10. Moderate hyperthermia onset chart for electric fan use under various extreme environmental conditions and electric fan speed of 0.8 m/s. Fan use is deemed effective (blue zone) when it maintains core temperatures below 38.0 °C, and detrimental (yellow zone) if it accelerates the rise to 38.0 °C compared to no-fan conditions. (a) Activity level of 1.8 PAR; (b) activity level of 2.8 PAR; and (c) activity level of 3.8 PAR.

As metabolic heat production increases due to higher-PAR activities, the body's ability to dissipate heat through sweat evaporation and convective cooling becomes insufficient. Higher metabolic heat production overwhelms the thermoregulatory system, leading to faster heat

accumulation and a significant reduction in the safe exposure duration. For example, at 45 °C and 50% RH, hyperthermia occurs in 1 hour at PAR-1.2, 0.75 hour at PAR-1.8, and 0.69 hour at PAR-2.8. At extreme temperatures such as 50 °C with 70% RH, hyperthermia occurs within 0.21 hour across all activity levels, rendering fan use ineffective. Overall, we found that fan use is beneficial at lower activity levels (PAR-1.2) under moderate environmental conditions but becomes increasingly detrimental as PAR increases or when temperatures and RH levels are high. The interplay among ambient heat, humidity, and metabolic heat production critically determines the effectiveness of fan use. Fans fail to provide sufficient relief under extreme heat stress or high activity levels, as the additional metabolic heat outweighs the evaporative cooling benefits provided by air movement, leading to accelerated hyperthermia onset.

The findings regarding the effects of different fan speeds and PAR levels on the onset of moderate hyperthermia are provided in the figures in Appendix A. At PAR 1.8, increasing the fan speed from 1.7 m/s to 3.0 m/s accelerates the onset of hyperthermia under higher ambient temperatures and humidity (Figure B 3). For example, at 45 °C and 40% RH, the onset time decreases from 0.84 hour at a fan speed of 1.7 m/s to 0.86 hour at 3.0 m/s. This trend becomes more pronounced at higher activity levels. As shown in Figure B 4, at PAR 2.8 and 43 °C with 30% RH, the onset time drops slightly when air speed increases. Figure B 5 depicts a similar trend in results at PAR 3.8. This comparison reveals that while fans provide cooling benefits at lower PAR and fan speeds, they are significantly less effective under higher metabolic heat production and greater air circulation, making their use less favourable in extreme heat and high humidity.

4.4 Discussion and Limitation

This study evaluated the effectiveness of electric fans under prolonged heatwave conditions through thermoregulation modeling across various environmental scenarios, fan speeds, and

physical activity levels. The findings highlight the complex interplay among air temperature, relative humidity, fan speed, and metabolic heat production in determining the onset of moderate hyperthermia. In present study, the hyperthermia onset charts were compared with thresholds reported in previous laboratory work. Through our present model, we found that at 47 °C and 10% RH, the moderate hyperthermia occurs after 2.34 hours (at 0.8 m/s fan speed) and core temperature in the fan case is higher than in the no-fan scenario. Moreover, in such scenario the increment in fan speed is more detrimental (see Figure A2 and A3) since sweat can easily evaporate even without elevated air movement, while higher fan speed increases heat gain. Similar results were observed in the Morris & Jay [13] laboratory study comprising 12 healthy men, which showed that for 47 °C and 10% RH with a fan speed of 2 m/s, fan use is not advisable. Furthermore, Morris & Jay's [13] and Bhuvad et al. [16] lab studies also showed that fans are beneficial at 40 °C and 50% RH (fan speed 2 m/s) and 41 °C and 35% RH (fan speed 1.7 m/s), respectively. Our model also predicted that in above scenarios fan use delays the onset of hyperthermia and is beneficial by enhancing evaporation despite additional sensible heat gain. At PAR of 1.2 (v-1.7 m/s), our hyperthermia onset chart shows fans are beneficial up to 42 °C at 10–20% RH, trivial around 43 °C at 10–30% RH, and increasingly detrimental above these limits (see Figure A2). Similar result trends are found in Morris et al. [23] and Tartarini's [25] studies; however, our present model is more conservative as it computes hyperthermia onset time which can be useful for understanding how human core temperature varies with time in extreme heat environments and provides detail on how much time individuals have before hyperthermia onset. This is crucial for people performing higher physical activity so that heatwave guidelines can regulate work–rest cycles and ensure breaks before core temperature accelerates above the hyperthermia threshold. Additionally, The results reported by Morris et al. [23] at a fan speed of 4.0 m/s may be difficult to generalize, as such high air velocities are rarely achievable with most commercially available fans [16],

and the airflow is unlikely to be distributed uniformly across the body. Furthermore, cross-study validation remains essential to strengthen these findings. It is also noted that the present predictions did not replicate Foster's [24] results. The fundamental difference between our chart and Foster chart [24] is that Foster's chart shows fans are detrimental in hot–dry air but become beneficial as RH increases, e.g., at 46 °C and 50% RH nonetheless in our study we found that are detrimental in such extreme scenarios. To clarify whether fans are beneficial or detrimental in such scenarios, more experimental studies are required under different physical activity levels. However, compared to the previous models the present thermoregulation model can be extended to integrate other simple and sustainable cooling strategies such as foot immersion, leg immersion, and dousing, due to its detailed thermoregulation modeling [49], thereby further understanding fan effectiveness to improve fan-use guidelines.

We found that at PAR 1.2 and a fan speed of 0.8 m/s, fans are beneficial up to 42 °C with 10–20% RH, becoming trivial around 43 °C with 10–30% RH, and detrimental above this range. Higher fan speeds provide added benefit only below 43 °C at very low humidity (10%), where they enhance evaporative heat loss. Beyond 46 °C with RH above 60%, fan use consistently becomes detrimental, with hyperthermia onset occurring rapidly. At even higher fan speeds (e.g., 3.0 m/s), sensible heat gain outweighs the benefits of evaporation, further shortening safe exposure times (e.g., at 50 °C and 40% RH). Increasing physical activity amplifies these effects: at PAR 1.8, fans are effective only under milder conditions (≤38 °C, 30% RH), with diminishing benefits at higher temperatures. By PAR 2.8, fan use is already trivial below 37 °C and becomes detrimental above 37 °C and 40% RH, while at PAR 3.8 fans are detrimental under nearly all conditions due to the compounding effect of metabolic heat production and environmental stress. The moderate hyperthermia onset charts provided a comprehensive visualization of fan effectiveness across varying environmental and activity conditions. The findings suggest that fans are beneficial only within specific temperature, humidity, and

activity thresholds. Above these thresholds, fans not only fail to prevent hyperthermia but may accelerate its onset; hence, there is a critical need for tailored public health guidelines for fan use during heatwaves.

The modified thermoregulation model proposed in this study shows promising results under severe heatwave conditions; nonetheless, several aspects require further refinement to improve accuracy. These include workload heat production, basal blood flow, sweat dripping from the skin, body movement effects, and the absence of heart rate responses. In addition, the present framework applies a single skin node for most body segments, which does not capture front–back asymmetries in local airflow; only the torso is represented with separate chest (anterior) and back (posterior) segments. While this limitation primarily affects local skin temperatures, effects on core thermal response are expected to be negligible. Addressing these factors in future work could enhance predictive accuracy under prolonged heat stress. Furthermore, the study focused exclusively on young, healthy adults, which limits the generalizability of the findings to other vulnerable populations, such as older adults, children, and individuals with chronic health conditions linked to heat vulnerability (e.g., cardiovascular diseases, diabetes, or obesity). Future studies should include these populations in order to provide a more comprehensive understanding of fan effectiveness. Additionally, future research should expand on the present findings by incorporating a variety of demographic groups and exploring the effects of extended heatwave durations. Moreover, additional variables, such as adaptive clothing strategies and mixed sustainable cooling technologies, should be investigated to optimize heat stress mitigation strategies under extreme environmental conditions.

4.5 Summary

The current study provides a detailed numerical assessment of electric fan effectiveness during extreme heatwaves by employing a modified multi-segment human thermoregulation model.

The model is built upon the JOS-3 framework and incorporates enhancements to account for physiological responses under dehydration, including alterations in set-point temperatures, sweat sensitivity, and vasodilation thresholds. The model was implemented in MATLAB and validated against multiple experimental datasets involving varying environmental conditions and activity levels. Strong agreement between model predictions and experimental data confirmed the model's accuracy in replicating core and skin temperature dynamics under heat stress.

The study systematically analyzed the interplay between environmental temperature, relative humidity, fan air speed, and metabolic heat load on the thermal state of the human body. Simulation results demonstrated that in moderate heat conditions—such as 40 °C with 50% RH—fans are highly effective, particularly at low activity levels and moderate fan speeds (e.g., 0.8 m/s). Under these conditions, fans enhance evaporative cooling, reduce skin and core temperatures, and delay the onset of moderate hyperthermia (core temperature ≥ 38 °C).

However, the results also highlighted critical thresholds beyond which fan use becomes counterproductive. At ambient temperatures exceeding 46 °C or relative humidity levels above 60%, fan use accelerated core temperature rise. This phenomenon is attributed to increased sensible heat gain from the hot ambient air when fans drive airflow over the skin, overwhelming the body's evaporative cooling capacity. At 50 °C and 40% RH, for instance, the onset of moderate hyperthermia occurred significantly faster with higher fan speeds, revealing that fans may exacerbate thermal strain under extreme conditions. These findings challenge the conventional assumption that fans are universally beneficial in hot environments.

The study further explored how physical activity levels influence the fan effectiveness. Simulations under four activity levels—sedentary (PAR-1.2), light (PAR-1.8), moderate (PAR-2.8), and strenuous (PAR-3.8)—revealed a strong correlation between metabolic heat

production and reduced fan effectiveness. At higher PAR levels, heat stress escalated regardless of fan use, and in many cases, fan-assisted air movement accelerated the onset of hyperthermia. For example, at PAR-2.8 under 43 °C and 40% RH, fans were no longer effective in preventing core temperature from exceeding 38 °C. At PAR-3.8, even mild conditions such as 36 °C with 40% RH led to hyperthermia within two hours of exposure. These results demonstrate that fan effectiveness is highly dependent on activity level, with higher metabolic heat loads diminishing their benefits.

Threshold charts developed in this study clearly identify the environmental and physiological boundaries for safe fan use. Fans are beneficial under air temperatures up to 43 °C and RH levels below 40%, especially at lower activity levels. However, beyond 46 °C or when RH exceeds 60%, the safety margin rapidly diminishes. This nuanced understanding offers an important tool for guiding public health decisions, enabling authorities to provide population-specific fan usage guidelines based on weather forecasts and activity levels. Overall, the study concludes that electric fans can effectively reduce thermal strain under moderately hot and dry conditions but lose their effectiveness—and may even increase risk—under extreme heat and humidity, particularly when combined with high physical exertion. These findings underscore the importance of tailoring cooling recommendations not only to ambient temperature but also to humidity, activity level, and fan speed. By providing evidence-based thresholds, the study contributes to developing smarter, more adaptive heatwave mitigation strategies.

CHAPTER 5. ASSESSMENT OF SUSTAINABLE AND ACCESSIBLE WATER-BASED COOLING INTERVENTIONS DURING HEAT EVENTS THROUGH THERMOREGULATION MODELING

The findings from Chapter 4 highlighted the conditional benefits and limitations of electric fan use during extreme heat events, especially under varying humidity levels and activity intensities. However, in situations where electricity access is limited or fan use becomes physiologically ineffective, alternative strategies become essential. In this context, Chapter 5 investigates passive water-based cooling methods, including foot immersion, leg immersion, and self-dousing, which offer simple and sustainable solutions for managing heat stress. By further refining the thermoregulatory model developed in the previous chapter, this study evaluates the practical effectiveness of these interventions across diverse climatic conditions, addressing the critical need for accessible cooling solutions in resource-constrained environments.

Extreme heat events are rapidly becoming more frequent, intense, and prolonged across many parts of the world, particularly in low- and middle-income countries. This rise in temperature poses a severe threat to public health, especially among vulnerable populations who lack access to advanced cooling infrastructure like air conditioning. In India, where less than 10% of households have air conditioning, the need for accessible, low-cost cooling solutions is especially urgent. Passive strategies such as water-based cooling, including foot immersion,

leg immersion, and self-dousing, have garnered attention for their simplicity, affordability, and potential effectiveness. These interventions offer the promise of thermal relief without requiring electrical power or specialized equipment, making them viable for widespread use in resource-constrained settings.

To rigorously evaluate these cooling strategies, this study employed a modified human thermoregulation model based on the JOS-3 framework. The model was enhanced to simulate realistic physiological responses by incorporating key factors such as hydration, dynamic sensor signal behavior, and modifications for water-based interventions. Unlike earlier models that did not account for localized immersion or intermittent skin wetting, the present model simulates foot and leg immersion by adjusting heat transfer coefficients and suppressing evaporation in submerged segments, while dousing effects were modeled by dynamically calculating evaporative cooling, water retention, and mass transfer across different body segments. These enhancements enable a more realistic simulation of how the human body responds to passive water-based cooling under various environmental stressors.

The model was validated against experimental datasets involving partial and full-body immersion and dousing under hot and humid conditions, showing strong agreement with measured core and skin temperatures. This validation supports its reliability in assessing the thermal impact of cooling interventions in real-world heatwave scenarios. The simulations were conducted for representative Indian cities across three major climate zones—hot and dry, warm and humid, and composite—using real ambient temperature and humidity profiles. A total of six cities were included, with extreme heat events drawn from historical data to create realistic boundary conditions for testing the interventions. The modeled subject was a healthy, non-acclimatized young adult in light clothing, exposed to indoor conditions with low activity levels during the day when heat stress is typically most pronounced. Cooling strategies were triggered only when ambient temperatures exceeded 35 °C, enthalpy crossed 55 kJ/kg, and the

time was between 8 AM and 5 PM, ensuring that interventions were activated only under physiologically stressful conditions.

Understanding the effectiveness of foot immersion, leg immersion, and dousing in mitigating heat-related illnesses during heatwaves requires the evaluation of key thermo-physiological responses through thermoregulation modeling. Therefore, the following section presents a detailed analysis of core and mean skin temperature variations over time, under real-world conditions. First, the cooling effects of foot immersion are discussed across hot-dry, warm-humid, and composite climates under varying water temperatures. Next, the role of immersion surface area in determining the cooling efficiency of leg immersion is examined. This is followed by the evaluation of dousing strategies and the influence of different body surface areas exposed to water. Finally, a comparative analysis synthesizes these results to provide climate-specific recommendations, offering practical guidance on the application of these passive water-based interventions.

5.1 Methodology

We used the JOS 3 model (Takahashi et al., 2021), which first modified to incorporates dehydration, updated sensor signals, sweating, and set-point temperature adjustments. This section presents the detailed numerical solution methodology, the formulation of the multi-segment model, and the fundamental mathematical equations used to solve the model. Furthermore, the modifications applied to the thermoregulation model, specifically for foot immersion and leg immersion, are explained. Additionally, adaptations related to the dousing cooling approach, considering parameters such as water application, retention, evaporation rate, sensible heat loss, and mass transfer coefficient, are described.

5.1.1 Overview of Thermoregulation Modelling

The present human thermoregulatory model was developed and simulated using a computational program written in MATLAB. The model simulates thermoregulation as a balance between heat production and heat dissipation. Internally, heat is produced through basal metabolism, external work, shivering thermogenesis, and non-shivering thermogenesis. This heat is transported via blood flow and dissipated externally by conduction, convection, radiation, evaporation of sweat, and respiration. During heat stress, evaporation is the dominant cooling pathway. Thermoregulatory control signals such as sweating and vasodilation are activated when deviations in core or skin temperature exceed set-point thresholds. These responses are further influenced by dehydration, which reduces sweating efficiency and shifts activation thresholds. In present study, the model considers environmental parameters (air temperature, relative humidity, air velocity) and anthropometric details of the subject as input (see Figure 5.1). Next, heat balance and physiological processes such as metabolic heat production, skin blood flow, and convective and radiative heat exchange equations are solved in each time step by applying the spatial discretization. The model also incorporates the effects of water immersion and dousing by considering various other parameters such as a water convective heat transfer coefficient, sweat suppression due to immersion, segments of the body, water application, retention, and evaporation rate. These aspects are described in detail in Sections 5.1.2 and 5.1.3. We used a modified human thermoregulation model that was adapted from the JOS-3 framework (Takahashi et al., 2021). The human body is discretized into 17 anatomical segments, each further divided into two concentric layers—core and skin—with the exception of the head and pelvis segments, which also consist of muscle and fat layers. All body parts are represented by simplified cylindrical geometry, with the exception of the head, which is modeled as a sphere. The segment-wise properties such as surface area, thermal

conductivity, and specific heat capacity are consistent with those defined in the JOS-3 model (Takahashi et al., 2021).

The following generalized heat balance equation is employed to compute heat transfer in the body (Takahashi et al., 2021):

$$C_{ap_{\mathrm{j}(i)}} \frac{d}{dt}(T_{\mathrm{j}(i)}) = Q_{\mathrm{j}(i)} + B_{\mathrm{j}(i)} - D_{\mathrm{j-j\&}(i)} - C_{\mathrm{j}(i)} - R_{\mathrm{j}(i)} - E_{\mathrm{j}(i)} - RES_{\mathrm{j}(i)} \quad (5.1)$$

Here, C_{ap} denotes the specific heat capacity, T is the temperature of different layers of the body, and t is time. The terms B, Q, D, C, R, E and RES represent heat transfer via blood flow, metabolic heat production, conduction, convection, radiation, evaporation, and respiration, respectively. The subscripts i, j and j' correspond to the body segment, body layer, and adjacent layer, respectively. Next, heat production in the body is evaluated using equation (5.2) (Takahashi et al., 2021),

$$Q_{\mathrm{j}(i)} = M_{base\mathrm{j}(i)} + M_{work(i)} + M_{shv(i)} + M_{nst(i)} \quad (5.2)$$

where M_{base}, M_{work}, M_{shiv}, and M_{nst} represent heat production by basal metabolism, external work, shivering thermogenesis, and non-shivering thermogenesis, respectively. The comprehensive details of heat production, heat transfer by blood circulation, conduction heat loss between different body layers, and respiration calculations can be found in the JOS 3 study (Takahashi et al., 2021).

The evaporation heat transfer (E) is calculated as (Takahashi et al., 2021),

$$E_{(i)} = w_{sweat(i)} \times E_{\max(i)} \quad (5.3)$$

Here, w is skin wettedness, and E_{max} is maximum evaporative heat loss obtained using equation (5.4),

$$E_{\max(i)} = ((P_{sks(i)} - p_{a(i)}) \times h_{et(i)} \times BSA_{(i)} \quad (5.4)$$

where P_{sks} and P_a are saturated water vapor pressure at the skin and water vapor pressure in the surroundings, respectively, and BSA *is* the body surface area.

Total evaporative heat transfer coefficient (h_{et}) is obtained as:

$$h_{et(i)} = \frac{i_{cl(i)} \times L_R}{0.155\, I_{cl(i)} + \frac{i_{cl(i)}}{f_{cl}\, h_c}} \tag{5.5}$$

Here, i_{cl} and L_R are clothing vapor permeation efficiency and Lewis ratio, respectively, while f_{cl} and h_c are clothing area factor and convective heat transfer coefficients, respectively.

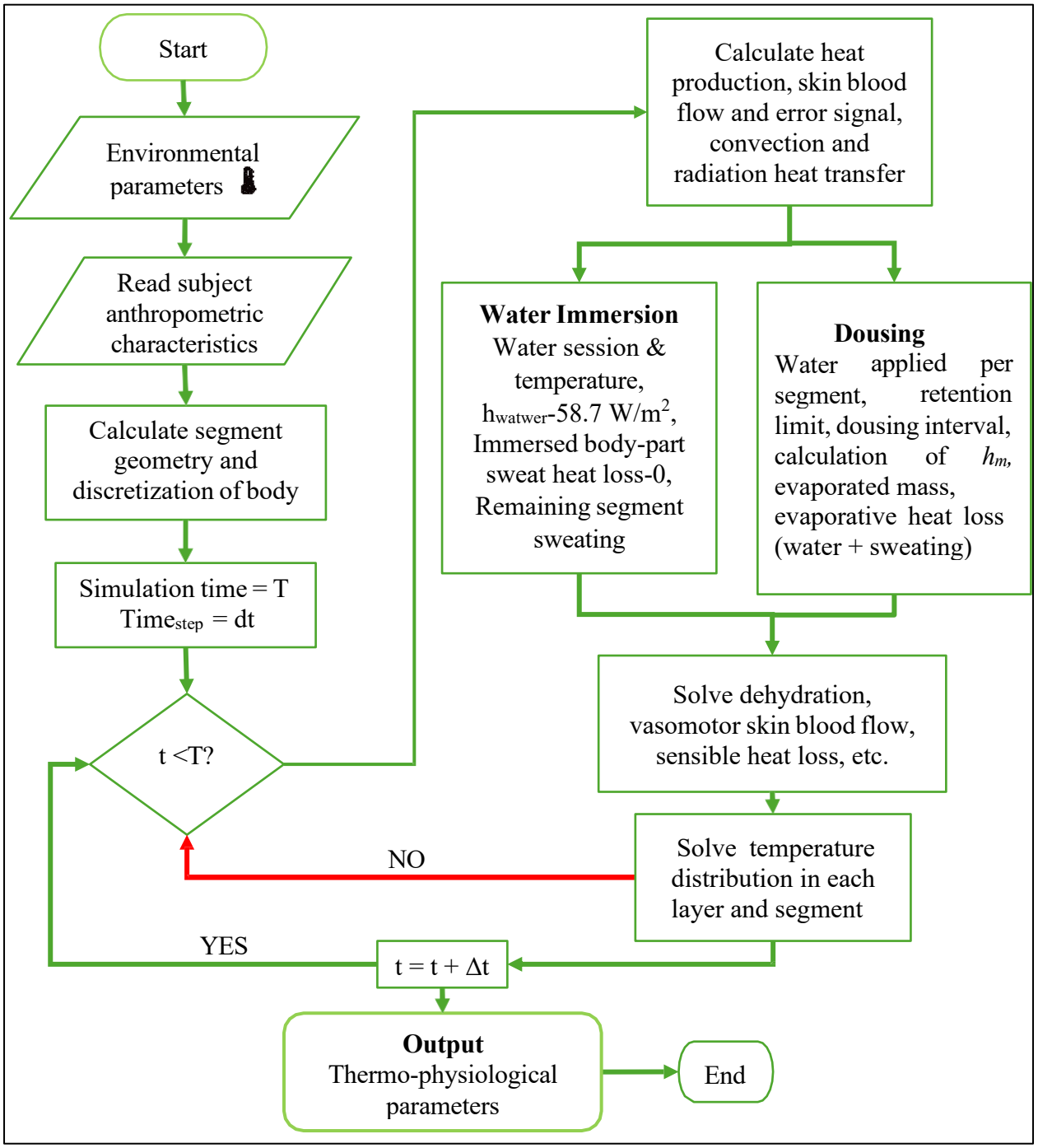

Figure 5.1. Flow chart to evaluate the human body temperature using the thermoregulation model in hot environment.

Evaporative heat loss by sweating (E_{sw}) is calculated as (Takahashi et al., 2021),

$$E_{sw(i)} = SKINS_{(i)} \times AGsweat_{(i)} \times SWEAT \times BSA_{ra} \times 2^{\frac{Err_{sk(i)}}{10}} \quad (5.6)$$

In the above equations, *SKINS* is the coefficient of sweating distribution, *SWEAT* is a signal for sweating, *Err* is the error signal, and *AGsweat* is a sweating aging factor.

The sensible heat exchange between the body skin surface and the environment consists mainly of heat transfer by convection [$C\ (W/m^2)$] and radiation [$R\ (W/m^2)$], and is calculated as (Takahashi et al., 2021),

$$C_{(i)} + R_{(i)} = h_{t(i)}(T_{sk(i)} - T_{o(i)}).BSA_{(i)} \quad (5.7)$$

where h_t is the total heat transfer coefficient, which is calculated using the convective heat transfer coefficient; T_{sk} is the local skin temperature; and T_o is the operative or ambient temperature.

Further, for immersed segments, the heat exchange

$$C_{(i)} = h_{c(i)}(T_{sk(i)} - T_{water}).BSA_{(i)} \quad (5.8)$$

In water cooling, radiative exchange is neglected, and heat loss is dominated by convection. Here, h_c is the convective heat transfer coefficient in water, and T_{water} is the water temperature.

The modified model calculates the percentage of sweat lost through the body in relation to total body weight as follows:

Sweat losses (*SL*) are expressed as:

$$SL = \frac{Initial\ body\ weight - current\ \ body\ weight}{Initial\ body\ weight} = \frac{\int_0^t Sweat.dt}{Initial\ body\ weight} \quad (5.9)$$

The sweat loss data is then used to compute the sensor signals from the head core layer ($Err_{[0]}$) as shown in equation (5.10) (Tanabe et l., 2002; Takahashi et al., 2021);

$$Err_{cr[0]} = T_{[0]} - [T_{setpt[0]} + (0.06\ x\ SL)] \quad (5.10)$$

When $Err_{cr(1)} \leq 0.01$ and $WRMS \leq 0.4$ then the sweating signal is:

$$SWEAT = (371.2 - 0.068xSL)\ xErr_{cr(0)} + 33.64\ x\ (WRMS - CLDS) \quad (5.11)$$

Otherwise, sweating signal (*SWEAT*) is,

$$SWEAT = (371.2 - 0.068xSL)\ xexp(Err_{cr(0)}) + 33.64\ x\ (WRMS - CLDS) \quad (5.12)$$

Next, the vasodilation signal (*DILAT*) is expressed by equation (5.13),

$$DILAT = (100.5 - 0.06xSL)xErr_{cr(0)} + 6.4x(WRMS - CLDS) \quad (5.13)$$

where WRMS and CLDS are integrated warm and cold signals which can be evaluated by different sensor signals for different body segments, respectively (Takahashi et al., 2021). Further, in line with JOS-3, our model accounts for heat exchange via blood circulation, including arterial and venous blood as well as arteriovenous anastomoses. These mechanisms were retained without modification. The detailed equations are available in the JOS-3 model (Takahashi et al., 2021).

5.1.2 Modification related to foot immersion and leg immersion

The previous thermoregulatory models do not incorporate local exposure to water immersion, particularly in a seated posture. However, local boundary effects become critical under water immersion conditions. In a water immersion cooling method, sweat evaporation is effectively suppressed, and radiative heat transfer is negligible. Instead, convective heat transfer becomes dominant due to the higher thermal conductivity of water compared to that of air. Unlike higher values reported under showering with forced flow (Munir et al., 2010), still-water immersion involves lower heat transfer. Therefore, we modifed the present model's convective heat transfer coefficient and evaporative heat loss by seting the values of 58.7 W/m²·K (Boutelier et al., 1977; Cooney & Cooney, 1976), and zero (Munir et al., 2010), respectively for the immersed segment. Figure 5.2 displays a schematic of the foot and leg immersion cooling method. In the case of foot immersion, only the foot is immersed in water, extending from the toes to the ankles. For leg immersion, the water level is assumed to reach the calf, including

the entire foot and lower leg segment. This approach allows us to model the physiological effects of immersion up to the calf while keeping the segmentation of the body intact.

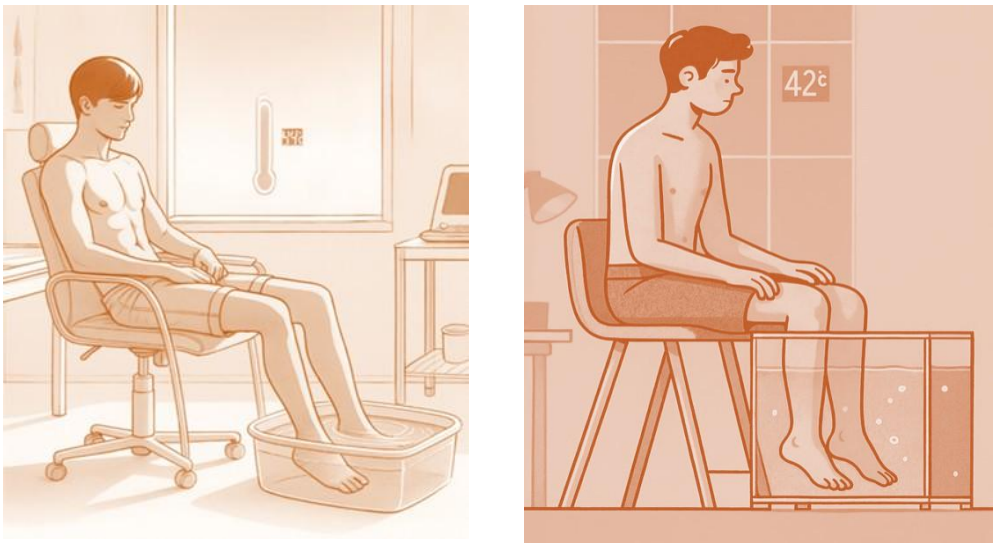

(a) (b)

Figure 5.2. (a) Foot immersion and (b) leg immersion for body cooling under extreme heat events.

5.1.3 Modification related to dousing

Dousing is a widely used cooling strategy during heat stress, where water is applied directly to the skin through spraying or sponging to enhance evaporative cooling (see Figure 5.3). Dousing increases the water-evaporative surface area, leading to greater heat dissipation without additional sweat and heat strain on the body. In the present study, the thermoregulatory model was modified to incorporate dousing in order to simulate its effect on skin and core temperatures under heatwave conditions. The modification included adjustments to the boundary conditions, evaporative heat loss calculation, sensible heat loss and skin temperature adjustment based on the applied water mass and thermal properties.

Figure 5.3. Self dousing for body cooling under extreme heat events.

Water was applied to different body parts, including the head, neck, chest, arms, legs, and feet, as these body parts have higher surface area and greater convective heat loss potential. The total amount of water applied per session was 0.6–1.0 L/hr, distributed across the segments based on body surface area (BSA) (Morris et al. 2019). Larger body parts received more water, while smaller areas received proportionally less water. To prevent unrealistic water accumulation, a maximum water retention limit was defined for each segment, beyond which excess water was considered to drip off without contributing to evaporative cooling. The maximum retention capacity was based on the known properties of human skin and experimental data (Parsons, 2014).

The amount of water applied was calculated using equation (5.14),

$$water\ mass\ init(\mathrm{i}) = \frac{\text{Total water appliedb per dousing} \times \text{BSA of segment (i)}}{BSA\ of\ all\ segments\ \text{with}\ water} \tag{5.14}$$

Next, the mass transfer coefficient (h_m) (Bird et al., 2007) was calculated as follow,

$$h_m(\mathrm{i}) = \frac{\mathrm{Sh} \times D_{water-air}}{\sqrt{\text{BSA (i)}}} \tag{5.15}$$

Here, *Sh* is the Sherwood number derived from the Chilton-Colburn analogy (Bird et al., 2007), which links heat and mass transfer (see equation 5.16). Further, under stagnant conditions, *Sh* = 2 was set as the lower bound to represent diffusion-limited evaporation. When airflow is

present, the Chilton–Colburn term dominates. Meanwhile, $D_{water\text{-}air}$ is the diffusion coefficient, which is calculated using equation (5.17).

$$Sh = 0.664.\left(\frac{\rho_{air} \times V \times \sqrt{BSA(i)}}{\mu_{air}}\right)^{1.75}.\left(\frac{\mu_{air}}{D_{water-air}}\right)^{1/3} \quad (5.16)$$

$$D_{water-air} = 2.26 \times 10^{-5}.\left(\frac{Tambient}{273.15}\right)^{1.75}.\left(\frac{101325}{P_a}\right) \quad (5.17)$$

Further, In the modified model, sweat evaporation and doused water evaporation are treated as parallel but independent processes, consistent with prior thermoregulation studies. Evaporation from sweat is driven by sudomotor activity and limited by skin wettedness and ambient vapor pressure, whereas evaporation from applied water is externally imposed, constrained by segmental retention capacity and local evaporation potential. The two processes are additive at the skin surface, with total wettedness (ω) expressed as the sum of sweat-induced (ω_{sweat}) and water-induced (ω_{water}) contributions (Equation 5.21). This formulation ensures that sweat-driven and dousing-driven evaporation remain physiologically distinct while their combined effect on heat dissipation is captured.

The evaporated mass of water was then evaluated using equation (5.18) (Parsons, 2014; Marrero & Mason, 1972),

$$evaporated\_mass(i) = \min\left(h_m(i).(P_{sks}(i) - P_a).dt, Water_{mass_{current}}(i), {}^{E_{max}}/_{L_v}\right) \quad (5.18)$$

The evaporated mass of water is limited by two conditions, the available evaporation capacity and the water available to evaporate (see equation (5.19)).

$$Water_{mass_{current}}(i) = min(water\ mass\ init\ (i), \max\_retention(i)) \quad (5.19)$$

Max_retention(i) is the maximum amount of water that can stay on the skin (kg/m²), such that any excess drips off and does not contribute to cooling. The maximum retention capacity values are taken from reference [50].

Next, evaporative heat loss due to water ($E_{water(i)}$) (Monteith & Unsworth, 2013) is calculated as follow,

$$E_{water(i)} = \frac{evaporated\ mass_{(i)}}{dt} . L_v . BSA(i) \quad (5.20)$$

Skin wettedness (ω), indicating the body's capacity for both water and sweat is then calculated by the following equation:

$$w_{(i)} = w_{water(i)} + w_{sweat(i)} \quad (5.21)$$

Where, $w_{water(i)} = \frac{E_{water(i)}}{E_{max(i)}}$ and $w_{sweat(i)} = 0.06 + 0.94 \frac{E_{sw(i)}}{E_{\max(i)}}$

In the present model, a critical $w_{sweat(i)}$ value of 0.85 was used [[60],[61]].

Further, the sensible heat loss is calculated as,

$$Q_{sensible(i)} = evaporated_{mass(i)} c_{pwater} (T_{skin(i)} - T_{water}) \quad (5.22)$$

Here, c_{pwater} is specific heat of water; $T_{skin(i)}$ and T_{water} are skin temperature and water temperature, respectively.

5.2 Model Validation

The present model was validated with previous experimental studies on water immersion and dousing to ensure model reliability and accuracy. Model prediction errors (ME, MAE, RMSE) were computed as time-averaged values across the entire simulation period rather than a single time point. The thermoregulation model was validated using experimental data from Castellani et al. (Castellani et al., 2023), which included prolonged water immersion trials with 18 participants for each of three water temperature settings, 18 ± 1 °C, 22 ± 1 °C, and 26 ± 1 °C. Subjects remained immersed from the neck down, wearing swimwear and Type 1 life jackets, while freely floating in the water. The simulations assumed resting subjects with a metabolic rate of 1.2 met. The Type 1 life jacket was added with a thermal resistance of approximately 0.3 clo [[39],[62],[63]].The simulated core temperature results showed excellent agreement

with the experimental data, with mean absolute errors of 0.13 °C, 0.07 °C, and 0.1 °C for water temperatures of 18 °C, 22 °C, and 26 °C, respectively (see Figure 5.4). The maximum error did not exceed 0.2 °C across all conditions. Similarly, the predicted mean skin temperature also aligned well, exhibiting RMSE values of 0.5 °C, 0.4 °C, and 0.5 °C for 18 °C, 22 °C, and 26 °C, respectively. These results indicate that the present model accurately captures thermal responses during immersion conditions.

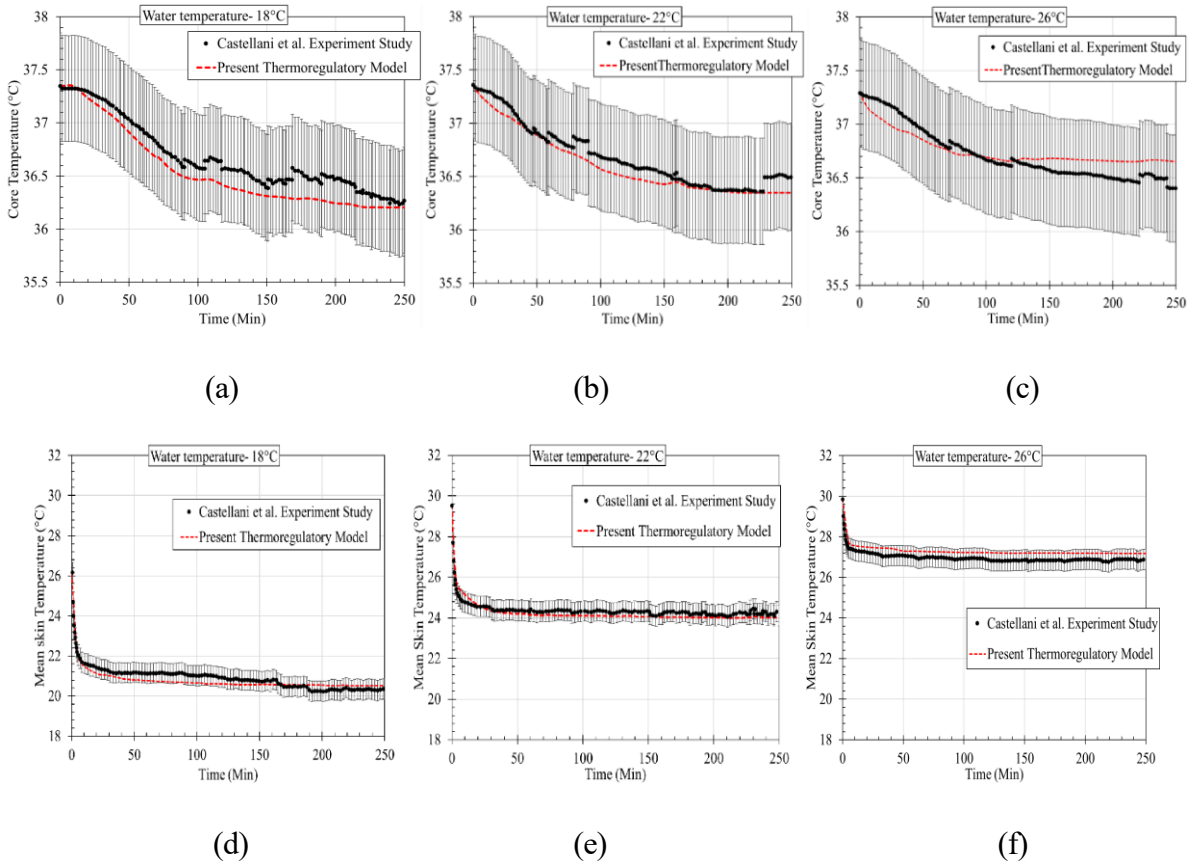

Figure 5.4. Comparison between simulated results from the present model and experimental data from Castellani et al. (Castellani et al., 2023) for core and mean skin temperatures under different water immersion conditions: 18 °C ((a) and (d)), 22 °C ((b) and (e)), and 26 °C ((c) and (f)).

The present model was also validated using experimental data from Morris et al. (Morris et al., 2019), which involved foot immersion under hot and dry environmental conditions (46°C, 11 % RH). Participants immersed their feet in 22 °C water for 20-minute intervals followed by

10-minute breaks, with each trail lasting of 120 minutes. The simulated core and mean skin temperatures showed excellent agreement with the experimental measurements. For core temperature, the model produced a mean absolute error (MAE) of 0.044 °C, a maximum deviation of 0.03 °C, and a root mean square error (RMSE) of 0.04 °C. For mean skin temperature, the MAE was 0.31 °C , the maximum error was 0.3°C, and the RMSE was 0.3°C (see Figure 5.5). These results confirm the model's accuracy in capturing the physiological response to foot immersion cooling under extreme heat conditions.

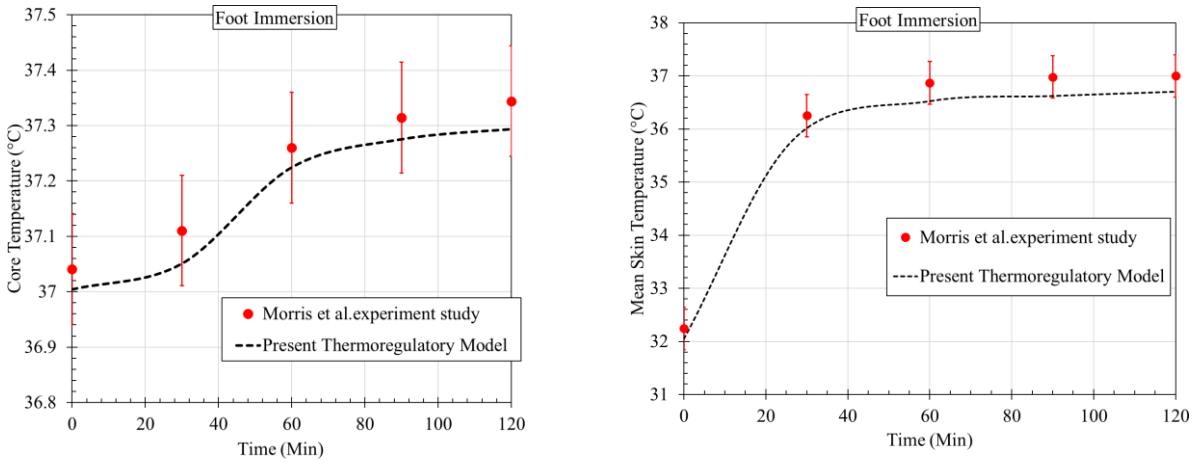

(a) (b)

Figure 5.5. Validation of present thermoregulatory model with Morris et al.'s experimental study on foot immersion: (a) core temperature; and (b) mean skin temperature.

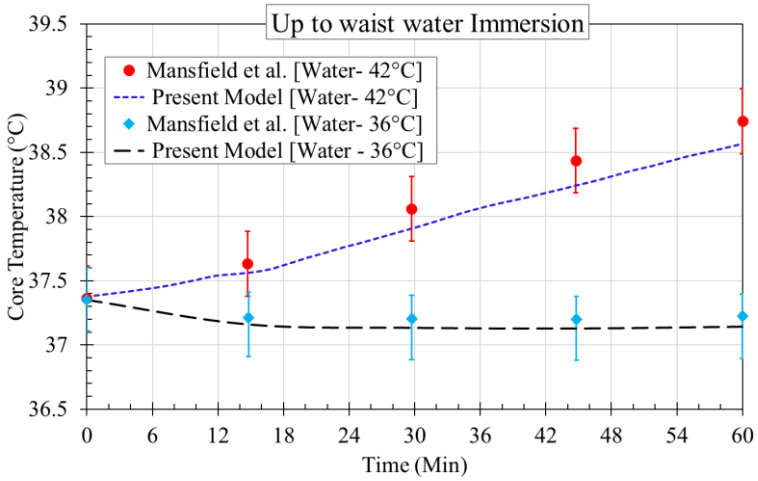

(a)

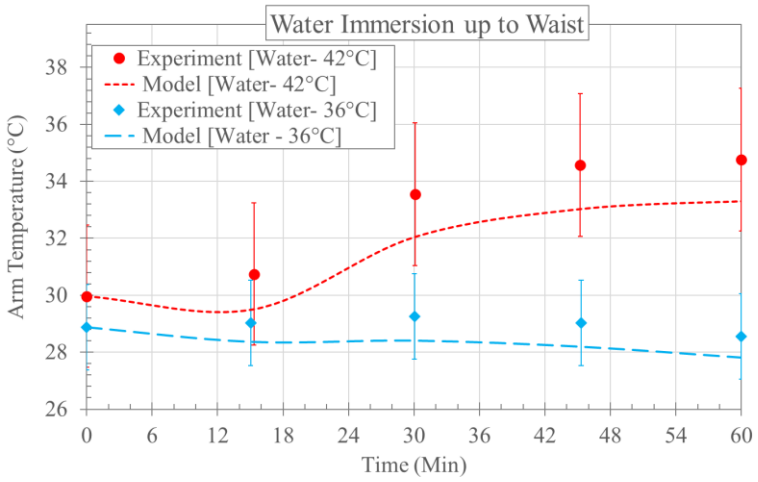

(b)

Figure 5.6. Validation of present thermoregulatory model with Mansfield et al.'s [41] experimental study on water immersion: (a) core temperature (b) arm temperature.

In addition, the model was validated using an experimental study conducted by Mansfield et al. (Mansfield et al., 2021), where nine healthy male participants were immersed up to the waist for 60 minutes in water at 42 °C and 36 °C. The predicted core temperatures closely matched the experimental results, with mean absolute error (MAE) values of 0.11°C and 0.05 °C, and root mean square error (RMSE) values of 0.1°C, for both 42 °C and 36 °C water, respectively (see Figure 5.6a). In addition, for arm temperature, at 42 °C immersion, MAE and RMSE were 1.15 °C and 1.29 °C, respectively, while at 36 °C immersion they were 0.62 °C and 0.69 °C (see Figure 5.6b). These larger discrepancies likely reflect spatial variability in skin temperature, vasomotor effects, and the simplified representation of peripheral thermoregulation, indicating that the model is more reliable for core than for local skin temperature predictions. Present study was validated using foot immersion data (Morris et al., 2019). However, validation with full-body and waist-level immersion data (Castellani et al., 2023, Mansfield et al., 2021) may introduce some uncertainty.

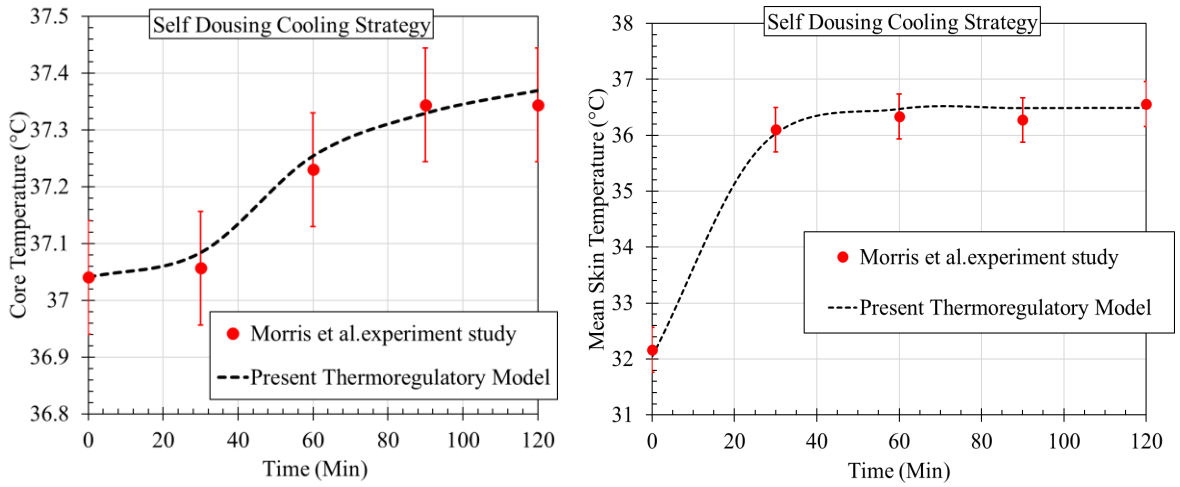

(a) (b)

Figure 5.7. Validation present thermoregulatory model with Morris et al. (Morris et al., 2019) dousing experiment study (a) core temperature; and (b) mean skin temperature.

The present model was also validated using Morris et al.'s experimental data (Morris et al., 2019) on dousing under hot and dry environmental conditions (46.0 ± 0.5 °C, 11 ± 4% RH), where participants applied 22 °C water externally to the chest, arms, back, legs, and face. Each intervention lasted 120 minutes. The predicted core and mean skin temperatures showed excellent agreement with the experimental results. For core temperature, the model yielded a mean absolute error (MAE) of 0.03 °C, a maximum error of 0.0271 °C, and a root mean square error (RMSE) of 0.0209 °C. For mean skin temperature, the MAE was 0.22 °C , the maximum error was 0.2 °C, and the RMSE was 0.2 °C (see Figure 5.7). Validation studies (Castellani et al., 2023, Morris et al., 2019, Mansfield et al., 2021) were selected because they provide experimental data directly relevant to the present work. Morris et al. (Morris et al., 2019) includes both foot immersion and dousing, Castellani et al. (Castellani et al., 2023) reports prolonged full-body immersion, and Mansfield et al. (Mansfield et al., 2021) provides waist-level immersion at multiple water temperatures. Validation with these studies confirms the model's reliability in capturing dynamic thermal responses during immersion and dousing,

thereby supporting its application to water-based cooling strategies under extreme heat exposure.

5.3 Case Study

As per the IPCC's sixth assessment report (IPCC, 2021), heatwaves in India are projected to increase in frequency, intensity, and duration, resulting in higher morbidity and mortality rates. With over a billion citizens and limited access to air conditioning (only 8% of households own air conditioning units), staying cool during extreme heat is a critical survival issue (IPCC, 2021). Furthermore, a 2021 study by The Lancet Planetary Health (Zhao et al., 2021) estimated that nearly 740,000 excess deaths in India each year are linked to temperature-related climate change, underscoring the urgent need for effective, low-cost cooling strategies. To ensure that the study outcomes are relevant to real-world conditions, we selected environmental data from Indian cities that experience extreme heat events. Although this study was focused on Indian climatic conditions, the findings can be extended to any extreme heat environments globally. According to the National Building Code 2016 (Bureau of Indian Standard, 2016), and the Energy Conservation Building Code 2017 (USAID-ECO III Project, 2017), India's climate is classified into five major zones: composite, warm-humid, hot-dry, cold, and temperate. In the present study, we excluded the cold and temperate zones, as they are less affected by extreme heat events. From the remaining three zones we selected two cities each (see Table 5.1). For present study, outdoor climatic data were applied directly as input. This assumption reflects conditions in naturally ventilated dwellings without air-conditioning, where field studies in Indian cities show indoor air temperatures during heatwaves closely follow outdoor values, often within 1–2 °C (Mani et al., 2012; Bhatia et al, 2011; NRDC, 2012). Accordingly, mean radiant temperature was assumed equal to air temperature, and air velocity was fixed at 0.1 m/s to represent still indoor air (Jay et al., 2021). Other than climate categorization, cities were

chosen due to their large populations, documented vulnerability, and infrastructure stress. For example, Ahmedabad recorded more than 1,300 excess deaths during the 2010 heatwave, leading to India's first Heat Action Plan (NRDC, 2012). Mumbai, Kolkata, and New Delhi are megacities where high density and infrastructure stress exacerbate risk. Nagpur's heat-prone districts are under special risk with frequent power and water shortages that amplify vulnerability (Shakti,2022). Although this study was focused on Indian climatic conditions, the findings can be extended to extreme heat environments globally. The heat event weather data for different cities were taken fromEnergyPlus Weather, 2021 (see Figure C1). Overall, the thermo-physiological simulations were performed using this environmental data to replicate real-world heat exposure scenarios.

Table 5.1. Heat event of selected cities from the three climate zones.

Sr. no	Climate zone type	City	Geographical position (National Portal of India, 2025)		Ambient temperature (°C)	Max. Relative Humidity (%)
			latitude	longitude		
1.	I-Hot & dry	Bikaner	28.0271° N	73.3022°E	48	28
2.	II-Hot & dry	Ahmedabad	23.0339° N	72.5714° E	46	21
3.	I- Warm & humid	Kolkata	22.5726° N	88.3639° E	41	61
4.	II- Warm & humid	Mumbai	19.0760° N	72.8777° E	38	60
5.	I-Composite	New Delhi	28.6139° N	77.2090° E	45	27
6.	II-Composite	Nagpur	21.1466° N	79.0889° E	48	20

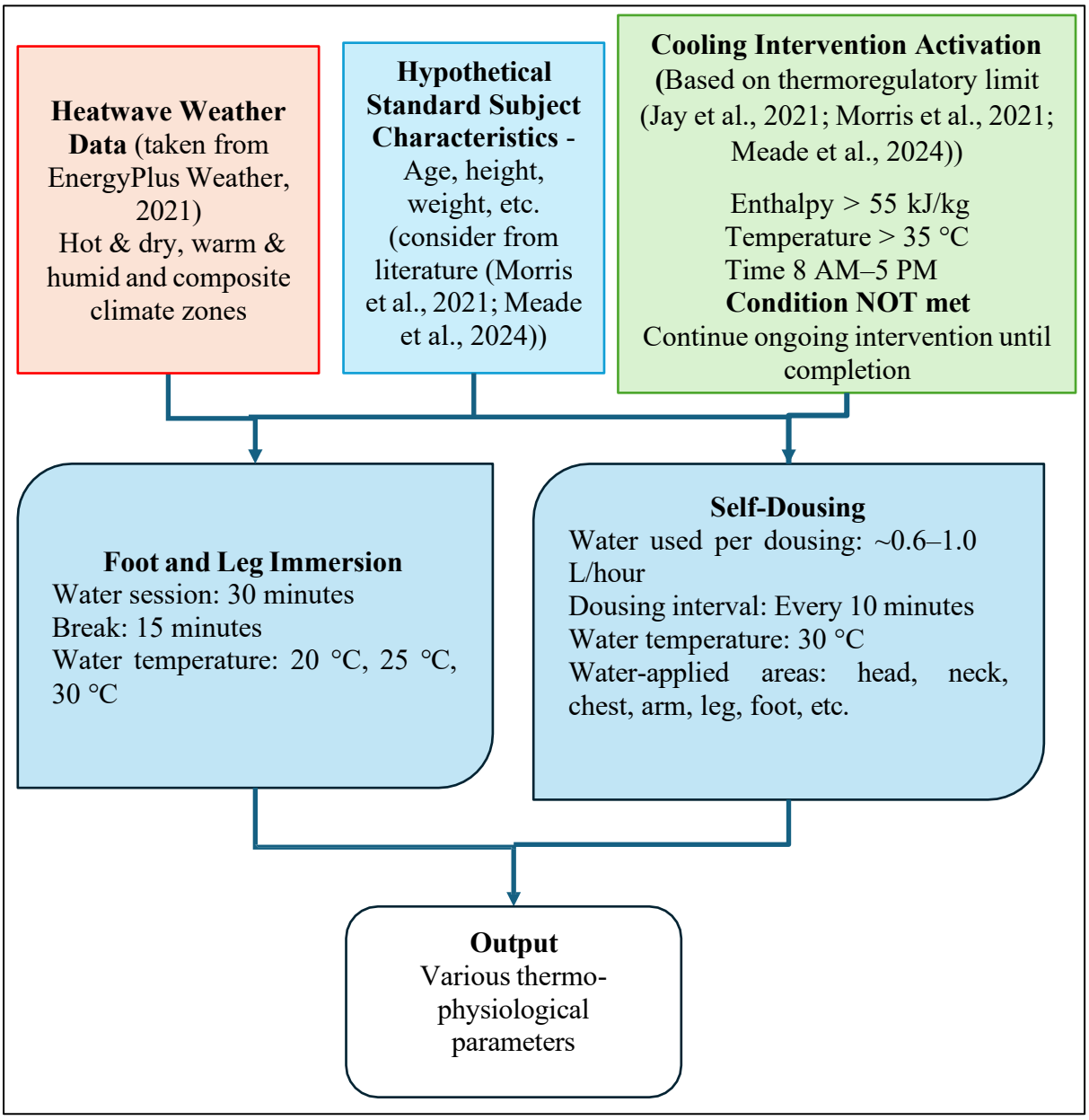

Figure 5.8. Basic operational structure of the case setup.

Figure 5.8 illustrates the operational structure used to compute the effectiveness of cooling strategies under extreme heatwave conditions. We considered a hypothetical healthy male occupant aged 24 years, with a height of 1.73 m, a body mass of 71.5 kg, and a body surface area (BSA) of 1.85 m² (Morris et al., 2021; Meade et al., 2024). The occupant was assumed to be in an indoor environment with a sedentary activity lifestyle (mean physical activity ratio of 1.53 or ~89 W/m²), which included 8 hours of sleep and seated activities such as office work, light leisure, eating etc. (World Health Organization, 2004). The occupant was assumed to wear

shorts, with the lower body clothed and the upper body uncovered. The overall thermal insulation was set to 0.2 clo, corresponding to minimal summer clothing (World Health Organization, 2004). Furthermore, the occupant was non-acclimatized to extreme heat (Morris et al., 2021; Meade et al., 2024). The cooling intervention was triggered only at the selected time, temperature and enthalpy. Typically, heat exposure is highest during daytime hours. Therefore, we choose the time window of 8:00 AM to 5:00 PM. Meanwhile, ambient threshold values of 35 °C for temperature and 55 kJ/kg for enthalpy (representing combined effects of humidity and temperature) were selected, as they mark the point at which the body's thermoregulatory capacity begins to struggle in dissipating heat, thereby increasing the risk of hyperthermia (Jay et al., 2021; Morris et al., 2021; Meade et al., 2024). The cooling intervention was initiated only when all these conditions were met, to ensure that the body was under actual heat strain. If any of these conditions were not satisfied, ongoing cooling intervention would continue until completion, but no new intervention would begin unless all conditions were true. Furthermore, water temperatures of 20, 25, and 30 °C were selected to represent typical water ranges in India, as reported for municipal and groundwater supplies with seasonal variation across climate zones.

5.4 Results

Understanding the effectiveness of foot immersion, leg immersion, and dousing in mitigating heat-related illnesses during heatwave requires the evaluation of key thermo-physiological responses through thermoregulation modeling. Based on the scenarios outlined in the previous section (case study), the present section presents core temperature and mean skin temperature variation with respect to time under real-world heat scenarios. First, we discuss the effectiveness of foot immersion in hot and dry, hot and humid, and composite climatic conditions under different water temperatures. Next, the effects of leg immersion are examined,

highlighting how different immersed surface areas affect the thermo-physiological parameters. The impact of dousing is then analyzed by evaluating the influence of the different body surface areas being doused. Finally, a comparative analysis of all three strategies is presented, and practical recommendations are provided on the basis of cooling mechanisms and climatic conditions. Overall, the present section provides insights into the practical application of water-based cooling methods as sustainable and accessible interventions for reducing core temperature and preventing hyperthermia during extreme heat events.

5.4.1 Foot Immersion Cooling

Figure 5.9a illustrates the core temperature variation in Bikaner (hot and dry climate) during an extreme heat event with foot immersion at 20 °C, 25 °C, and 30 °C, compared to no cooling method (NCM). On 7th June, ambient conditions were severe, with enthalpy reaching approximately 95.7 kJ/kg. Under NCM, core temperature rose rapidly between daytime, exceeding the moderate hyperthermia threshold (~38 °C) and reaching to 38.4 °C. Foot immersion provided limited thermal relief, with a maximum reduction of ~0.3 °C observed at 20 °C. However, this reduction was insufficient to bring the core temperature below 38 °C, indicating the limitations of this method under extreme hot-dry conditions. Further, during peak hours (12:00–16:00), foot immersion reduced average core temperature by ~0.2–0.3 °C compared to no cooling, with the largest reduction at 20 °C water. During nighttime hours, in all cases the temperature was same as cooling intervention was inactive. The repeated activation of foot immersion throughout the day highlights its physiological relevance, but also its limited capacity in mitigating thermal strain in such harsh climates.

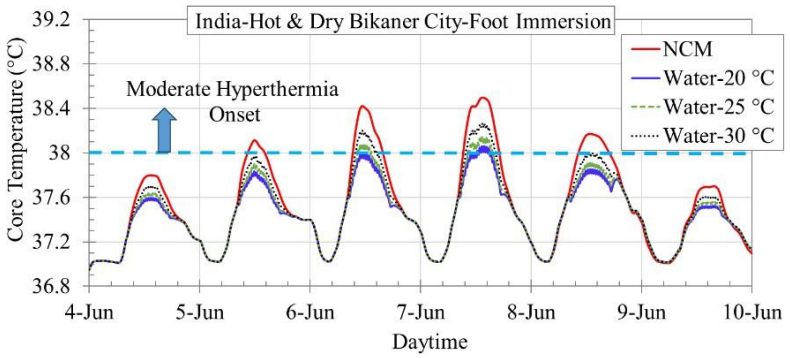

(a)

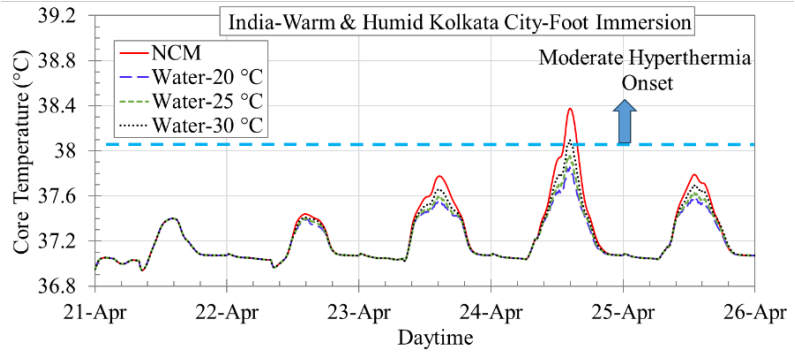

(b)

Figure 5.9. Core temperature variation during a heat event for foot immersion interventions at different water temperatures and no cooling method (NCM) in (a) the hot and dry city of Bikaner and (b) the warm and humid city of Kolkata.

Figure 5.9b shows a similar comparison in Kolkata (hot and humid climate) under foot immersion. Although ambient temperatures were lower, high humidity drove enthalpy to nearly 120 kJ/kg, intensifying thermal stress on extreme days. Under NCM, core temperature reached to 38.4 °C. Foot immersion, particularly at 20 °C, reduced core temperature by up to 0.4 °C. In Kolkata, the average daytime reduction in core temperature during peak hours was smaller (~0.1–0.2 °C). The cooling response was slower than in Bikaner, reflecting the diminished evaporative heat loss in high-humidity environments. At night, core temperatures again aligned across all scenarios due to inactive cooling. Despite the environmental constraints, foot immersion demonstrated consistent daytime effectiveness in humid climates, confirming its utility as a simple and practical intervention. Further, foot immersion at higher

water temperatures was less effective because the reduced skin–water temperature gradient lowered convective heat transfer, limiting cooling capacity.

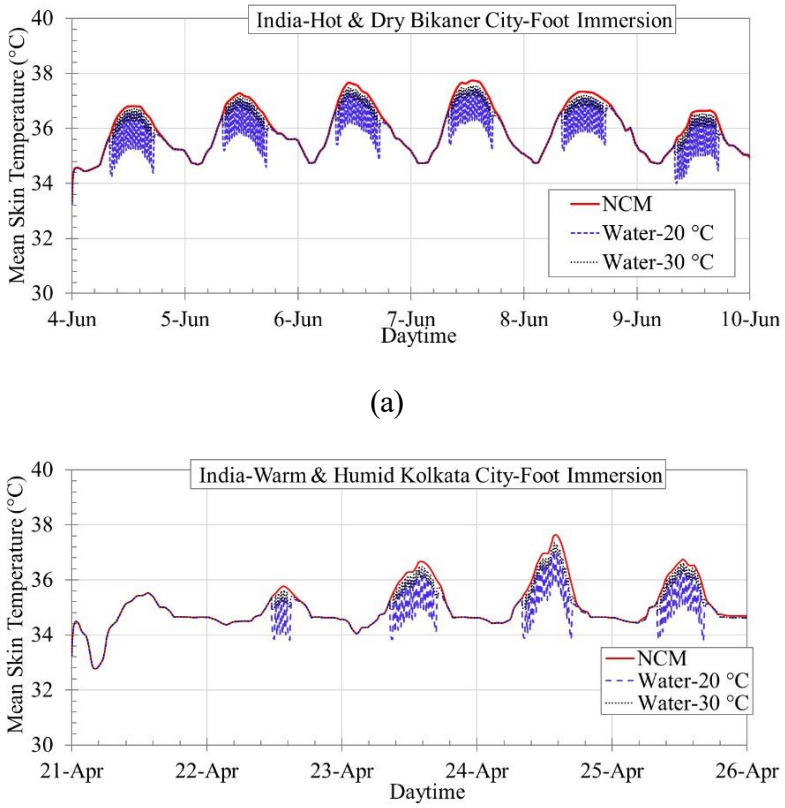

Figure 5.10. Mean skin temperature variation during a heat event for foot immersion interventions at different water temperatures and no cooling method (NCM) in (a) the hot and dry city of Bikaner and (b) the warm and humid city of Kolkata.

Figure 5.10a llustrates the diurnal variation in mean skin temperature under foot immersion and no cooling method in Bikaner. In the NCM scenario, mean skin temperature peaked at 37.6 °C, indicating high thermal stress. Foot immersion reduced skin temperature to 34.4–37.2 °C, with the most significant cooling achieved at 20 °C due to enhanced convective heat loss. In contrast, NCM relied solely on evaporative cooling, which was less effective in hot-dry conditions due to rapid sweat evaporation. Foot immersion consistently maintained lower skin temperatures during peak heat hours, demonstrating its effectiveness in reducing skin thermal strain. Further, the average daytime skin temperature reduction was ~1.2–1.8°C during

peak heat hours, depending on water temperature. At night, all cases converged, reflecting reduced environmental stress and inactive cooling. Furthermore, Figure 5.10b shows similar patterns in Kolkata (hot and humid climate), where 20 °C foot immersion provided up to ~0.4 °C greater cooling than 30 °C immersion. The average reduction in mean skin temperature during peak hours was ~0.6–0.9 °C. Although the overall reduction was smaller than in Bikaner, cooler water still delivered better thermal relief. Nighttime temperatures again converged across all cases. Additional results for Ahmedabad, Mumbai, New Delhi, and Nagpur (representing hot-dry, warm-humid, and composite climates) are included in the Figure C 2. Across all regions, skin and core temperature responses followed the trends observed in Bikaner and Kolkata, reaffirming the broad applicability and daytime effectiveness of foot immersion in mitigating thermal strain during extreme heat events.

5.4.2 Leg Immersion Cooling

Figure 5.11a presents core temperature variations in Bikaner (hot-dry climate) during a heat event for leg immersion at 20 °C, 25 °C, and 30 °C, compared to no cooling method. Under NCM, core temperature exceeded the moderate hyperthermia threshold (~38 °C). Leg immersion effectively maintained core temperatures below this threshold across all water temperatures, with the maximum reduction (~0.7 °C) observed at 20 °C. This enhanced performance is attributed to the greater thermal gradient and larger immersed surface area, which promotes efficient convective heat loss. Even at 30 °C, leg immersion successfully prevented hyperthermia, demonstrating its robustness under extreme ambient temperatures exceeding 45 °C. Further, on extreme heat days, leg immersion delayed the time to reach the moderate hyperthermia threshold (38 °C) by 2.45 hours at 30 °C compared with NCM. At lower water temperatures, the hyperthermia condition was never reached throughout the day.

Moreover, under NCM, the moderate hyperthermia condition persisted throughout the daytime (09:00–17:00).

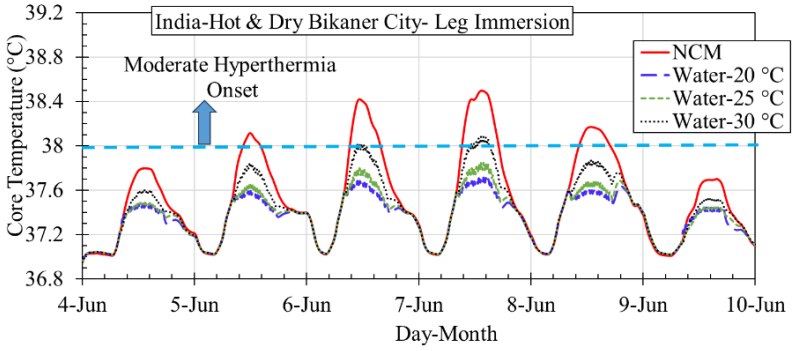

(a)

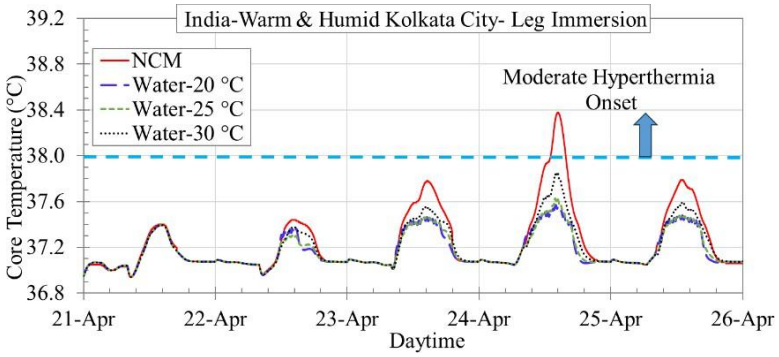

(b)

Figure 5.11. Core temperature variation during a heat event for leg immersion interventions at different water temperatures and no cooling method (NCM) in (a) the hot and dry city of Bikaner and (b) the warm and humid city of Kolkata.

Figure 5.11b shows similar trends in Kolkata (hot-humid climate), where high humidity (61%) and enthalpy (~120 kJ/kg) intensified thermal strain. NCM conditions led to rapid core temperature rise beyond 38 °C, whereas leg immersion maintained core temperatures below this threshold throughout the exposure. The strongest cooling again occurred at 20 °C, with diminishing but still effective results at 25 °C and 30 °C. While temperature fluctuations were smaller than in Bikaner, reduced evaporative potential in humid air made conductive cooling via leg immersion especially important. The consistent effectiveness of leg immersion in both

climates confirms its utility as a reliable intervention for managing heat stress across diverse environmental conditions.

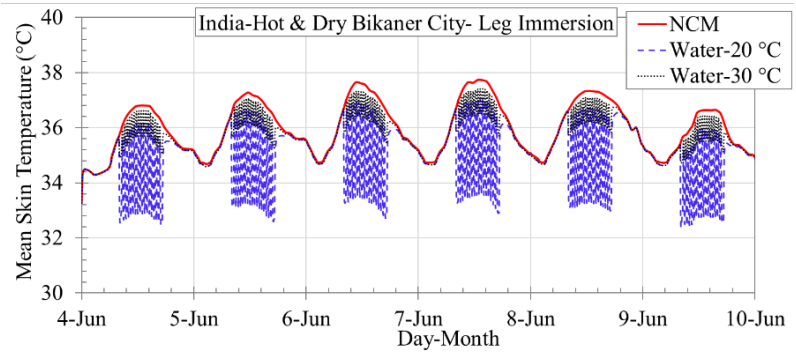

(a)

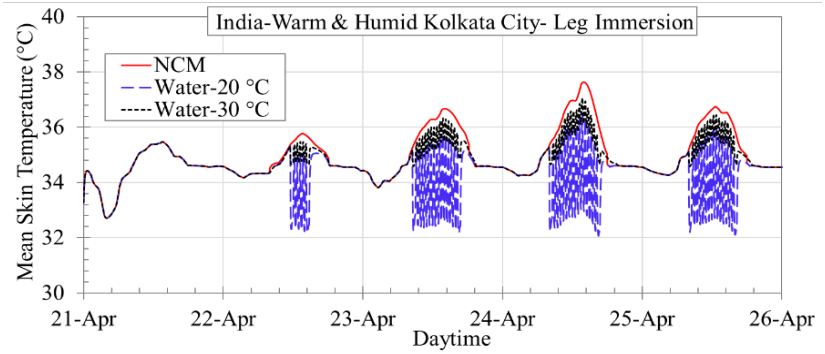

(b)

Figure 5.12. Mean skin temperature variation during a heat event for leg immersion interventions at different water temperatures and no cooling method (NCM) in (a) the hot and dry city of Bikaner and (b) the warm and humid city of Kolkata.

Figure 5.12a illustrates mean skin temperature variation in Bikaner during leg immersion at 20 °C and 30 °C, compared to the no-cooling method. Leg immersion significantly reduced skin temperature, with 20 °C water achieving a ~3–4 °C drop due to a stronger thermal gradient enhancing conductive and convective heat loss. At 30 °C, a moderate reduction (~1–2 °C) was observed, still beneficial but less effective. These results confirm that lower water temperatures enhance leg immersion performance in hot-dry climates. At night, skin temperatures converged across all conditions due to inactive interventions and reduced environmental stress. Figure 5.12b shows comparable outcomes in Kolkata (hot-humid climate). Leg immersion at 20 °C

reduced mean skin temperature by ~2–3 °C, while 30 °C water yielded a smaller (~1 °C) reduction. Although high humidity limits evaporative cooling, conductive mechanisms remained effective, particularly at lower water temperatures. As in Bikaner, nighttime convergence occurred, reinforcing the finding that immersion is most effective during daytime thermal peaks. Additional cities in the supplementary file exhibited consistent patterns (see Figure C 3). In Ahmedabad and New Delhi (hot-dry and composite), 20 °C immersion-maintained core temperature below hyperthermia thresholds. In Mumbai (humid climate), leg immersion remained effective. However, the implementation of leg immersion may be constrained by the need for a suitably sized vessel and a seated posture that further restricts mobility compared to foot immersion. Overall, these results support leg immersion as a robust, climate-resilient cooling strategy, with effectiveness strongly tied to water temperature and time of application..

5.4.3 Dousing Cooling Effects

Figure 5.13a displays core temperature variation in Bikaner during a heat event for three dousing strategies compared to no cooling method. All dousing methods effectively reduced core temperature, with the greatest reduction (~0.35 °C) observed in Dousing 3, which included application to the head, neck, chest, back, arms, and legs. This approach maintained core temperature below the moderate hyperthermia threshold during peak hours, attributable to the larger wetted surface area enhancing evaporative and convective heat loss. Dousing 1 (head, neck, shoulders, arms, legs) and Dousing 2 (head, neck, chest, arms, legs), involving fewer application regions, also improved thermal response but were less effective than Dousing 3.

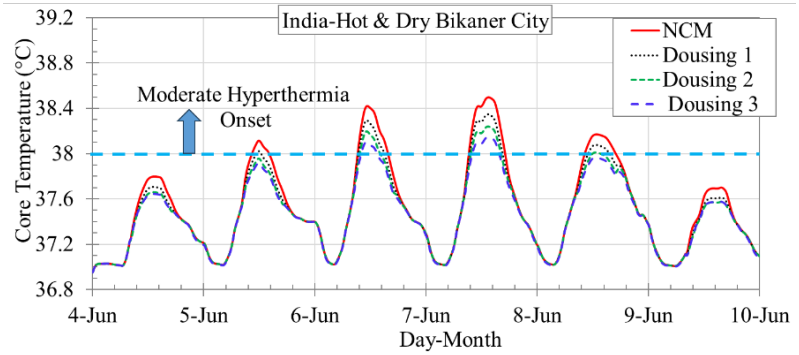

(a)

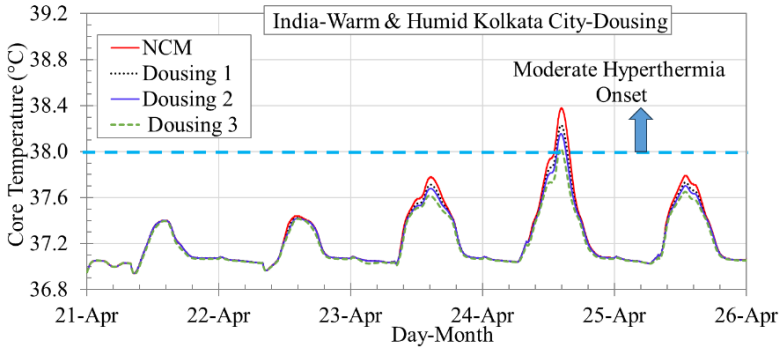

(b)

Figure 5.13. Core temperature variation during a heat event for dousing interventions and no cooling method (NCM) in (a) the hot and dry city of Bikaner and (b) the warm and humid city of Kolkata.

Figure 5.13b presents similar results in Kolkata (hot-humid climate), where high enthalpy (~120 kJ/kg) caused core temperatures under NCM to exceed 38 °C. All dousing strategies reduced core temperature, with Dousing 3 again providing the most effective cooling. Due to Kolkata's elevated humidity (~61%), differences among the three dousing approaches were smaller than in Bikaner, though including the chest (in Dousing 2 and 3) led to improved cooling performance. This is because the higher ambient humidity reduced the vapor pressure gradient between skin and air, thereby limiting evaporation. These findings confirm that dousing, particularly when applied over broader surface areas, is a practical and effective cooling method under both dry and humid conditions.

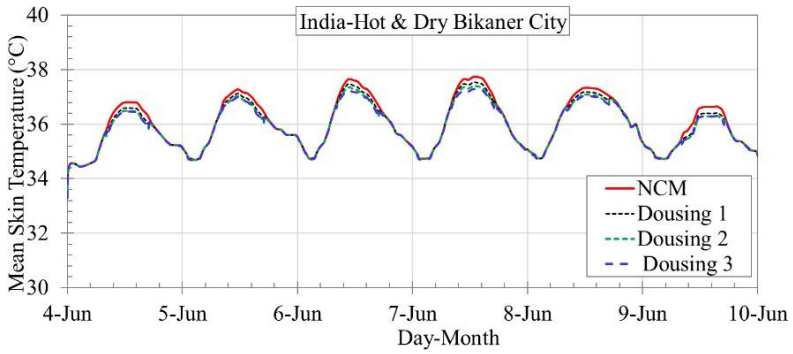

(a)

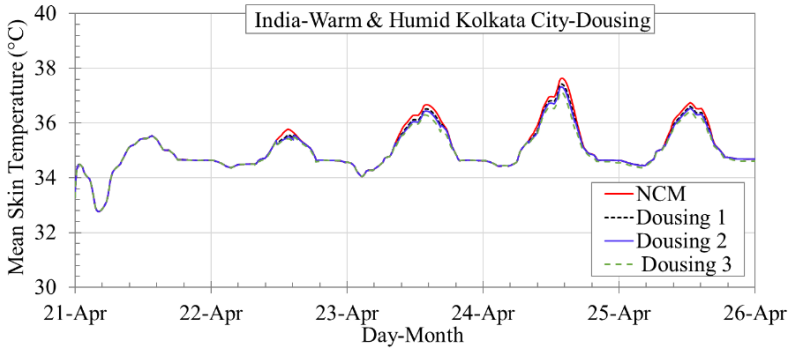

(b)

Figure 5.14. Mean skin temperature variation during a heat event for dousing interventions at different water temperatures and no cooling method (NCM) in (a) the hot and dry city of Bikaner and (b) the warm and humid city of Kolkata.

Figure 5.14(a) shows that in Bikaner (hot-dry climate), dousing interventions provide more stable and consistent mean skin temperature reduction compared to no cooling method. Dousing 3, which covers the face, neck, chest, back, arms, legs, and feet, yields the most pronounced and stable cooling effect. This can be attributed to enhanced evaporation across a larger wetted surface area, effectively minimizing thermal fluctuations and reducing discomfort associated with rapid temperature changes. Next, Figure 5.14(b) displays similar trends in Kolkata (hot-humid climate), where all dousing methods consistently reduce skin temperature and maintain thermal stability despite high humidity. While the differences among the dousing scenarios are less pronounced in humid conditions, their overall effectiveness highlights the contribution of surface evaporation to thermal comfort. While expanded surface

coverage enhanced cooling potential, the high humidity constrained the additional benefits, leading to diminishing returns. Results from additional cities, presented in the supplementary material (Figure C 4), support the trends observed in Bikaner and Kolkata. In Ahmedabad and composite climates like New Delhi and Nagpur, Dousing 3 consistently lowered skin temperatures and minimized variability. In Mumbai, the limited evaporative potential due to high humidity reduces the effectiveness of dousing as a cooling intervention. These results underscore dousing as a practical and reliable passive cooling strategy across diverse climates.

5.4.4 Comparative Analysis and Practical Recommendations

For comparative analysis, all cooling interventions were evaluated at the same water temperature (30 °C), with Dousing 3 considered for the dousing strategy. In Bikaner (hot-dry climate), the highest core temperature (~38.5 °C) was observed when no cooling method was used, indicating severe thermal strain. Leg immersion provided the greatest reduction (0.5 °C), followed by dousing (0.4 °C) and foot immersion (0.2 °C) (Figure 5.15a). In Kolkata (hot-humid climate), where elevated humidity and enthalpy (~120 kJ/kg) intensified thermal stress, leg immersion achieved a larger reduction of 2.0 °C, while dousing and foot immersion reduced core temperature by 0.6 °C and 0.3 °C, respectively (Figure 5.15b). These results highlight the superior conductive cooling capacity of leg immersion due to the larger contact area, while dousing benefits from evaporative and convective mechanisms. Furthermore, unlike foot and leg immersion, which require users to remain seated with access to a water container, dousing allows for more flexible and mobile application during daily activities, making it more practical for certain users. Foot immersion, limited by a smaller wetted area, was the least effective. Results for remaining cities, presented in the supplementary material. Similar patterns were observed in other climate conditions, reinforcing leg immersion as the most robust intervention across varied conditions. Table 5.2 summarizes the maximum core temperature under the no

cooling method (NCM), foot immersion, leg immersion, and dousing at a common water temperature of 30 °C. In New Delhi and Nagpur (hot–dry), the reductions were modest (~0.3 °C), whereas in Bikaner and Kolkata (hot–humid) leg immersion achieved the largest reduction. Across all climates, leg immersion consistently provided the greatest cooling effect, followed by dousing and foot immersion. These results highlight leg immersion as the most robust strategy across diverse climates.

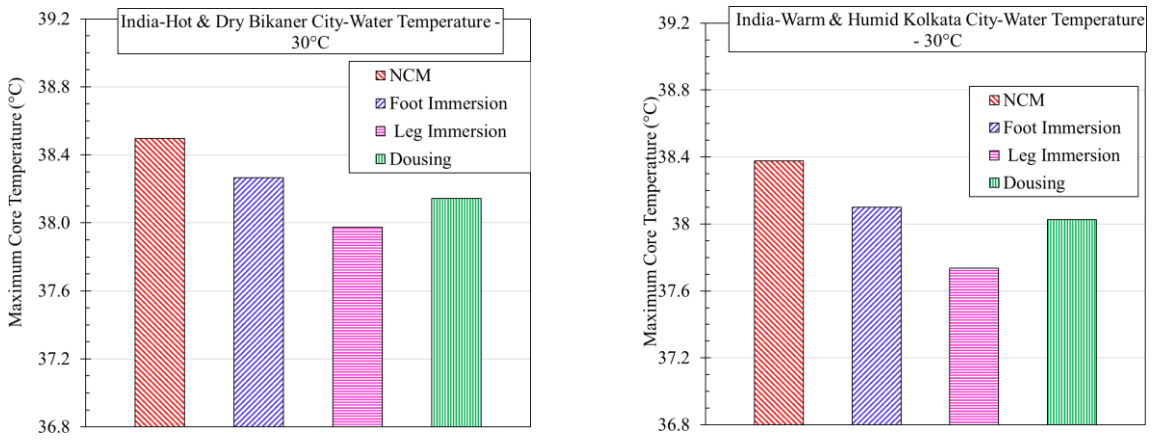

(a) (b)

Figure 5.15. Maximum core temperature for foot immersion, leg immersion, and dousing compared to no cooling method in (a) Bikaner (hot-dry) and (b) Kolkata (hot-humid) cities.

Table 5.2. Maximum core temperature (°C) reported in case of no cooling method (NCM), foot immersion, leg immersion, and dousing across Indian cities at a common water temperature of 30 °C.

City	No cooling method (NCM) (°C)	Foot immersion (°C)	Leg immersion (°C)	Dousing (°C)
Bikaner	38.5	38.3	38.0	38.1
Ahmedabad	38.0	37.8	37.7	37.8
Kolkata	38.3	38.1	37.7	38.0
Mumbai	37.5	37.4	37.3	37.5
New Delhi	38.0	37.8	37.7	37.8

Nagpur	38.2	38.0	37.9	37.9

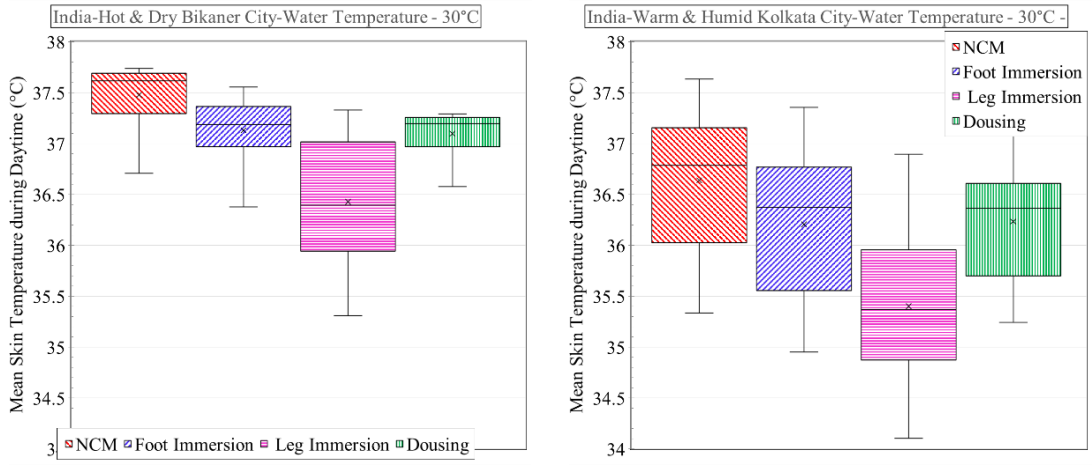

(a) (b)

Figure 5.16. Mean skin temperature for no cooling method, foot immersion, leg immersion, and dousing during daytime hours (08:00–17:00) on an extreme heatwave day for (a) Bikaner (hot-dry) and (b) Kolkata (hot-humid) cities.

Figure 5.16 presents the mean skin temperature variation during daytime hours (08:00–17:00) in Bikaner and Kolkata. NCM resulted in the highest skin temperatures (~38.49 °C), indicating substantial thermal stress. Leg immersion achieved the lowest skin temperatures due to enhanced conductive cooling but also exhibited the largest fluctuations, likely due to intermittent immersion cycles. Foot immersion provided intermediate relief with moderate variability. Dousing maintained lower skin temperatures than foot immersion and exhibited the least fluctuation, attributable to frequent and distributed water application enabling stable evaporative cooling. Results for remaining cities, presented in the supplementary material. Similar patterns were observed in other climate conditions, reinforcing leg immersion as the most robust intervention across varied conditions. These findings suggest that while leg immersion provides stronger physiological cooling, dousing enhances perceptual comfort by maintaining greater thermal stability of skin temperature.

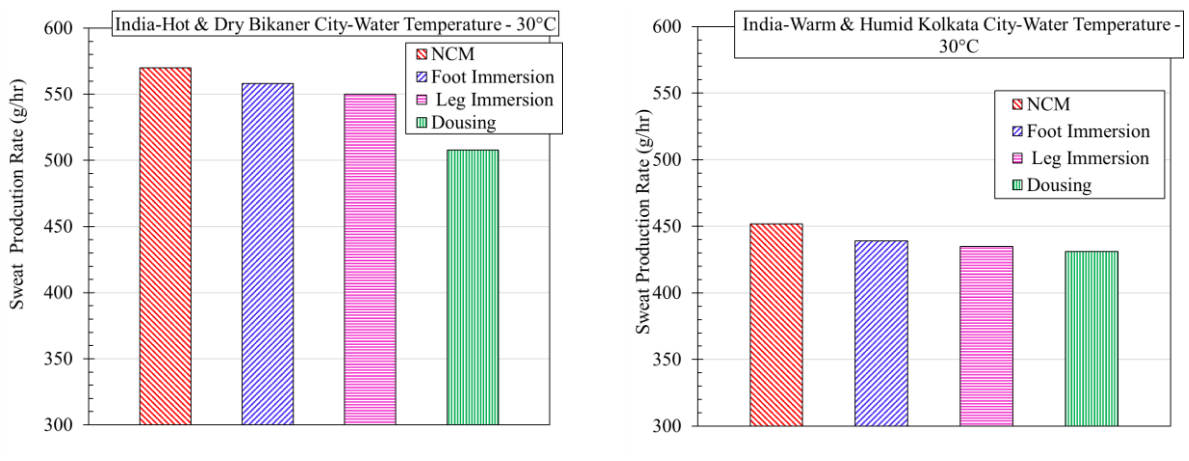

(a) (b)

Figure 5.17. Average sweat loss reduction for foot immersion, leg immersion, and dousing compared to no cooling method in (a) Bikaner (hot-dry) and (b) Kolkata (hot-humid) cities.

Figure 5.17 illustrates average sweat production rate during daytime hours (08:00–17:00) on an extreme heatwave day under different interventions compared to no cooling method. In Bikaner, NCM produced the highest sweat rate (~570 g/hr), with dousing exhibiting the largest reduction (62 g/hr), followed by leg immersion (20 g/hr) and foot immersion (12 g/hr). In Kolkata, overall sweat rates were lower due to reduced ambient temperature, but high humidity hindered evaporation. Dousing again yielded the most significant reduction (21 g/hr). These results show that all interventions reduce sweat burden, with dousing being the most effective in limiting perspiration, potentially reducing dehydration risk. Similar observations were noted in other cities (see Figure C 5, Figure C 6, Figure C 7). Overall, leg immersion delivers stronger thermo-physiological cooling, while dousing provides more stable skin temperatures and lower sweat rates, indicating a trade-off between cooling intensity and comfort.

5.5 Discussion and Limitation

This study systematically assessed the thermal effectiveness of three passive cooling interventions—foot immersion, leg immersion, and dousing—using a thermoregulation model under real-world heatwave conditions. Among the evaluated strategies, leg immersion

demonstrated the greatest potential to reduce core temperature, particularly when 20 °C water was used. The increased surface contact between the lower limbs and the water allowed for enhanced conductive heat loss, maintaining core temperature consistently below the moderate hyperthermia threshold. Foot immersion, though logistically simpler and still beneficial, exhibited limited effectiveness under more intense heat exposure, especially in hot and dry climatic conditions with ambient temperatures above 45 °C. In such scenarios, core temperature remained closer to the hyperthermia threshold, indicating that foot immersion alone may not provide sufficient physiological relief under severe thermal stress.

Dousing interventions, particularly Dousing 3, proved most effective in reducing and stabilizing mean skin temperature. By targeting a larger body surface area, dousing 3 allowed for uniform evaporative and convective cooling, thereby preventing abrupt skin temperature fluctuations and reducing thermal discomfort. Furthermore, unlike foot and leg immersion, which require users to remain seated with access to a water container, dousing allows for more flexible application during daily activities. Across water immersion strategies, cooler water temperatures (20 °C) were consistently more effective than warmer water (25–30 °C), because the steeper thermal gradient between the body and water enhanced conductive heat loss. While leg immersion demonstrated the strongest performance in lowering core temperature, dousing showed superiority in stabilizing skin temperature, and foot immersion provided a balance between ease of implementation and moderate effectiveness.

From a public health perspective, these findings highlight the potential of water-based cooling strategies as accessible, low-cost interventions in low- and middle-income countries (LMICs), where air conditioning coverage is limited and power outages are frequent. Incorporating such strategies into community heat-health action plans could reduce the risk of heat-related illness, particularly among vulnerable population. However, behavioral and social factors may influence real-world applicability. For instance, while leg immersion is highly effective, it

requires water access and time in a seated posture, which may not be feasible for outdoor laborers. Similarly, willingness to douse in public settings may vary depending on cultural and social norms. Such factors should be considered when translating model-based findings into practical public health guidelines.

Furthermore, the present study has several limitations. The simulations were based on a standard subject in good health and physical fitness, with other parameters such as water temperature and timing of intervention held constant. The model did not account for inter-individual variability (e.g., age, sex, or pre-existing health conditions), nor for sensitivity analyses that could capture a broader range of physiological responses. Moreover, outdoor weather conditions were assumed to represent indoor environments, which may not accurately reflect real-world scenarios. Therefore, future studies should expand to include diverse body types, acclimatization states, and varying clothing insulation to better capture population-level responses. However, despite these constraints, the model provides robust insights into the practical application of water-based cooling interventions under extreme heat stress.

5.6 Summary

This study presents a comprehensive computational evaluation of foot immersion, leg immersion, and dousing cooling interventions using a modified thermoregulation model under real-world heatwave conditions in representative Indian cities. The model simulated the physiological responses of a hypothetical healthy male under realistic conditions, incorporating environmental parameters such as air temperature, relative humidity, and air speed, along with physiological processes like metabolic heat generation and thermoregulatory feedback loops. Foot immersion was found to provide meaningful but moderate relief in both hot and dry and warm and humid environments, with cooling performance highly dependent on water temperature. In hot and dry regions like Bikaner, where daytime temperatures exceeded 45 °C

and enthalpy surpassed 90 kJ/kg, foot immersion with 20 °C water resulted in a reduction in core temperature of approximately 0.27 °C during peak thermal stress. However, even with cooling, core temperature remained near or slightly above the moderate hyperthermia threshold (~38 °C), suggesting that foot immersion alone may be insufficient during the most extreme heat events.

In warm and humid regions like Kolkata, foot immersion also proved effective, reducing core temperature by up to 0.35 °C during periods of high enthalpy (~120 kJ/kg). The high humidity in such regions limits sweat evaporation, making conductive cooling more critical. Foot immersion provided stable mean skin temperature reductions in the range of 0.4 to 0.8 °C, with the cooler water temperature offering more noticeable benefits. However, cooling was only effective during the daytime when environmental stress exceeded intervention thresholds, and benefits diminished at night when cooling was not applied. Across the different cities studied, including Ahmedabad, Mumbai, New Delhi, and Nagpur, similar trends emerged—foot immersion consistently lowered both core and skin temperatures but struggled to bring core temperatures below the hyperthermia threshold during the most severe heat days.

Leg immersion demonstrated significantly greater thermal effectiveness than foot immersion. In hot and dry conditions, leg immersion with 20 °C water consistently maintained core temperatures below the hyperthermia threshold, with temperature reductions reaching approximately 0.7 °C compared to no cooling. Even water at 25 °C and 30 °C proved sufficient to prevent core temperature escalation above 38 °C, owing to the larger skin surface area involved and the enhanced conductive and convective heat loss from the lower limbs. In humid climates like Kolkata, leg immersion remained effective, particularly with cooler water, showing consistent mitigation of core and mean skin temperatures even during high humidity periods when evaporative cooling was impaired. The cooling performance of leg immersion

was clearly superior to foot immersion, both in terms of magnitude and consistency, and it remained effective across diverse climate zones.

Dousing interventions further enhanced cooling performance by enabling large-scale evaporative and convective heat transfer from multiple body regions. Among the three dousing strategies tested, the one involving water application to the face, neck, chest, back, arms, legs, and feet consistently outperformed others. This approach reduced core temperature by up to 0.7 °C during peak thermal stress in Bikaner and helped maintain temperatures near or below the hyperthermia threshold even under high ambient heat and low humidity. In humid regions like Kolkata, dousing also significantly reduced thermal strain, although the absolute cooling effect was smaller due to limited evaporative capacity. Importantly, dousing was particularly effective in stabilizing skin temperatures, reducing abrupt thermal fluctuations and maintaining user comfort throughout the day. Its flexible application and independence from immersion setups made it a promising intervention for various activity levels and settings. Across the range of environmental conditions and intervention types modeled, it was evident that the selection of cooling strategy, water temperature, and the extent of body surface involved were critical factors in determining effectiveness.

CHAPTER 6. CONCLUSIONS AND RECOMMENDATIONS FOR FUTURE STUDY

This chapter presents a summary of the primary findings derived from research and subsequently discusses potential future investigations.

6.1 Conclusions

This research set out to evaluate and optimize accessible cooling strategies under extreme heat events, focusing specifically on electric fan use and water-based passive cooling interventions. Using a combination of experimental trials and advanced thermoregulation modeling, this work contributes new insights into the physiological and perceptual impacts of commonly used yet under-researched cooling methods. The findings support the development of evidence-based guidelines for mitigating thermal strain during prolonged heatwaves, particularly in low-resource and high-risk settings.

The experimental evaluation of electric fan usage revealed that both ceiling fans and table fans improved thermal comfort and delayed physiological strain compared to the no-fan condition under controlled hot environments. Although both fan types lowered core and skin temperatures and reduced cardiovascular strain, the table fan provided slightly better outcomes in terms of thermal sensation and subjective comfort. This advantage was attributed to the table fan's proximity to the body, which allowed for more targeted airflow and enhanced evaporative cooling. Notably, these findings challenge the blanket assumption that ceiling fans are universally optimal and underscore the need to tailor fan strategies according to placement and user needs. The improved thermal comfort and extended tolerance times observed in the fan-

assisted scenarios further reinforce the practical utility of fans as viable tools in heat mitigation, especially for sedentary individuals in moderate heat conditions.

Beyond the experimental setup, the research extended to the use of a modified JOS-3 thermoregulation model to simulate complex scenarios of fan usage under varying environmental and physical activity conditions. The model integrated dehydration-dependent physiological adjustments, such as dynamic changes in set-point temperature, vasodilation response, and sweat regulation, enabling a realistic simulation of body responses under extreme heatwave conditions. The simulations revealed that while electric fans are beneficial under moderately hot and dry environments, their use under more extreme heat and humidity conditions—especially above 50°C and RH exceeding 60%—may become counterproductive. In such cases, fans can exacerbate thermal strain by increasing sensible heat gain, particularly when airflow accelerates heat absorption rather than facilitating evaporation. This risk is further magnified with increased physical activity, which compounds internal heat production. These model-based insights highlight the nuanced role fans play across varying environmental conditions and call for region-specific and condition-specific usage guidelines to avoid misuse and potential harm during critical heat events.

In parallel, the research evaluated three passive water-based cooling interventions—foot immersion, leg immersion, and dousing—using the same thermoregulation modeling framework under real-world heatwave scenarios drawn from Indian climate zones. The simulations captured diverse environmental conditions, body surface coverage, and water temperatures to holistically assess the physiological effectiveness of each method. Among the interventions tested, leg immersion emerged as the most effective at reducing core body temperature, particularly when using 20°C water. This method consistently prevented the onset of moderate hyperthermia across all climatic regions evaluated, including hot-dry, warm-

humid, and composite zones. The superior performance of leg immersion was attributed to the larger surface area in contact with water, which enabled sustained conductive and convective heat transfer from the lower limbs to the cooler water medium.

Foot immersion, while less effective than leg immersion, still proved valuable, particularly in humid climates where evaporative cooling is restricted. Although its limited surface coverage reduced its capacity to meaningfully lower core temperature under more severe conditions, foot immersion offered a logistically simpler option for individuals without access to larger water containers or immersion setups. In contrast, the dousing method, which involved applying water to various parts of the body, showed significant potential in stabilizing mean skin temperatures, especially when applied to a wider surface area. Dousing 3, which targeted multiple body segments including the chest, back, arms, and legs, demonstrated the most consistent cooling response and thermal stability. This finding underscores the critical role of body surface coverage and water distribution in maximizing the cooling benefits of self-dousing strategies.

Across all interventions, the study found that water temperature played a critical role in determining cooling efficiency. Cooler water consistently produced greater thermal relief, although even water at 30°C was sufficient to prevent hyperthermia during leg immersion. This suggests that passive cooling interventions remain effective even when access to cold water is limited, thereby enhancing their applicability in resource-constrained settings. The timing and activation of these interventions, based on ambient temperature and enthalpy thresholds, further ensured their relevance in realistic heat stress conditions, aligning intervention onset with periods of greatest physiological risk.

Together, the experimental and simulation-based findings of this research provide a comprehensive and actionable understanding of how simple, affordable cooling strategies can

mitigate thermal strain in extreme heat conditions. The implications span public health policy, urban planning, and disaster preparedness, especially in heat-vulnerable populations with limited access to energy-intensive cooling technologies like air conditioning. The conclusions underscore the importance of refining and contextualizing heat-mitigation strategies to specific climates, user behaviors, and physiological responses, ensuring that interventions are both effective and safe under a range of extreme conditions.

6.2 Scope of Future Research

While this thesis provides meaningful contributions toward understanding and optimizing passive and fan-based cooling strategies, several avenues remain for future exploration and refinement. First, although the present study examined healthy young adults in both experimental and simulated settings, future work should extend this investigation to other vulnerable demographic groups, such as older adults, individuals with chronic health conditions, and children. These populations often experience altered thermoregulatory responses and may face heightened risks under extreme heat exposure. Integrating age-specific or health-adjusted physiological parameters into the thermoregulation model would enhance its predictive accuracy and broaden its applicability to public health planning.

Moreover, the current model simulations used well-controlled, static environmental conditions representative of real-world heat events. However, in reality, heatwave exposures are dynamic, and indoor thermal conditions can vary due to fluctuating ventilation, shading, occupancy, and building materials. Future work should incorporate transient and spatially heterogeneous boundary conditions to reflect indoor thermal microenvironments more realistically. This can be achieved through coupling the thermoregulation model with dynamic building energy simulation tools or environmental sensors that track real-time temperature and humidity

variations. Such integrated approaches would allow for individualized, adaptive cooling recommendations that respond to real-time risk levels.

Another area for future investigation is the behavioral dimension of cooling intervention. While this study focused on physiological and perceptual responses, actual user compliance, preferences, and adaptation strategies during heatwaves remain underexplored. Investigating how individuals perceive the usability and acceptability of foot immersion, leg immersion, or dousing—especially in community or occupational settings, would provide important context for translating research findings into scalable public health interventions. In particular, understanding cultural perceptions, water availability, and privacy constraints will be critical in designing interventions that are both effective and adopted on a scale.

Additionally, future work should explore the long-term and cumulative effects of repeated cooling interventions. The current study examined single-day or short-duration interventions, but in prolonged heatwave scenarios, individuals may use cooling strategies over multiple days or weeks. Repeated exposure to water immersion or fan usage could have compounding effects on hydration status, skin integrity, and cardiovascular strain, which were not assessed in this work. Modeling the impact of chronic exposure or developing longitudinal studies could reveal whether cooling benefits persist, diminish, or even reverse over time.

The present thermoregulation model includes several innovative features such as dehydration-adjusted thermophysiological responses and segment-specific heat transfer properties. However, further enhancements are warranted to address current limitations. For example, improvements in modeling the sweat-drip dynamics, water retention on irregular skin surfaces, and interactions between clothing and cooling interventions could yield more accurate simulations of real-life conditions. Incorporating high-resolution anatomical data, either from

imaging or anthropometric databases, may improve model geometry and enable finer spatial mapping of temperature and sweat distribution.

Future experimental validation is also critical. Although the model was validated against several existing studies, there remains a need for controlled chamber trials to specifically test fan usage and water immersion strategies under a wider range of environmental, clothing, and activity conditions. Collaborative studies with thermal physiology laboratories could help generate richer datasets and validate model predictions under diverse, standardized protocols.

Finally, the insights from this work offer a foundation for developing decision-support tools or mobile applications that can advise users when and how to apply specific cooling interventions based on weather forecasts, indoor conditions, and personal health profiles. Such tools could integrate wearable sensor data with thermoregulation algorithms to deliver tailored alerts and guidance in real-time. This would translate scientific findings into usable technologies, empowering individuals and healthcare systems to proactively respond to extreme heat threats.

In summary, future work should aim to diversify the studied populations, expand modeling to real-world conditions, account for behavioral dimensions, and develop interactive tools for public use. Addressing these gaps will strengthen the science behind accessible cooling interventions and support scalable, equitable solutions to the growing global burden of extreme heat events.

APPENDIX A ELECTRIC FAN EXPERIEMTAL ANALYSIS

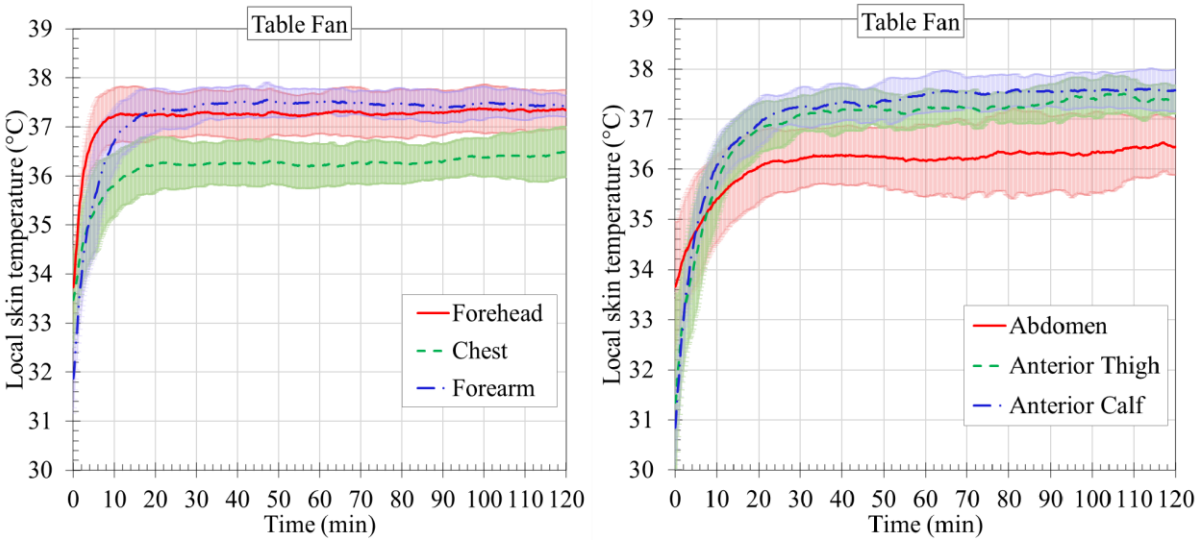

(a) (b)

Figure A 1. Variation in local skin temperatures in table-fan condition: (a) forehead, chest, and forearm; (b) abdomen, anterior thigh, and anterior calf.

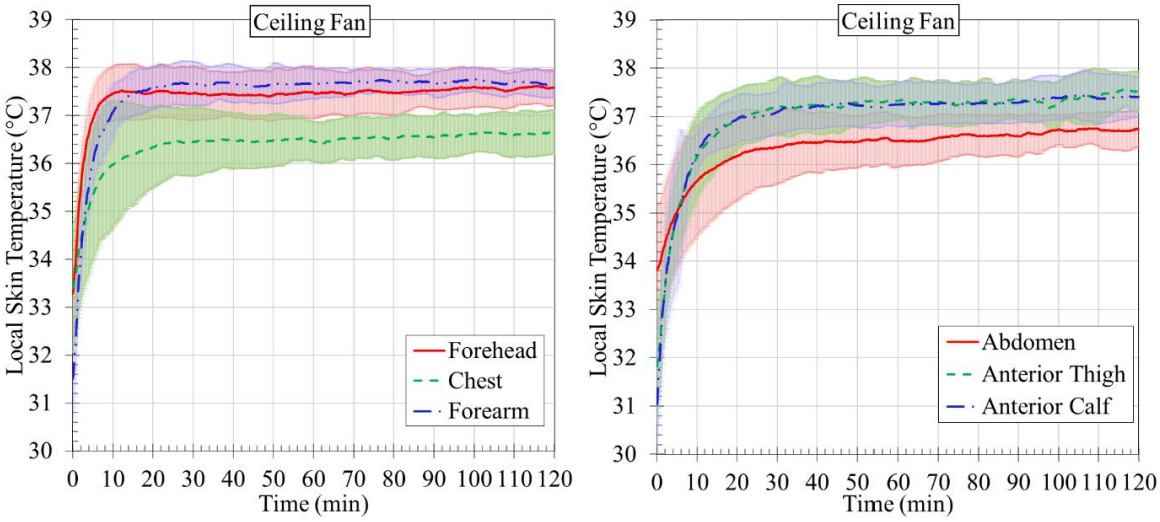

(a) (b)

Figure A 2. Variation in local skin temperatures in ceiling-fan condition: (a) forehead, chest, and forearm; (b) abdomen, anterior thigh, and anterior calf.

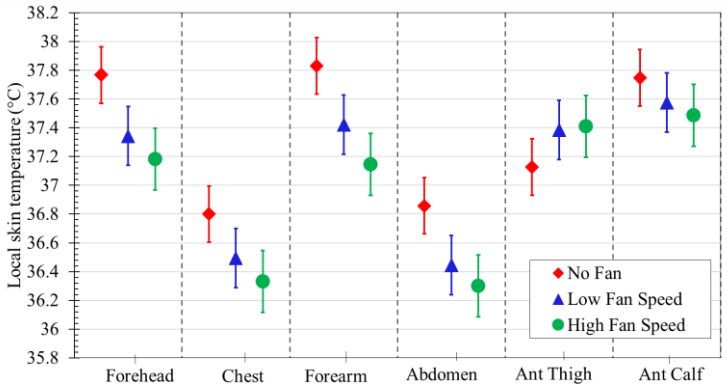

Figure A 3. Local skin temperature at the end trail during no fan, low fan and high fan speed scenarios.

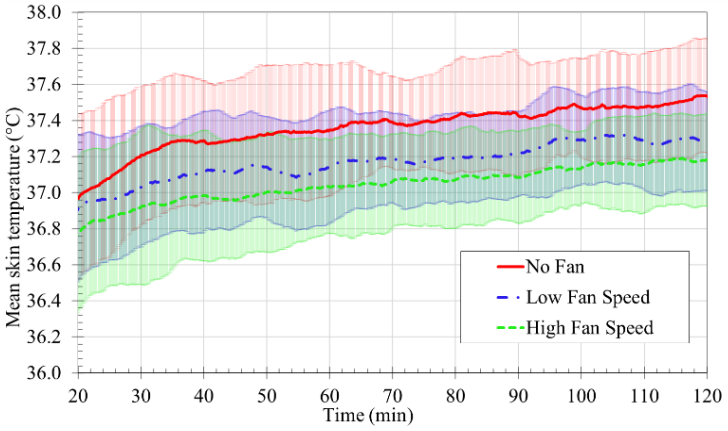

Figure A 4. Mean skin temperatures across no fan, low fan and high fan speed scenarios.

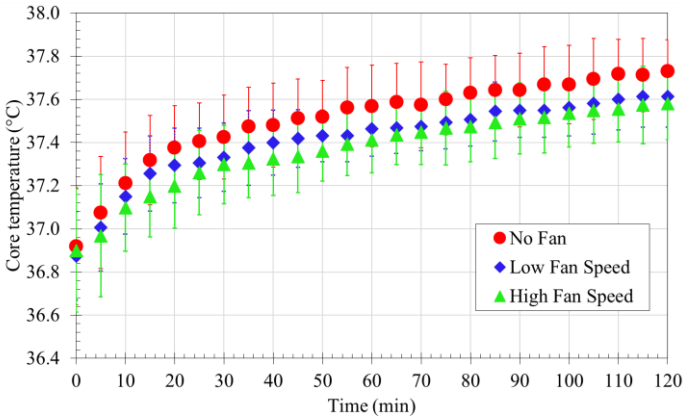

Figure A 5. Core temperature variation under no fan, low fan and high fan speed scenarios.

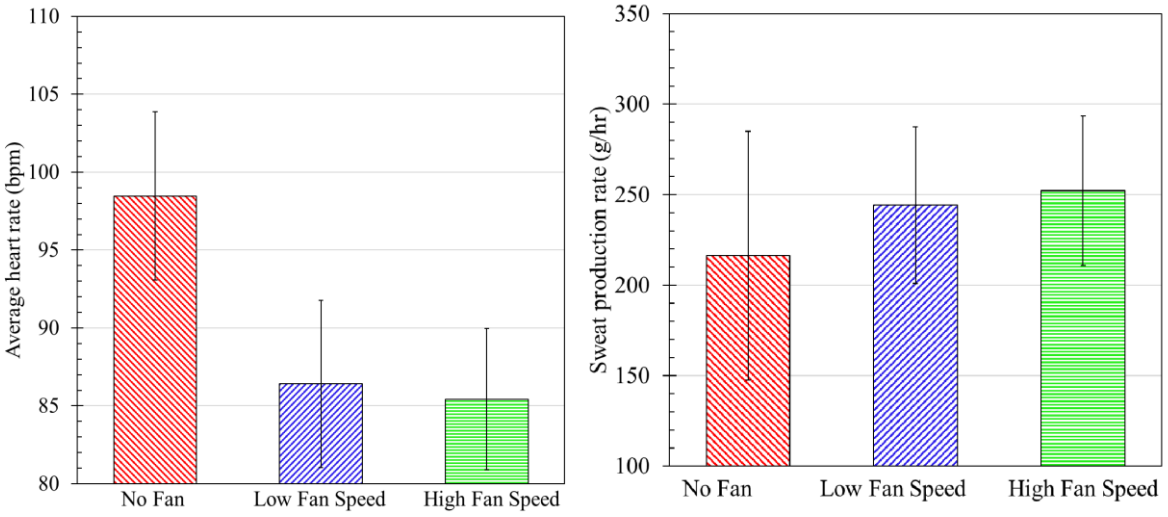

(a) (b)

Figure A 6. (a) Cardiovascular response and (b) sweat production under no fan, low fan and high fan speed scenarios.

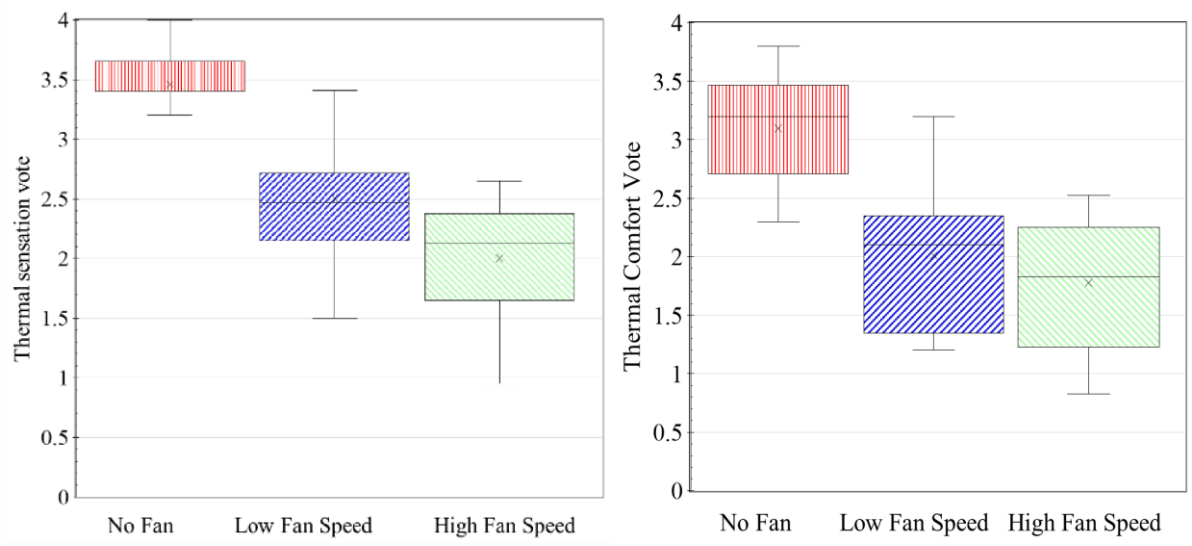

(a) (b)

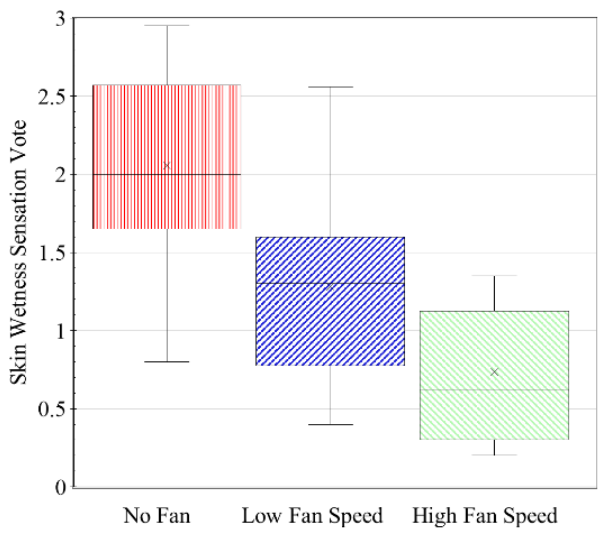

(c)

Figure A 7. (a) Thermal sensation, (b) thermal comfort and (c) skin wetness votes under no fan, low fan and high fan speed scenarios at the end of the trial.

APPENDIX B SWEATING SIGNAL, EVAPORATION LOSS AND MODERATE HYPERTHERMIA ONSET CHART UNDER VARIOUS PAR ACTIVITY

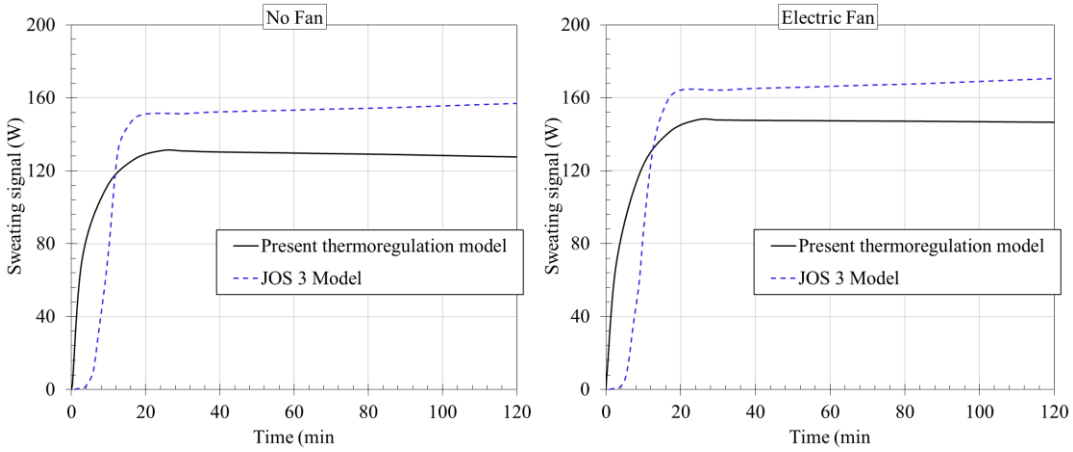

(a) (b)

Figure B 1. Comparison of the sweating signals obtained by the JOS-3 model and the present thermoregulatory model in case of Bhuvad et al. [16] experimental study: (a) No fan and (b) fan scenario.

Table B1. Model-predicted whole-body sweat loss (mL/hour) across varying ambient temperatures and relative humidity levels under no-fan (air velocity = 0.1 m/s) condition.

Ambient Temperature (°C)	Relative Humidity (%)								
	10	20	30	40	50	60	70	80	90
36	182	201	213	304	341	371	425	452	542

38	220	261	287	345	390	470	512	581	630
40	305	370	420	506	540	570	600	610	650
42	360	430	480	540	589	620	650	650	650
44	400	440	500	560	610	640	650	650	650
46	430	480	520	580	620	640	650	650	650
48	510	540	560	610	630	650	650	650	650
50	540	560	590	630	641	650	650	650	650

Table B2. Model-predicted whole-body sweat loss (mL/hour) across varying ambient temperatures and relative humidity levels under fan (air speed 0.8 m/s) condition.

Ambient Temperature (°C)	Relative Humidity (%)								
	10	20	30	40	50	60	70	80	90
36	178	200	206	292	327	361	420	441	532
38	213	266	277	335	383	449	486	560	615
40	325	385	441	521	530	558	586	593	636
42	385	450	501	552	549	599	625	640	640
44	435	465	515	565	610	630	650	650	650
46	461	515	540	615	625	640	650	650	650
48	537	565	580	625	640	650	650	650	650
50	567	595	620	640	646	650	650	650	650

Table B3. Rate of evaporative heat loss from skin (W/m2) under no-fan (air velocity = 0.1 m/s) and fan (air speed 0.8 m/s) conditions.

Ambient Temperature (°C)	No-fan conditions (0.1 m/s)		Fan conditions (0.8 m/s)	
	RH=30%	RH=60%	RH=30%	RH=60%
36	65	55	78	60
38	78	60	96	75
40	105	62	121	80
42	120	55	167	75
44	143	45	210	65
46	128	35	197	55
48	121	25	191	45
50	113	15	184	35

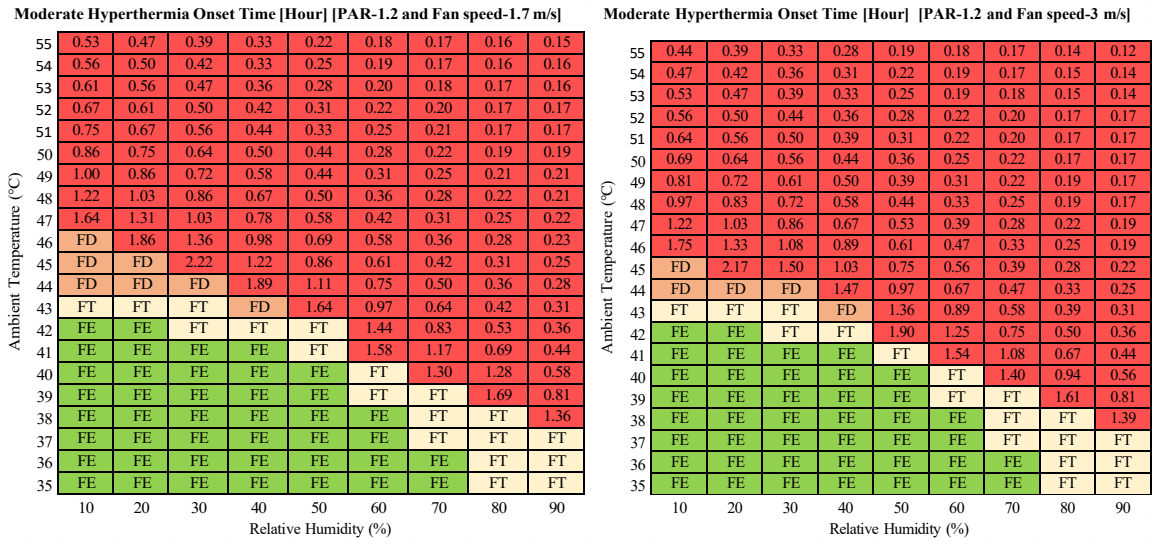

(a) (b)

Figure B 2. Moderate hyperthermia onset chart for electric fan use under various extreme environmental conditions during activity level of 1.2 PAR. Fan use is effective (green zone- FE) when Tc-fan < 38.0 °C and Tc-fan reduction relative to no-fan by ≥ 0.1 °C; trivial (yellow zone- FT) when Tc-fan < 38.0 °C with a reduction relative to no-fan < 0.1 °C; detrimental

(orange zone- FD) when Tc-fan < 38.0 °C but exceeds no-fan; and detrimental (red zone) when Tc-fan > 38.0 °C and exceeds no-fan: (a) Electric fan speed of 1.7 m/s; and (b) electric fan speed of 3.0 m/s.

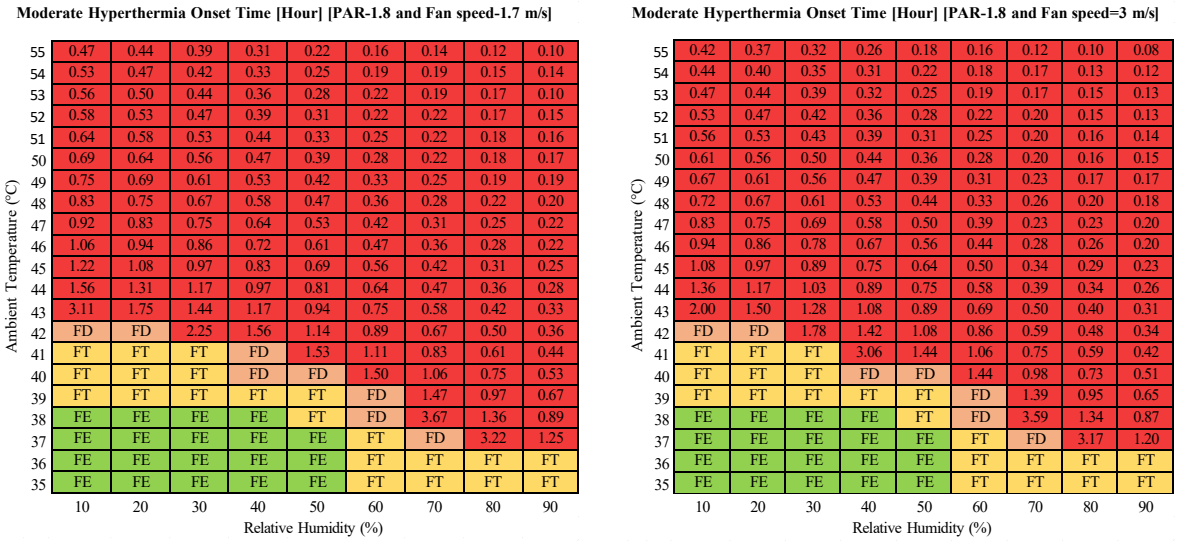

(a) (b)

Figure B 3. Moderate hyperthermia onset chart for electric fan use under various extreme environmental conditions during activity level of 1.2 PAR. Fan use is effective (green zone- FE) when Tc-fan < 38.0 °C and Tc-fan reduction relative to no-fan by ≥ 0.1 °C; trivial (yellow zone- FT) when Tc-fan < 38.0 °C with a reduction relative to no-fan < 0.1 °C; detrimental (orange zone- FD) when Tc-fan < 38.0 °C but exceeds no-fan; and detrimental (red zone) when Tc-fan > 38.0 °C and exceeds no-fan: (a) Electric fan speed of 1.7 m/s; and (b) electric fan speed of 3.0 m/s.

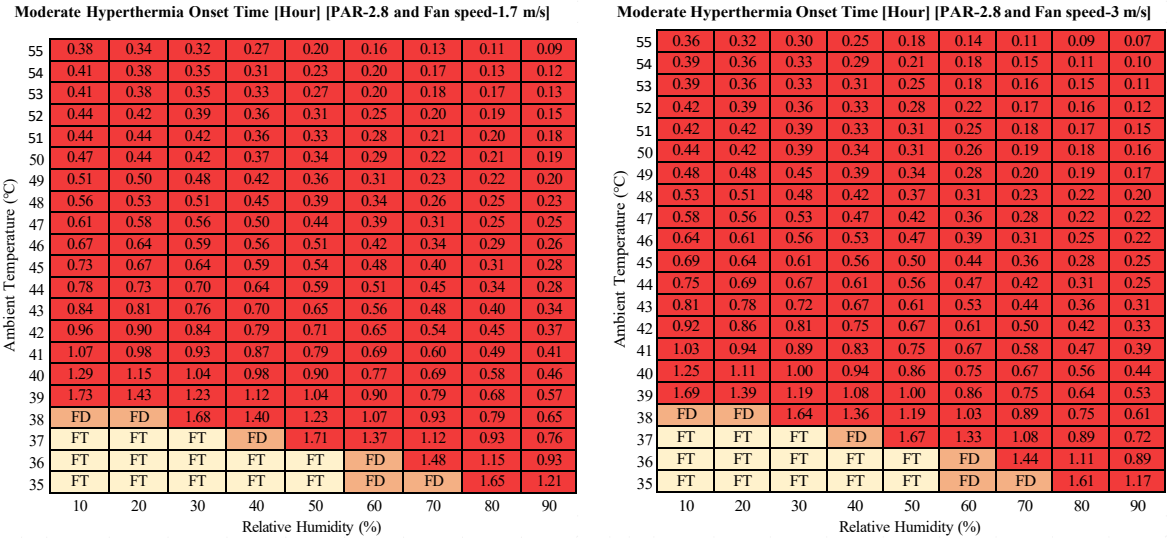

(a) (b)

Figure B 4. Moderate hyperthermia onset chart for electric fan use under various extreme environmental conditions during activity level of 2.8 PAR. Fan use is effective (green zone- FE) when Tc-fan < 38.0 °C and Tc-fan reduction relative to no-fan by ≥ 0.1 °C; trivial (yellow zone- FT) when Tc-fan < 38.0 °C with a reduction relative to no-fan < 0.1 °C; detrimental (orange zone- FD) when Tc-fan < 38.0 °C but exceeds no-fan; and detrimental (red zone) when Tc-fan > 38.0 °C and exceeds no-fan: (a) Electric fan speed of 1.7 m/s; and (b) electric fan speed of 3.0 m/s.

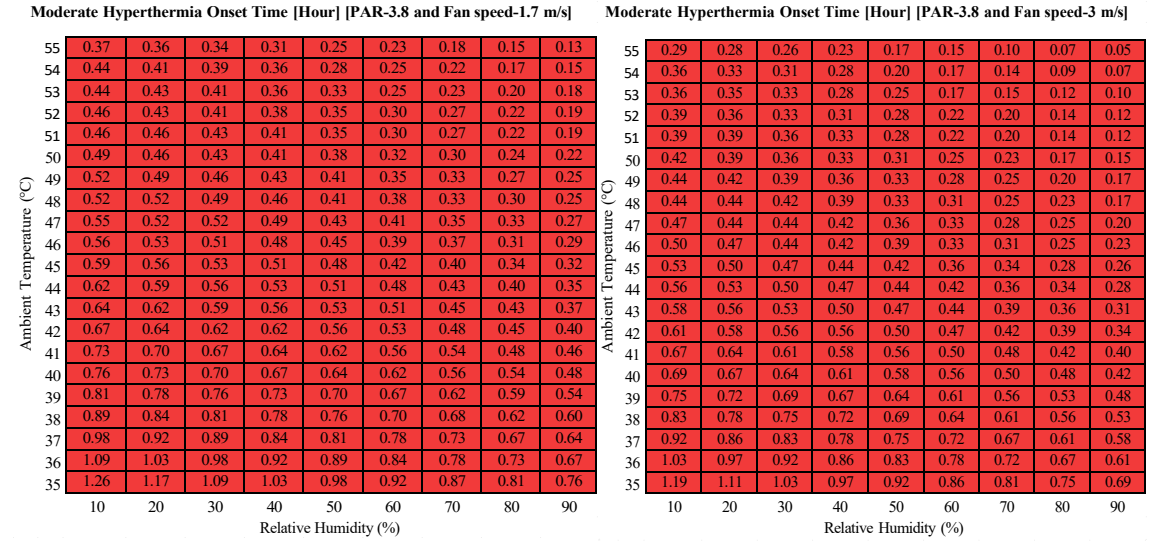

(a) (b)

Figure B 5. Moderate hyperthermia onset chart for electric fan use under various extreme environmental conditions during activity level of 3.8 PAR. Fan use is effective (green zone- FE) when Tc-fan < 38.0 °C and Tc-fan reduction relative to no-fan by ≥ 0.1 °C; trivial (yellow zone- FT) when Tc-fan < 38.0 °C with a reduction relative to no-fan < 0.1 °C; detrimental (orange zone- FD) when Tc-fan < 38.0 °C but exceeds no-fan; and detrimental (red zone) when Tc-fan > 38.0 °C and exceeds no-fan: (a) Electric fan speed of 1.7 m/s and (b) electric fan speed of 3.0 m/s.

APPENDIX C WEATHER DATA, FOOT IMMERSION, LEG IMMERSION AND DOUSING RESULTS

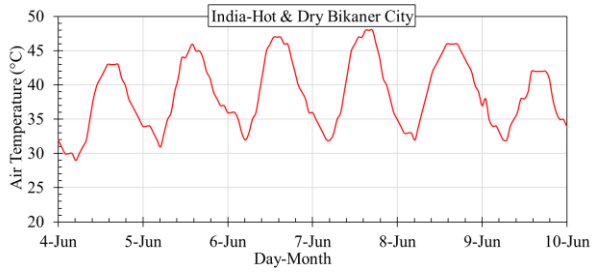

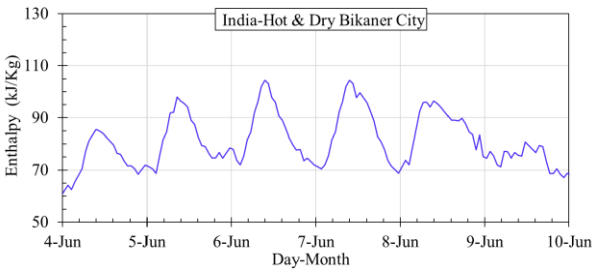

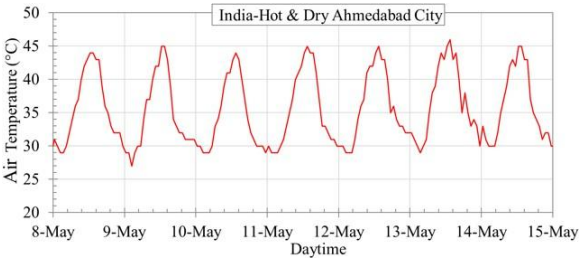

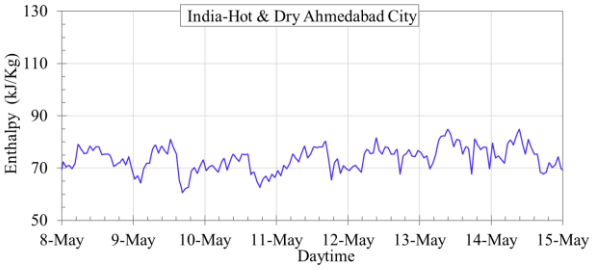

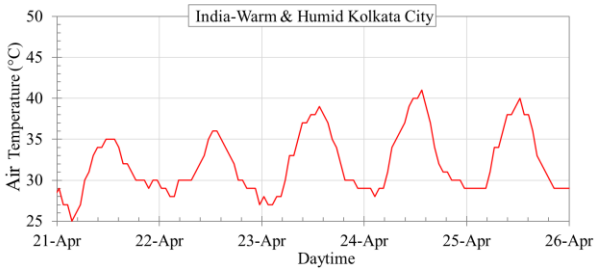

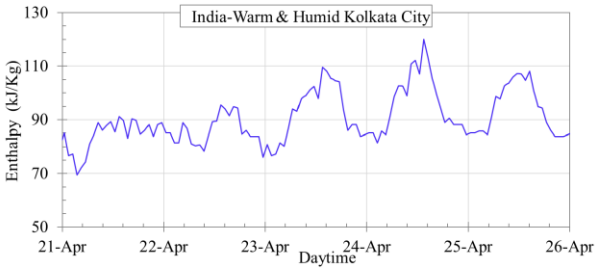

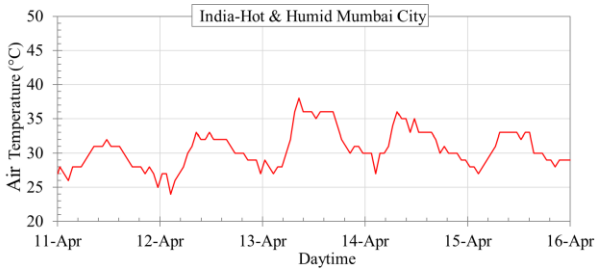

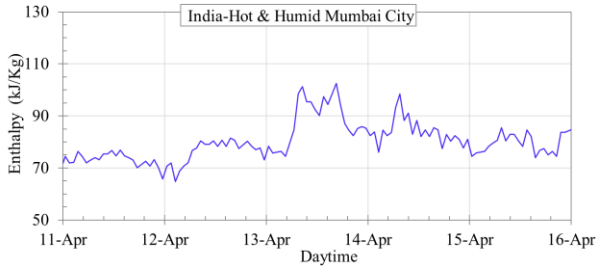

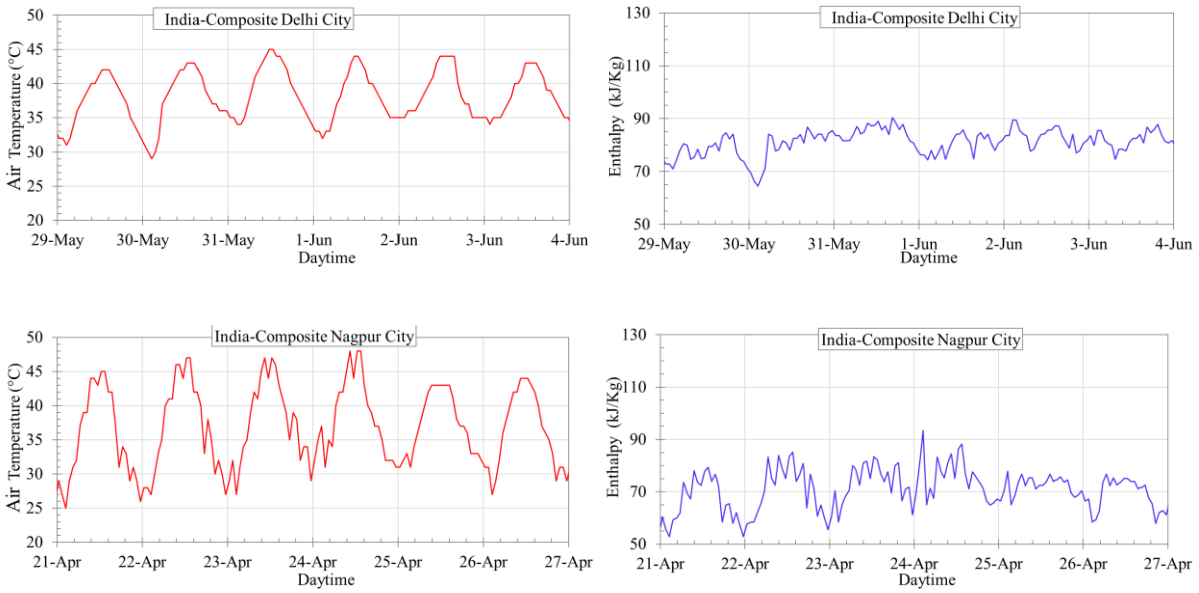

Figure C1.Air temperature and enthalpy variations over time during a heat event across six different climatic cities of India.

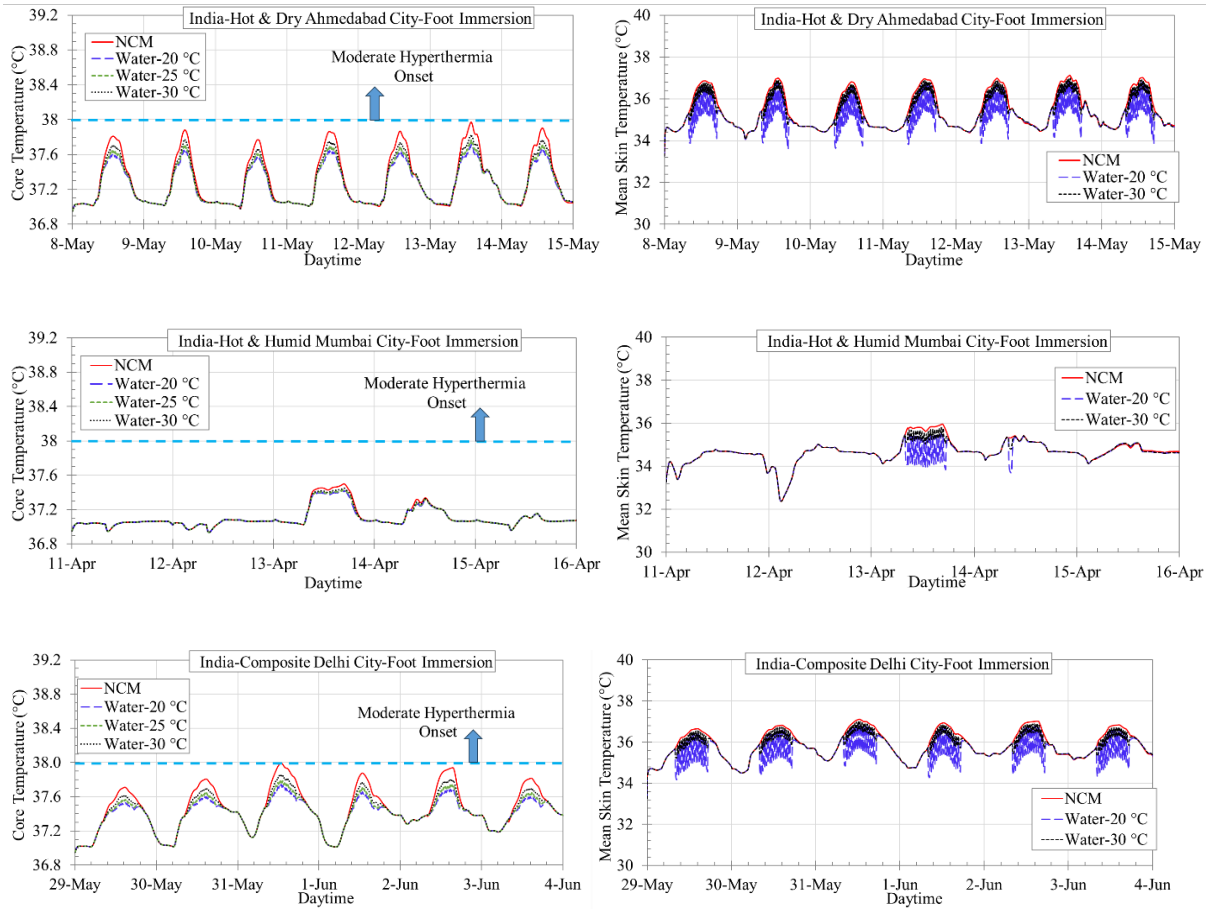

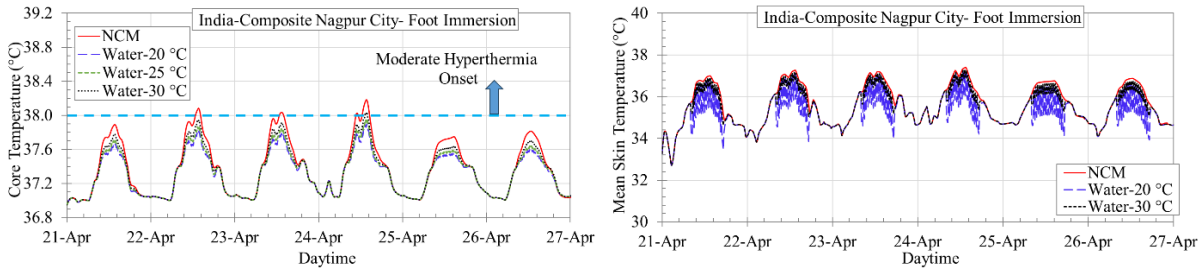

Figure C 2. Core and mean skin temperature variation during a heat event for foot immersion interventions at different water temperatures and with no cooling method (NCM) in across different climatic cities of India.

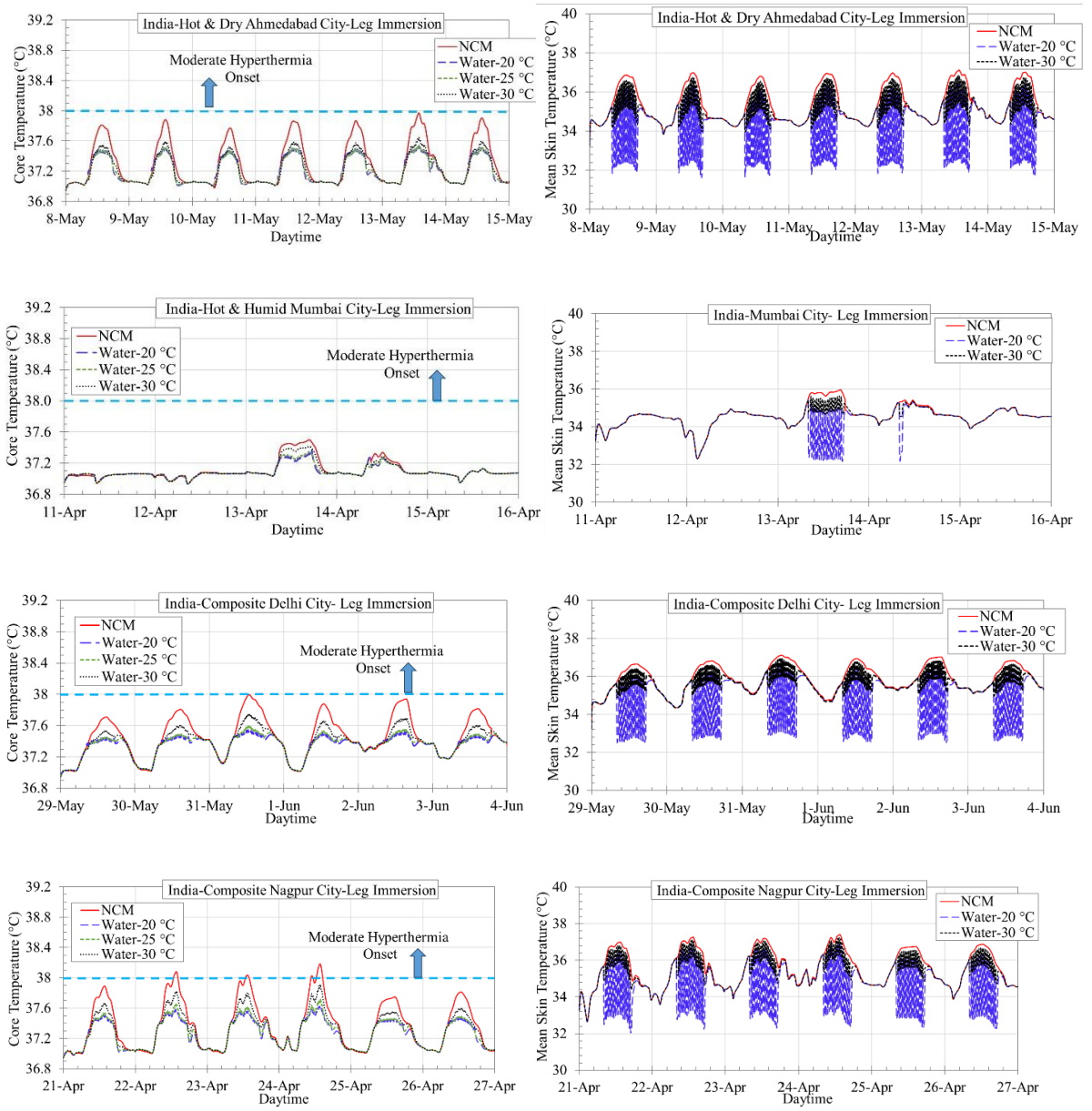

Figure C 3. Core and mean skin temperature variation during a heat event for leg immersion interventions at different water temperatures and with no cooling method (NCM) in across different climatic cities of India.

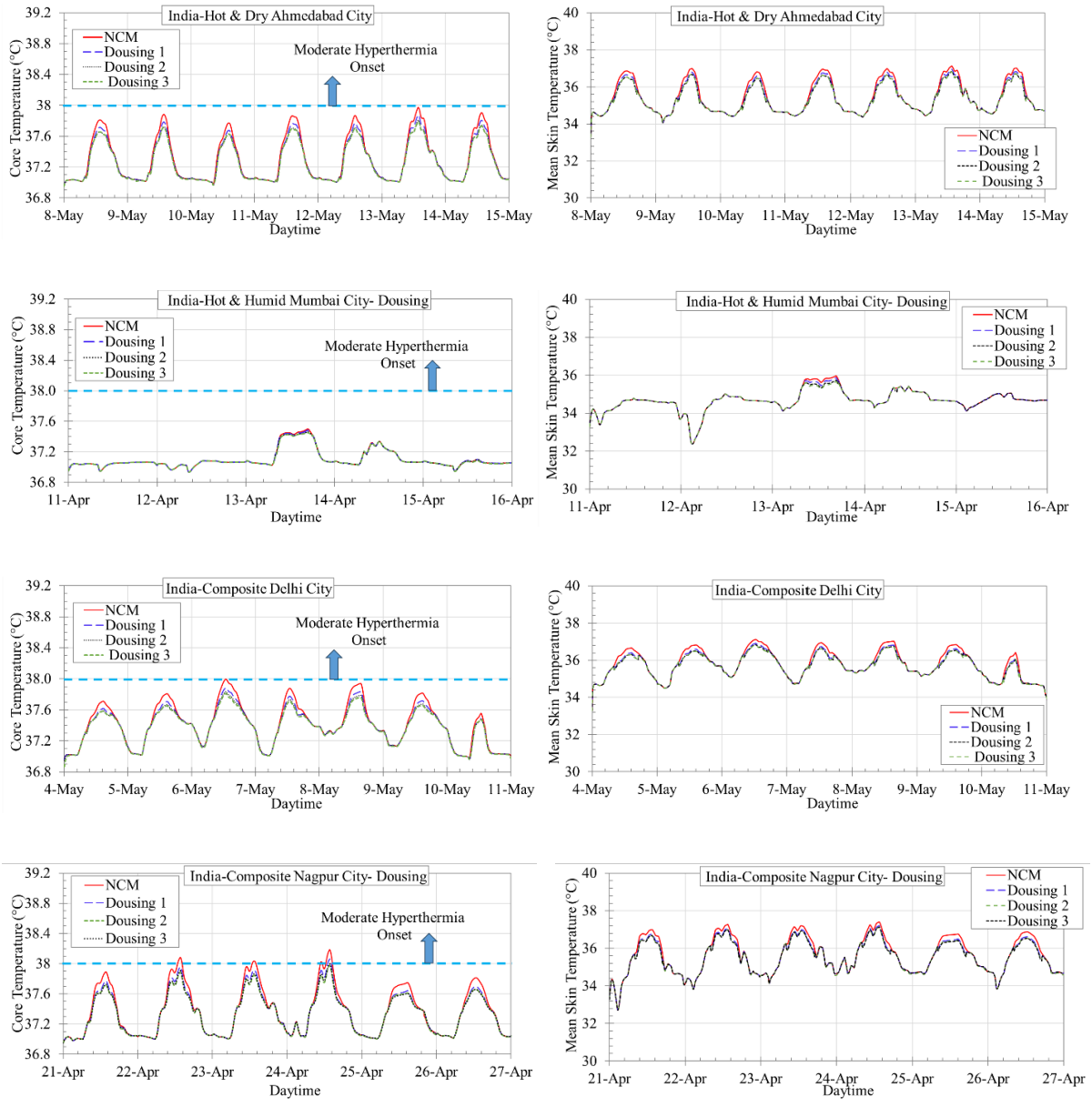

Figure C 4. Core and mean skin temperature variation during a heat event for dousing interventions at different water temperatures and with no cooling method (NCM) in across different climatic cities of India.

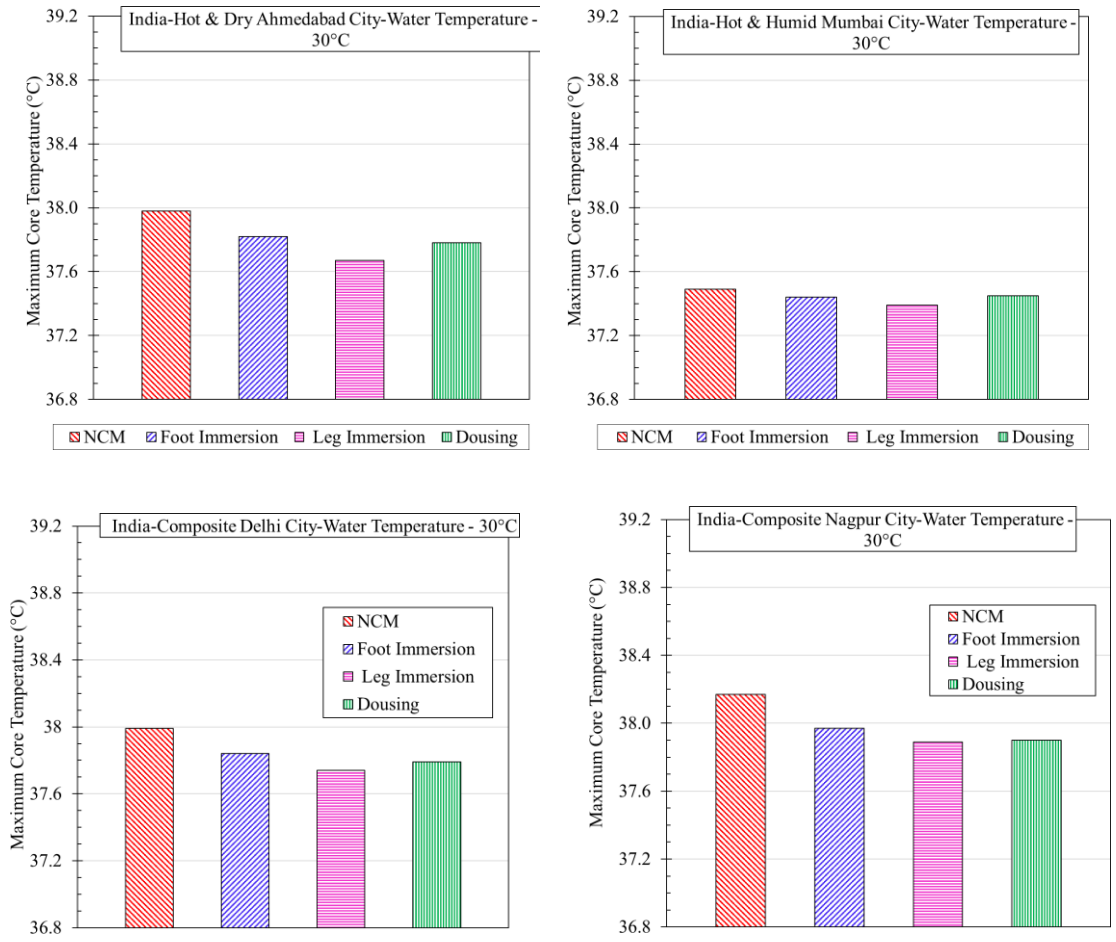

Figure C 5. Maximum core temperature for foot immersion, leg immersion, and dousing compared to no cooling method in across different climatic cities of India.

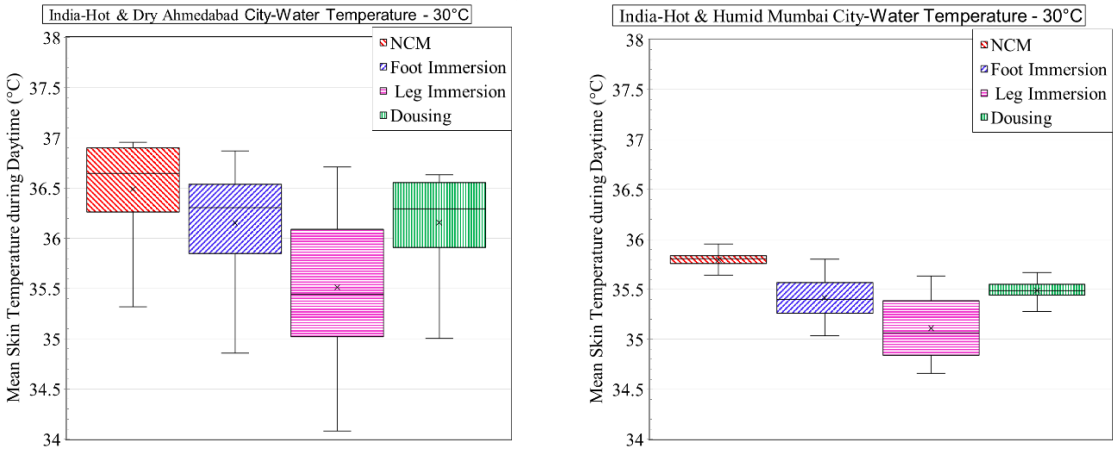

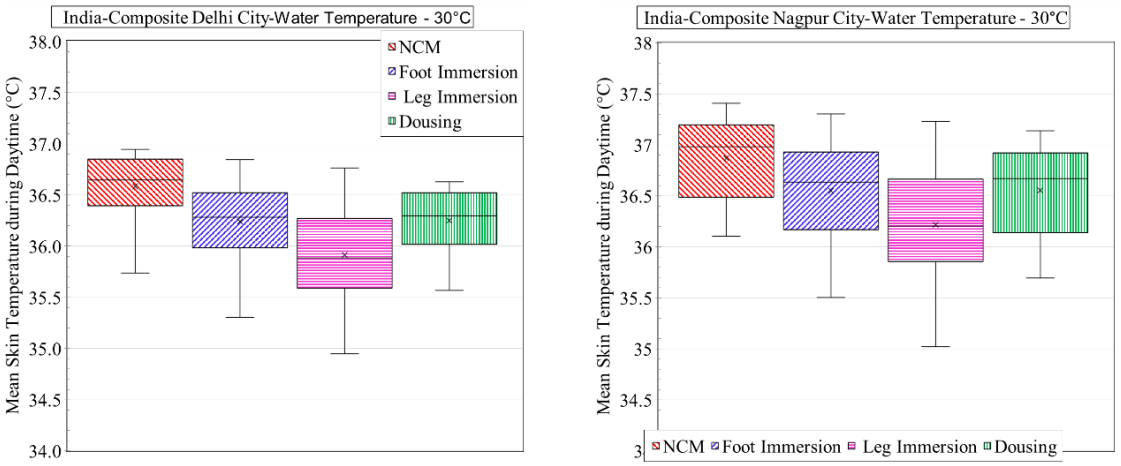

Figure C 6. Mean skin temperature for no cooling method, foot immersion, leg immersion, and dousing during daytime hours (08:00–17:00) on an extreme heatwave day in across different climatic cities of India.

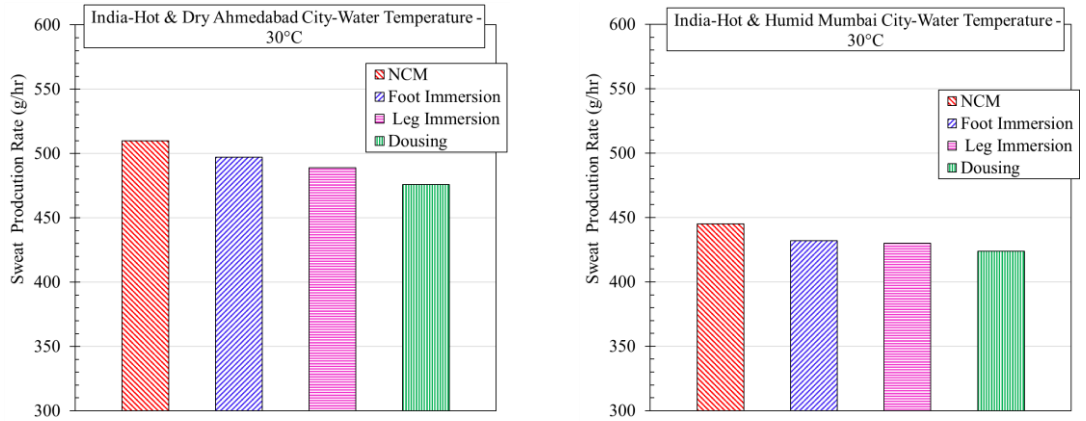

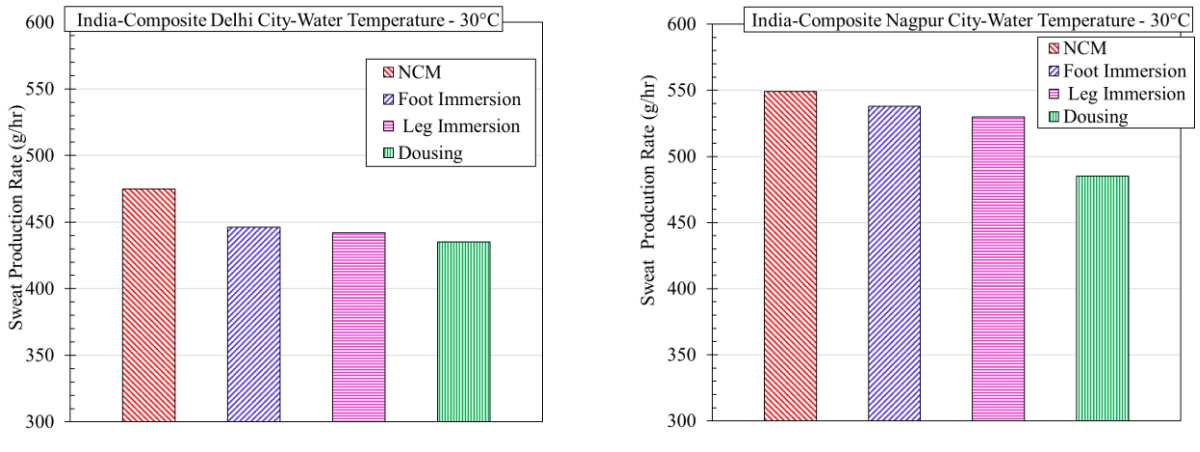

Figure C 7. Sweat production rate for the no cooling method, foot immersion, leg immersion, and dousing across different climatic cities of India.

BIBLIOGRAPHY

- Adnan, M. S. G., Dewan, A., Botje, D., Shahid, S., & Hassan, Q. K. (2022). Vulnerability of Australia to heatwaves: A systematic review on influencing factors, impacts, and mitigation options. *Environmental Research*, 213, 113703. https://doi.org/10.1016/j.envres.2022.113703
- AECOM; Delta-EE; University of Exeter. (2021). *Cooling in the U.K.* Department for Business, Energy & Industrial Strategy: London, UK.
- Alexander, L., Hope, P., Collins, D., Trewin, B., Lynch, A., & Nicholls, N. (2007). Trends in Australia's climate means and extremes: a global context. *Australian Meteorological Magazine*, 56, 1–18.
- Anderson, M., Bellenger, C., Chaseling, G. K., & Chalmers, S. (2024). The effect of water dousing on heat strain and performance during endurance running in the heat. *International Journal of Sports Physiology and Performance*, 1(aop), 1–8.
- Arens, E. A., & Zhang, H. (2006). The skin's role in human thermoregulation and comfort. https://escholarship.org/uc/item/3f4599hx
- Arens, E., Turner, S., Zhang, H., & Paliaga, G. (2009). Moving air for comfort. *ASHRAE Journal*, 51(5), 18–29.
- ASHRAE. (2004). *ASHRAE Standard 55-2004: Thermal Environmental Conditions for Human Occupancy*. ASHRAE.
- Ayushi Sharma, Priya Dutta, Priyanka Shah, Veena Iyer, Hao He, Amir Sapkota, Chuansi Gao, Yu-Chun Wang (2024). Characterizing the effects of extreme heat events on all-cause mortality: A case study in Ahmedabad city of India, 2002–2018. Urban. Climate, 54 Article 101832.

- Ballester, J., Quijal-Zamorano, M., Méndez Turrubiates, R. F., Pegenaute, F., Herrmann, F. R., Robine, J. M., Basagaña, X., Tonne, C., Antó, J. M., & Achebak, H. (2023). Heat-related mortality in Europe during the summer of 2022. *Nature Medicine*, 29(7), 1857–1866. https://doi.org/10.1038/s41591-023-02419-z
- Bhatia, R. Tiwari, J. Mathur (2011). Thermal comfort in naturally ventilated residential buildings in India: field measurements and implications. Build Env., 46 (2), pp. 370-378
- Bhuvad, S. S., You, R., & Chen, Q. (2024). Evaluation of physiological and thermal comfort effectiveness of ceiling fan and table fan during a heat wave. *Energy and Buildings*, 322, 114706. https://doi.org/10.1016/j.enbuild.2024.114706
- Bird, R. B., Stewart, W. E., & Lightfoot, E. N. (2007). *Transport Phenomena* (2nd ed.). Wiley.
- Boutelier, C., Bougues, L., & Timbal, J. (1977). Experimental study of convective heat transfer coefficient for the human body in water. *Volume 42*, 93–100.
- Bureau of Indian Standards. (2016). *National Building Code of India 2016, Part 1* (3rd ed.). Bureau of Indian Standards, India.
- Cabanac, M. (2006). Adjustable set point: To honor Harold T. Hammel. *Journal of Applied Physiology*, 100(4), 1338–1346.
- Cabanac, M. (2006). Adjustable set point: to honor Harold T. Hammel. *Journal of Applied Physiology*, 100(4), 1338–1346.
- Campbell, S., Remenyi, T. A., White, C. J., & Johnston, F. H. (2018). Heatwave and health impact research: A global review. *Health & Place*, 53, 210–218. https://doi.org/10.1016/j.healthplace.2018.08.017
- Castellani, M. P., Rioux, T. P., Castellani, J. W., Reed, M. D., Whalen, S., Cisternelli, M., Python, G., Lewandowski, M. J., & Xu, X. (2023). Validation of a human

thermoregulatory model during prolonged immersion in warm water. *Computers in Biology and Medicine*, 167, 107575.

- CDC. (2012). Frequently asked questions (FAQ) about extreme heat. *Centers for Disease Control and Prevention*. https://www.cdc.gov/disasters/extremeheat/faq.html (Accessed on 10/01/2025)
- Cheuvront, S. N., & Kenefick, R. W. (2017). CORP: Improving the status quo for measuring whole body sweat losses. *Journal of Applied Physiology*, 123(3), 632–636. https://doi.org/10.1152/japplphysiol.00433.2017
- Choudhary, B. (2025). A modified multi-node human thermoregulation model with improved sweating response to simulate human physiological behaviours in warm and hot environments. *Building and Environment*, 267, 112164.
- Connell, W., Houghten, F., & Yagloglou, C. (1924). Air motion—high temperatures and various humidities—reactions on human beings. *Transactions of the American Society of Heating and Ventilating Engineers*, 30, 199–224.
- Cooney, D. O. (1976). *Biomedical Engineering Principles: An Introduction to Fluid, Heat, and Mass Transport Processes*. Dekker.
- CoreBodyTemp. (n.d.). *Core temperature monitoring technology*. https://corebodytemp.com (Accessed on 15/10/2023)
- Cramer, M. N., Huang, M., Moralez, G., et al. (2020). Keeping older individuals cool in hot and moderately humid conditions: Wetted clothing with and without an electric fan. *Journal of Applied Physiology*, 128(3), 604–611. https://doi.org/10.1152/japplphysiol.00786.2019
- De Dear, R. J. (1998). A global database of thermal comfort field experiments. *ASHRAE Transactions*, 104, 1141.

- De Dear, R. J., Arens, E., Hui, Z., & Oguro, M. (1997). Convective and radiative heat transfer coefficients for individual human body segments. *International Journal of Biometeorology*, 40(3), 141–156.
- DeGroot, D. W., Gallimore, R. P., Thompson, S. M., & Kenefick, R. W. (2013). Extremity cooling for heat stress mitigation in military and occupational settings. *Journal of Thermal Biology*, 38(6), 305–310.
- Dickie, G. (2024). Extreme heat kills hundreds, millions more sweltering worldwide as summer begins. *Reuters*. (Accessed on 07/01/2025)

- Dickie, G. (2024). Extreme heat kills hundreds, millions more sweltering worldwide as summer begins. *Reuters*. (Accessed on 07/01/2025)

- EnergyPlus. (2021). *Climate data for building performance simulation*. http://www.climate.onebuilding.org
- FAO/WHO/UNU Expert Consultation. (2005). Human energy requirements: Report of a joint FAO/WHO/UNU expert consultation. *Food and Nutrition Bulletin*, 26(1), 166.
- Fiala, D., Havenith, G., Bröde, P., Kampmann, B., & Jendritzky, G. (2012). UTCI-Fiala multi-node model of human heat transfer and temperature regulation. *International Journal of Biometeorology*, 56(3), 429–441.

- Fiala, D., Havenith, G., Bröde, P., Kampmann, B., & Jendritzky, G. (2012). UTCI-Fiala multi-node model of human heat transfer and temperature regulation. *International Journal of Biometeorology*, 56(3), 429–441.

- Fiala, D., Lomas, K. J., & Stohrer, M. (1999). A computer model of human thermoregulation for a wide range of environmental conditions: The passive system. *Journal of Applied Physiology*, 87(5), 1957–1972.

- Fiala, D., Lomas, K. J., & Stohrer, M. (1999). A computer model of human thermoregulation for a wide range of environmental conditions: The passive system. *Journal of Applied Physiology*, 87(5), 1957–1972.
- Gagnon, D., & Kenny, G. P. (2012). Does sex have an independent effect on thermoeffector responses during exercise in the heat? *Journal of Physiology*, 590(23), 5963–5973.
- Gagnon, D., & Kenny, G. P. (2012). Does sex have an independent effect on thermoeffector responses during exercise in the heat? *Journal of Physiology*, 590, 5963–5973.
- Gagnon, D., Romero, S. A., Cramer, M. N., Jay, O., & Crandall, C. G. (2016). Cardiac and thermal strain of elderly adults exposed to extreme heat and humidity with and without electric fan use. *JAMA*, 316(9), 989–991. doi:10.1001/jama.2016.10550
- Grahn, D. A., Dillon, J. L., & Heller, H. C. (2009). Heat loss through the glabrous skin surfaces of heavily insulated, heat-stressed individuals. *Journal of Biomechanical Engineering*, 131(7), 071005. doi:10.1115/1.3157184
- Hagobian, T. A., Jacobs, K. A., Kiratli, B. J., & Friedlander, A. L. (2004). Foot cooling reduces exercise-induced hyperthermia in men with spinal cord injury. *Medicine and Science in Sports and Exercise*, 36(3), 411.
- Hailes, W. S., Cuddy, J. S., Cochrane, K., & Ruby, B. C. (2016). Thermoregulation during extended exercise in the heat: Comparisons of fluid volume and temperature. *Wilderness & Environmental Medicine*, 27(3), 386–392. https://doi.org/10.1016/j.wem.2016.06.00
- Haines, A., & Ebi, K. (2019). The imperative for climate action to protect health. *New England Journal of Medicine*, 380(3), 263–273. https://doi.org/10.1056/nejmra1807873

- House, J. (1998). Extremity cooling as a method for reducing heat strain. *Journal of Defense Science*, 3, 108–114.
- Huizenga, C., Hui, Z., & Arens, E. (2001). A model of human physiology and comfort for assessing complex thermal environments. *Building and Environment*, 36(6), 691–699.
- Huizenga, C., Hui, Z., & Arens, E. (2001). A model of human physiology and comfort for assessing complex thermal environments. *Building and Environment*, 36, 691–699.
- iButtonLink. (n.d.). *DS1922L temperature logger*. https://www.ibuttonlink.com/products/ds1922l (Accessed on 15/10/2023)
- International Energy Agency (IEA). (2018). *The future of cooling*. Paris: IEA. (Accessed on 07/01/2024)
- International Organization for Standardization (ISO). (1998). *ISO 7726: Ergonomics of the thermal environment – Instruments for measuring physical quantities*.
- IPCC. (2021). *Climate change 2021: The physical science basis*. Cambridge University Press. (Accessed on 12/10/2023)
- Ivanov, K. P. (2006). The development of the concepts of homeothermy and thermoregulation. *Journal of Thermal Biology*, 31, 24–29.
- Jay, O., Capon, A., Berry, P., Broderick, C., de Dear, R., Havenith, G., Honda, Y., Kovats, R. S., Ma, W., Malik, A., & Morris, N. B. (2021). Reducing the health effects of hot weather and heat extremes: from personal cooling strategies to green cities. *The Lancet*, 398(10301), 709–724. doi:10.1016/S0140-6736(21)01156-0
- Jay, O., Cramer, M. N., Ravanelli, N. M., & Hodder, S. G. (2015). Should electric fans be used during a heat wave? *Applied Ergonomics*, 46, 137–143. doi:10.1016/j.apergo.2014.07.013
- Jay, O., Hoelzl, R., Weets, J., Morris, N., English, T., Nybo, L., Niu, J., de Dear, R., & Capon, A. (2019). Fanning as an alternative to air conditioning–a sustainable solution for

reducing indoor occupational heat stress. *Energy and Buildings*, 193, 92–98. doi:10.1016/j.enbuild.2019.03.037

- Kanti, F. S., Alari, A., Chaix, B., & Benmarhnia, T. (2022). Comparison of various heat waves definitions and the burden of heat-related mortality in France: Implications for existing early warning systems. *Environmental Research*, 215, 114359. doi:10.1016/j.envres.2022.114359
- Kern & Sohn GmbH. (n.d.). *Precision weighing and measuring solutions*. https://www.kern-sohn.com (Accessed on 15/10/2023)
- Kingma, B. R. M., Schellen, L., Frijns, A. J. H., & van Marken Lichtenbelt, W. D. (2012). Thermal sensation: A mathematical model based on neurophysiology. *Indoor Air*, 22(3), 253–262.
- Kingma, B. R. M., Schellen, L., Frijns, A. J. H., & van Marken Lichtenbelt, W. D. (2012). Thermal sensation: a mathematical model based on neurophysiology. *Indoor Air*, 22(3), 253–262.
- Kobayashi, Y., & Tanabe, S. (2013). Development of JOS-2 human thermoregulation model with detailed vascular system. *Building and Environment*, 66, 1–10.
- Kobayashi, Y., & Tanabe, S. (2013). Development of JOS-2 human thermoregulation model with detailed vascular system. Building and Environment, 66, 1–10.
- Kotharkar, R., & Ghosh, A. (2022). Progress in extreme heat management and warning systems: a systematic review of heat-health action plans (1995–2020). *Sustainable Cities and Society*, 76, 103487. doi:10.1016/j.scs.2021.103487
- Lei, T. H., Lan, L., & Wang, F. (2023). Indoor thermal comfort research using human participants: Guidelines and a checklist for experimental design. *Journal of Thermal Biology*, 113, 103506. doi:10.1016/j.jtherbio.2023.103506

- Li, Z., Ke, Y., Wang, F., & Yang, B. (2018). Personal cooling strategies to improve thermal comfort in warm indoor environments: comparison of a conventional desk fan and air ventilation clothing. *Energy and Buildings*, 174, 439–451. doi:10.1016/j.enbuild.2018.06.065
  - Livingstone, S. D., Nolan, R. W., & Keefe, A. A. (1995). Heat loss caused by cooling the feet. *Aviation, Space, and Environmental Medicine*, 66, 232–232.
- Malik, A., Bongers, C., McBain, B., Rey-Lescure, O., de Dear, R., Capon, A., Lenzen, M., & Jay, O. (2022). The potential for indoor fans to change air conditioning use while maintaining human thermal comfort during hot weather: an analysis of energy demand and associated greenhouse gas emissions. *The Lancet Planetary Health*, 6(4), e301–e309. doi:10.1016/S2542-5196(22)00042-0
- Mani M., Y. Shukla, R. Rawal, L. Thomas, A. Meno. Thermal performance of typical residential buildings in India under climate change scenarios. Build. Simul., 5 (2012), pp. 25-37.
- Mansfield, R. G., Hoekstra, S. P., Bill, J. J., & Leicht, C. A. (2021). Local cooling during hot water immersion improves perceptions without inhibiting the acute interleukin-6 response. *European Journal of Applied Physiology*, 121(5), 1581–1591.
- Marrero, T. R., & Mason, E. A. (1972). Gaseous diffusion coefficients. *Journal of Physical and Chemical Reference Data*, 1(1), 3–118.
- Masood, I., Majid, Z., Sohail, S., Zia, A., & Raza, S. (2015). The deadly heat wave of Pakistan, June 2015. *International Journal of Occupational and Environmental Medicine*, 6, 247–248. https://doi.org/10.15171/ijoem.2015.672
- McDermott, B. P., Casa, D. J., O'Connor, F. G., Adams, W. B., Armstrong, L. E., Brennan, A. H., Lopez, R. M., Stearns, R. L., Troyanos, C., & Yeargin, S. W. (2009).

Cold-water dousing with ice massage to treat exertional heat stroke: a case series. *Aviation, Space, and Environmental Medicine*, 80(8), 720–722.

- McGregor, G. R., Bessmoulin, P., Ebi, K., & Menne, B. (2015). *Heatwaves and health: Guidance on warning-system development*. World Meteorological Organization.
- Meade, R. D., Atkins, W. C., Bach, A. J., Foster, J., Hutchins, K. P., McKenna, Z. J., & Notley, S. R. (2024). Human heat resilience in a warming climate: Biophysical and physiological underpinnings of heat vulnerability and personal cooling strategies. *One Earth*, 7(10), 1343–1350. doi:10.1016/j.oneear.2024.06.007
- Meade, R. D., Notley, S. R., Kirby, N. V., & Kenny, G. P. (2024). A critical review of the effectiveness of electric fans as a personal cooling intervention in hot weather and heatwaves. *The Lancet Planetary Health*, 8(4), e256–e269. doi:10.1016/S2542-5196(24)00030-5
- MedicineNet. (n.d.). *11 Tips on How To Survive A Heat Wave Without Air-Conditioning*. https://www.medicinenet.com/script/main/art.asp?articlekey=63080
- Mekjavic, I. B., & Eiken, O. (2006). Contribution of thermal and nonthermal factors to the regulation of body temperature in humans. *Journal of Applied Physiology*, 100, 2065–2072.
- Mekjavic, I. B., & Eiken, O. (2006). Contribution of thermal and nonthermal factors to the regulation of body temperature in humans. *Journal of Applied Physiology*, 100(6), 2065–2072.
- Montain, S. J., Latzka, W. A., & Sawka, M. N. (1995). Control of thermoregulatory sweating is altered by hydration level and exercise intensity. *Journal of Applied Physiology*, 79(5), 1434–1439.

- Montain, S. J., Latzka, W. A., & Sawka, M. N. (1995). Control of thermoregulatory sweating is altered by hydration level and exercise intensity. *Journal of Applied Physiology*, 79(5), 1434–1439.
- Montain, S. J., Sawka, M. N., Latzka, W. A., & Valeri, C. R. (1998). Thermal and cardiovascular strain from hypohydration: influence of exercise intensity. *International Journal of Sports Medicine*, 19(2), 87–91.
- Monteith, J. L., & Unsworth, M. H. (2013). *Principles of Environmental Physics* (4th ed.). Academic Press.
- Morris, N. B., & Jay, O. (2016). To drink or to pour: How should athletes use water to cool themselves? *Temperature*, 3(2), 191–194.
- Morris, N. B., Bain, A. R., Cramer, M. N., & Jay, O. (2014). Evidence that transient changes in sudomotor output with cold and warm fluid ingestion are independently modulated by abdominal, but not oral thermoreceptors. *Journal of Applied Physiology*, 116(9), 1088–1095.
- Morris, N. B., Chaseling, G. K., English, T., Gruss, F., Maideen, M. F. B., Capon, A., & Jay, O. (2021). Electric fan use for cooling during hot weather: a biophysical modelling study. *The Lancet Planetary Health*, 5(6), e368–e377. doi:10.1016/S2542-5196(21)00136-4
- Morris, N. B., Coombs, G., & Jay, O. (2016). Ice slurry ingestion leads to a lower net heat loss during exercise in the heat. *Medicine & Science in Sports & Exercise*, 48(1), 114–122.
- Morris, N. B., English, T., Hospers, L., Capon, A., & Jay, O. (2019). The effects of electric fan use under differing resting heat index conditions: a clinical trial. *Annals of Internal Medicine*, 171(9), 675–677. doi:10.7326/M19-0512

- Morris, N. B., Gruss, F., Lempert, S., English, T., Hospers, L., Capon, A., & Jay, O. (2019). A preliminary study of the effect of dousing and foot immersion on cardiovascular and thermal responses to extreme heat. *JAMA*, 322(14), 1411–1413. doi:10.1001/jama.2019.13051
- Munir, A., Takada, S., Matsushita, T., & Kubo, H. (2010). Prediction of human thermophysiological responses during shower bathing. *International Journal of Biometeorology*, 54(2), 165–178.
- National Portal of India. (2025). *Districts of India*. https://www.india.gov.in/india-glance/districts-india
- NRDC & Indian Institute of Public Health (IIPH). (2013). Ahmedabad heat and Climate study.
- Parsons, K. (2014). *Human thermal environments: The effects of hot, moderate, and cold environments on human health, comfort and performance* (3rd ed.). CRC Press.
- Ravanelli, N. M., Hodder, S. G., Havenith, G., & Jay, O. (2015). Heart rate and body temperature responses to extreme heat and humidity with and without electric fans. *JAMA*, 313(7), 724–725. doi:10.1001/jama.2015.153
- Ready.gov. (2020). *Extreme heat*. https://www.ready.gov/heat (Accessed on 10/01/2025)
- Robine, J. M., Cheung, S. L. K., Le Roy, S., Van Oyen, H., Griffiths, C., Michel, J. P., & Herrmann, F. R. (2008). Death toll exceeded 70,000 in Europe during the summer of 2003. *C R Biologies*, 331(2), 171–178. doi:10.1016/j.crvi.2007.12.001

- Robine, J. M., Cheung, S. L. K., Le Roy, S., Van Oyen, H., Griffiths, C., Michel, J. P., & Herrmann, F. R. (2008). Death toll exceeded 70,000 in Europe during the summer of 2003. *C R Biologies*, 331(2), 171–178. doi:10.1016/j.crvi.2007.12.001

- Romanello, M., Walawender, M., Hsu, S. C., Moskeland, A., Palmeiro-Silva, Y., Scamman, D., Ali, Z., Ameli, N., Angelova, D., Ayeb-Karlsson, S., Basart, S., et al.

(2024). The 2024 report of the Lancet Countdown on health and climate change: facing record-breaking threats from delayed action. *The Lancet*, 404(10387), 1847–1896. doi:10.1016/S0140-6736(24)01822-1

- Romanovsky, A. A. (2007). Thermoregulation: Some concepts have changed. Functional architecture of the thermoregulatory system. *American Journal of Physiology-Regulatory, Integrative and Comparative Physiology*, 292(1), R37–R46.
- Romanovsky, A. A. (2007). Thermoregulation: some concepts have changed. Functional architecture of the thermoregulatory system. *American Journal of Physiology-Regulatory, Integrative and Comparative Physiology*, 292(1), R37–R46.
- Saman, W., Boland, J., Pullen, S., de Dear, R. J., Soebarto, V., Miller, W. F., Pocock, B., Belusko, M., Bruno, F., & Whaley, D. (2013). *A framework for adaptation of Australian households to heat waves*. National Climate Change Adaptation Research Facility.
- Santamouris, M., Cartalis, C., Synnefa, A., & Kolokotsa, D. (2015). On the impact of urban heat island and global warming on the power demand and electricity consumption of buildings—A review. *Energy and Buildings*, 98, 119–124.
- Scheatzle, D. G., Wu, H., & Yellott, J. (1989). Extending the summer comfort envelope with ceiling fans in hot, arid climates. *ASHRAE Transactions*, 95, 269–280.
- Schlader, Z. J., Johnson, B. D., Pryor, R. R., Stooks, J., Clemency, B. M., & Hostler, D. (2020). Human thermoregulation during prolonged exposure to warm and extremely humid environments expected to occur in disabled submarine scenarios. *American Journal of Physiology-Regulatory, Integrative and Comparative Physiology*, 318(5), R950–R960.
- Schranner, D., Scherer, L., Lynch, G. P., Korder, S., Brotherhood, J. R., Pluim, B. M., Periard, J. D., & Jay, O. (2017). In-play cooling interventions for simulated match-play

tennis in hot/humid conditions. *Medicine & Science in Sports & Exercise*, 49(5), 991–998. https://doi.org/10.1249/MSS.0000000000001183

- Selkirk, G. A., & McLellan, T. M. (2001). Influence of aerobic fitness and body fatness on tolerance to uncompensable heat stress. *Journal of Applied Physiology*, 91(5), 2055–2063. https://doi.org/10.1152/jappl.2001.91.5.2055
- Selkirk, G. A., McLellan, T. M., & Wong, J. (2004). Active versus passive cooling during work in warm environments while wearing firefighting protective clothing. *Journal of Occupational and Environmental Hygiene*, 1(8), 521–531. https://doi.org/10.1080/15459620490475216
- Semenza, J. C., Rubin, C. H., Falter, K. H., Selanikio, J. D., Flanders, W. D., Howe, H. L., & Wilhelm, J. L. (1996). Heat-Related Deaths during the July 1995 Heat Wave in Chicago. *New England Journal of Medicine*, 335(2), 84–90.
- Sherman, P., Lin, H., & McElroy, M. (2022). Projected global demand for air conditioning associated with extreme heat and implications for electricity grids in poorer countries. *Energy and Buildings*, 268, 112198. https://doi.org/10.1016/j.enbuild.2022.112198
- Song, W., Wang, F., & Zhang, C. (2019). Intermittent wetting clothing as a cooling strategy for body heat strain alleviation of vulnerable populations during a severe heatwave incident. *Journal of Thermal Biology*, 79, 33–41. https://doi.org/10.1016/j.jtherbio.2018.11.012
- Staff Writers. (2011). Natural disasters killed 295,000 in 2010: reinsurer. *Terra Daily*. (Accessed on 07/01/2025)
- Stolwijk, J. A. J. (1971). A mathematical model of physiological temperature regulation in man. *NASA CR-1855*, 77.

- Stolwijk, J. A. J. (1971). *A mathematical model of physiological temperature regulation in man* (NASA CR-1855: 1–77). National Aeronautics and Space Administration.
- Takahashi, Y., Nomoto, A., Yoda, S., Hisayama, R., Ogata, M., Ozeki, Y., & Tanabe, S. I. (2021). Thermoregulation model JOS-3 with new open source code. *Energy and Buildings*, 231, 110575.
- Takahashi, Y., Nomoto, A., Yoda, S., Hisayama, R., Ogata, M., Ozeki, Y., & Tanabe, S. I. (2021). Thermoregulation model JOS-3 with new open source code. Energy and Buildings, 231, 110575.
- Tanabe, S. I., Kobayashi, K., Nakano, J., Ozeki, Y., & Konishi, M. (2002). Evaluation of thermal comfort using combined multi-node thermoregulation (65MN) and radiation models and computational fluid dynamics (CFD). *Energy and Buildings*, 34(6), 637–646.
- Tanabe, S. I., Kobayashi, K., Nakano, J., Ozeki, Y., & Konishi, M. (2002). Evaluation of thermal comfort using combined multi-node thermoregulation (65MN) and radiation models and computational fluid dynamics (CFD). *Energy and Buildings*, 34, 637–646.
- Tartarini, F., Schiavon, S., Jay, O., Arens, E., & Huizenga, C. (2022). Application of Gagge's energy balance model to determine humidity-dependent temperature thresholds for healthy adults using electric fans during heatwaves. *Building and Environment*, 207, 108437. doi:10.1016/j.buildenv.2021.108437
- USAID-ECO III Project. (2017). *Energy Conservation Building Code User Guide*. April 2017.
- Vaughan, A. (2021). The heat is on out west. *New Scientist*, 250(3342), 10–11.
- Vaughan, A. (2021). The heat is on out west. *New Scientist*, 250(3342), 10–11.
- Vellei, M., Pigliautile, I., & Pisello, A. L. (2023). Effect of time-of-day on human dynamic thermal perception. *Scientific Reports*, 13(1), 2367. https://doi.org/10.1038/s41598-023-29615-8

- Wang, F., Deng, Q., Lei, T. H., Wang, X., & Wang, A. R. (2023). Biophysical modelling predicts unreliable core temperature responses on healthy older adults using electric fans at residential homes during heatwaves. *Building and Environment*, 228, 109888. doi:10.1016/j.buildenv.2022.109888
- Wang, Y., Lin, L., Xu, Z., Wang, L., Huang, J., Li, G., & Zhou, M. (2023). Have residents adapted to heat wave and cold spell in the 21st century? Evidence from 136 Chinese cities. *Environment International*, 173, 107811. https://doi.org/10.1016/j.envint.2023.107811
- Watts, N., Amann, M., Arnell, N., Ayeb-Karlsson, S., Belesova, K., Boykoff, M., Byass, P., Cai, W., Campbell-Lendrum, D., Capstick, S., & Chambers, J. (2019). The 2019 report of The Lancet Countdown on health and climate change: ensuring that the health of a child born today is not defined by a changing climate. *The Lancet*, 394(10211), 1836–1878. https://doi.org/10.1016/S0140-6736(19)32596-6
- World Health Organization. (2018). Heat and health. https://www.who.int/news-room/fact-sheets/detail/climate-change-heat-and-health (Accessed on 12/10/2023)
- World Meteorological Organization & World Health Organization. (2015). Heat waves and health: guidance on warning-system development. http://www.who.int/globalchange/publications/heatwaveshealth-guidance/en (Accessed on 07/01/2025)
- Wright-Beatty, H. E., Hardcastle, S. G., Boulay, P., Flouris, A. D., & Kenny, G. P. (2015). Increased air velocity reduces thermal and cardiovascular strain in young and older males during humid exertional heat stress. Journal of Occupational and Environmental Hygiene, 12, 625–634. www.terradaily.com/reports/Natural_disasters_killed_295000_in_2010

- Yang, L., Gao, S., Zhao, S., Zhang, H., Arens, E., & Zhai, Y. (2020). Thermal comfort and physiological responses with standing and treadmill workstations in summer. Building and Environment, 185, 107238. https://doi.org/10.1016/j.buildenv.2020.107238
- Zhai, Y., Zhang, H., Zhang, Y., Pasut, W., Arens, E., & Meng, Q. (2013). Comfort under personally controlled air movement in warm and humid environments. Building and Environment, 65, 109–117. https://doi.org/10.1016/j.buildenv.2013.03.022
- Zhao, J., Wang, F., Ou, D., Zhou, B., Li, Y., Wang, H., & Deng, Q. (2023). Thermoregulatory analysis of warm footbaths before bedtime: Implications for enhancing sleep quality. Building and Environment, 227, 109788.
- Zhao, Q., Guo, Y., Ye, T., Gasparrini, A., Tong, S., & Overcenco, A. (2021). Global, regional, and national burden of mortality associated with non-optimal ambient temperatures from 2000 to 2019: a three-stage modelling study. The Lancet Planetary Health, 5(7), E415–E425.
- World Disasters Report 2020: Come Heat or High Water - Tackling the Humanitarian Impacts of the Climate Crisis Together. reliefweb.int/report/world/world-disasters-report-2020-come-heat-or-high-water-tackling-humanitarian-impacts.